National Library of Canada
Acquisitions and Bibliographic Services Branch
395 Wellington Street
Ottawa, Ontario
K1A 0N4

Bibliothèque nationale du Canada
Direction des acquisitions et des services bibliographiques
395, rue Wellington
Ottawa (Ontario)
K1A 0N4

Your file Votre référence

Our file Notre référence

NOTICE

The quality of this microform is heavily dependent upon the quality of the original thesis submitted for microfilming. Every effort has been made to ensure the highest quality of reproduction possible.

If pages are missing, contact the university which granted the degree.

Some pages may have indistinct print especially if the original pages were typed with a poor typewriter ribbon or if the university sent us an inferior photocopy.

Reproduction in full or in part of this microform is governed by the Canadian Copyright Act, R.S.C. 1970, c. C-30, and subsequent amendments.

AVIS

La qualité de cette microforme dépend grandement de la qualité de la thèse soumise au microfilmage. Nous avons tout fait pour assurer une qualité supérieure de reproduction.

S'il manque des pages, veuillez communiquer avec l'université qui a conféré le grade.

La qualité d'impression de certaines pages peut laisser à désirer, surtout si les pages originales ont été dactylographiées à l'aide d'un ruban usé ou si l'université nous a fait parvenir une photocopie de qualité inférieure.

La reproduction, même partielle, de cette microforme est soumise à la Loi canadienne sur le droit d'auteur, SRC 1970, c. C-30, et ses amendements subséquents.

Canada

University of Alberta

Internal Structure of Realistic Black Holes

by

Serge Patrice Droz-Georget

A thesis submitted to the Faculty of Graduate Studies and Research in partial fulfillment of the requirements for the degree of **Doctor of Philosophy**

in

Theoretical Physics

Department of Physics

Edmonton, Alberta

Spring 1996

National Library
of Canada

Acquisitions and
Bibliographic Services Branch

395 Wellington Street
Ottawa, Ontario
K1A 0N4

Bibliothèque nationale
du Canada

Direction des acquisitions et
des services bibliographiques

395, rue Wellington
Ottawa (Ontario)
K1A 0N4

Your file Votre référence

Our file Notre référence

The author has granted an irrevocable non-exclusive licence allowing the National Library of Canada to reproduce, loan, distribute or sell copies of his/her thesis by any means and in any form or format, making this thesis available to interested persons.

L'auteur a accordé une licence irrévocable et non exclusive permettant à la Bibliothèque nationale du Canada de reproduire, prêter, distribuer ou vendre des copies de sa thèse de quelque manière et sous quelque forme que ce soit pour mettre des exemplaires de cette thèse à la disposition des personnes intéressées.

The author retains ownership of the copyright in his/her thesis. Neither the thesis nor substantial extracts from it may be printed or otherwise reproduced without his/her permission.

L'auteur conserve la propriété du droit d'auteur qui protège sa thèse. Ni la thèse ni des extraits substantiels de celle-ci ne doivent être imprimés ou autrement reproduits sans son autorisation.

ISBN 0-612-10580-6

Canada

University of Alberta

Library Release Form

Name of Author: Serge Patrice Droz-Georget

Title of Thesis: Internal Structure of Realistic Black Holes

Degree: Doctor of Philosophy

Year this Degree Granted: 1996

Permission is hereby granted to the University of Alberta Library to reproduce single copies of this thesis to lend or sell such copies for private, scholarly, or scientific research purposes only.

The author reserves all other publication and other rights in association with copyright in the thesis, and except as hereinbefore, neither the thesis nor any substantial portion thereof may be printed or otherwise reproduced in any material form whatever without the author's prior written permission.

S. Droz

Serge Patrice Droz-Georget
530 Rowhouse, Michener Park
Edmonton Alberta
T6H 4M5, Canada

Date: 2. Feb 1996

University of Alberta

Faculty of Graduate Studies and Research

The undersigned certify that they have read, and recommend to the Faculty of Graduate Studies and Research for acceptance, a thesis **Internal Structure of Realistic Black Holes** submitted by **Serge Patrice Droz-Georget** in partial fulfillment of the requirement for the degree of **Doctor of Philosophy** in **Theoretical Physics**.

Werner Israel

Werner Israel (Supervisor)

B.A. Campbell

Bruce Campbell

Valery Frolov

Douglas Hube (Chairman)

Hans Künzle

Richard Matzner (External Examiner)

Date: 31 Jan 96

Wenn Gott in seiner Rechten alle Wahrheit und in seiner Linken den einzigen immer regen Trieb nach Wahrheit, obschon mit dem Zusatze, mich immer und ewig zu irren, verschlossen hielte und spräche zu mir: Wähle! ich fiele ihm mit Demut in seine Linke und sagte: Vater, gieb! Die reine Wahrheit ist ja doch nur für Dich allein.

G.E. Lessing, In der Bibliothek zu Wolfenbüttel (1770-1781)

If God were to hold out enclosed in His right hand all Truth, and in His left hand the everlasting search for Truth, though with the condition that I should ever err therein, and should say to me: Choose! I should humbly take His left and say: Father, this one! The final Truth belongs to Thee alone.

G.E. Lessing, From the library of Wolfenbüttel (1770-1781)

Abstract

Every realistic black hole possesses an inner or Cauchy horizon which signals the breakdown of the two cornerstones of physics: causality and predictability. It has long been known that that this inner horizon is unstable and it was generally assumed that in a realistic black hole it would be preceded by a spacelike BKL type singularity. A more detailed analysis of the black hole core shows that this in not quite so.

The key observation that allows a detailed treatment of the problem is that descent into a black hole necessarily is progress in time. Thus the analysis of the outer layers does not require the knowledge of the physics of the Planckian core of the black hole.

A detailed analysis of the evolution of the kind of perturbations expected in a stellar collapse shows that the singularity that forms at the Cauchy horizon is actually lightlike and mild. It slowly contracts to a strong, zero-volume singularity which is expected to be spacelike and of BKL (oscillatory) type. This so called mass inflation singularity is characterized by a divergence of the conformal curvature.

To study the structure of this singularity for a generic collapse a new double null formalism is developed which formulates Einstein's equations in a concise and transparent way. This is achieved by working with manifestly geometric objects.

The application of this formalism to the present situation shows that the mass inflation singularity is mild and smooth in the sense that the shear and the expansion stay finite. Asymptotically the spacetime becomes of Petrov Type N, indicating the presence of a collapsing gravitational shock wave.

Acknowledgements

First of all, I would like to thank my wife Silvia Gamper. Without her agreeing to come to Canada and her support throughout the years spent in Edmonton this thesis probably would have never been written. Many thanks to you Silvia!

An equally important role in finishing this thesis was played by my supervisor Werner Israel. Werner's constant support during my time here as a graduate student has been invaluable in pursuing my research and writing up my thesis. I should also mention Werner's help in converting my thesis into a readable form.

From the staff here at the Physics department I would especially like to thank Don Page for his warm welcome and help when we first arrived in Edmonton on a cold December 31st, Bruce Campbell for all the termpapers he made me write (and the beer he bought a the Power Plant) and finally Valery Frolov for his encouraging criticism of my work.

I also should not forget my fellow graduate students, especially Warren Anderson, Pat Brady and Sharon Morsink, all of whom I always could ask the "stupid questions". I hope we will find time to discuss more of these. Many thanks also for the many relaxing hours to the Knights of the coffee table Jason, Dave, Dave, Shaun, Bahman, Alick, Warren, Sharon, André and Rob. Nothing clears out the mind more after a long calculation than our coffee table discussions, especially when continued at the bar.

Many thanks also to my supervisory committee Bruce Campbell, Valery Frolov, Doug Hube, Werner Israel and Hans Künzle for their time and advice. This also includes my external examiner Richard Matzner who read my thesis so carefully. I really appreciated this.

I also would like to express my thanks to Lynn Chandler in the general office and Lee Grimard in the theoretical physics institute office for their help and support during the past four years.

Finally I would like to thank my parents Romie and Gaby Droz who always supported and respected my career wishes. Without their support I could not have gone through University.

Space is too limited to list all the friends I made here in Canada. They all contributed to make this stay in a foreign country a warm and welcoming experience.

Contents

1 Introduction 1

2 Review of basic black hole physics 8

2.1 The Schwarzschild solution 8

2.2 Formation of black holes 12

2.3 Black hole uniqueness and Price's theorem 15

2.4 The Kerr-Newman solution 16

3 Simple models of mass inflation 21

3.1 The Ori model 22

3.2 Plane mass inflation 25

4 Initial conditions for mass inflation 29

4.1 The scattering problem 31

4.2 Effects on the Cauchy horizon 35

5 Double null dynamics of Einstein gravity 42

5.1 Introduction 42

5.2 $(2+2)$-split of the metric 44

5.3 Two-dimensionally covariant objects embodying first derivatives of the metric: extrinsic curvatures K_{Aab}, twist ω^a and normal Lie derivatives D_A 47

5.4 Ricci tensor 49

5.5 Bianchi identities. Bondi's lemma 50

5.6 Co-ordinate conditions and gauge-fixing 51

5.7 Characteristic initial-value problem 52

5.8 Lagrangian 55
5.9 Gauss-Weingarten (first order) relations 56
5.10 Rationalized operators $\widetilde{\nabla}$, $\widetilde{D}_A$, ∇_a 59
5.11 Rationalized Ricci commutation rules 61
5.12 Contracted Gauss-Codazzi (second order) relations. Ricci tensor . . . 62
5.13 Riemann tensor 63
5.14 Concluding remarks 64

6 Generic structure of the Cauchy horizon **65**
6.1 Plane wave mass-inflation revisited 66
6.2 The generic structure of the Cauchy horizon 70
6.2.1 Gauge and initial conditions 70
6.2.2 Integration of Einstein's equations 71

7 Conclusions **80**

Appendices **83**
A Spherical Spacetimes 83
B Computing Ricci components: some intermediate details 84
C The operator D_A: commutation rules and other properties 85
D Solving the inhomogeneous shear equations 87

List of Figures

1 Kruskal diagram of the Schwarzschild manifold 10
2 Penrose diagram of the Schwarzschild manifold 11
3 Gravitational collapse in Eddington-Finkelstein coordinates 14
4 Penrose diagram of the exterior of a collapsing star 16
5 Maximal extension of the Reissner-Nordström spacetime 18
6 The Ori model 23
7 A spacetime diagram of the interior of a black hole 30
8 A conformal diagram of the interior of a black hole 33
9 Scattering and reflection coefficients 34
10 The $2+2$ splitting of the four dimensional spacetime 46
11 Initial data for the general case 67
12 Flow chart for the numerical integration of the shear 76
13 Numerical results for Price power law initial conditions 78
14 Numerical results for Gaussian initial conditions 79

Chapter 1

Introduction

Black holes are probably the best examples of a successful marketing campaign. Before 1967, when John Archibald Wheeler coined the term "black hole", most scientists considered their existence rather unlikely if not impossible. Things have changed since then and black holes have become a popular topic of conversation for the general public. But also the interest of scientists has risen dramatically as black holes have become the key ingredient to the possible resolution of many puzzles ranging from the structure of quasars to the problem of quantum gravity, a yet unknown theory. A quick search in the literature database Spires yields only 537 documents before 1990 dealing with black holes, but over a thousand since then.

Black hole physics has made enormous progress since its birth at the beginning of the century[1]. But there are still many unsolved problems in black hole physics. This thesis tries to shed some light on one particular question that has hardly received any attention: What is the internal structure of black holes? Even though one of the first questions that comes to mind when thinking about black holes is "What happens if I fall into one?" many physicists consider it meaningless to think about this because no explorer can ever communicate his findings to the outside world. On the other hand there are several reasons besides the classic "Because it's there!" why studying black hole interiors is worth the effort.

[1]The first person to talk of something like black holes was Rev. John Michell in 1783. But he was thinking of very massive newtonian stars, which cannot be treated as "true" black holes. The escape velocity of a star exceeding the speed of light does not mean that there is no escape from that star, in contrast to a "real" black hole where the causal structure of spacetime prevents any escape from a black hole.

There is no a priori reason to believe that the laws of physics suddenly lose their validity once the event horizon is crossed. Studying Einstein's equations in such extreme regimes of gravity as the black hole interior on the contrary might reveal new insight into this complicated nonlinear field theory. Furthermore all known (vacuum) solutions of Einstein's equations describing black holes can be continued analytically past the event horizon, but with rather bizarre consequences. The interior, with the exception of the special Schwarzschild case, possesses a so-called inner or Cauchy horizon [1], behind which a direct view onto the $r = 0$ singularity is possible. This means physics loses its predictive power, one of the cornerstones of modern science. Furthermore the inner horizon is the entrance to a tunnel that opens into a white hole (the time reverse of a black hole). To save causality we have to assume that it opens into another universe.

The good news is, as was first pointed out by Roger Penrose [2], that the inner horizon generically is unstable [3, 4]. Every tiniest perturbation falling into the black hole gets exponentially amplified as it approaches the inner horizon and eventually leads to its destruction. The butterfly flapping its wings in China not only causes bad weather here but also rids us of the embarrassment of naked singularities and new universes.

In this thesis I will take a closer look at the structure of the inner singular horizon. The remainder of this chapter gives an overview of the various chapters to follow.

Review of basic black hole physics

In Chapter 2 I briefly review some facts about black holes of importance to the main part of the thesis. Rather than building up the general theory, which is beyond the scope of this introduction, I choose to demonstrate important issues on simple examples. A more detailed treatment is found in standard texts [5, 6, 7].

The simplest solution to Einstein's field equations describing a black hole is the Schwarzschild solution which describes a spherically symmetric black hole in empty space [8]. This simple solution already possesses many of the properties of the more realistic Reissner-Nordström and Kerr-Newman solutions. Many basic ideas and tools are best explained for the Schwarzschild spacetime. These methods — suitably modified — will then be applied later to more complicated situations.

The next section deals with the formation of actual black holes. We will discusses

a simple, yet powerful model due to Oppenheimer and Snyder [9] of a stellar collapse into a black hole.

We then briefly discuss the "no-hair" theorems which essentially tell us that black holes are among the simplest objects found in nature. Their mass, angular momentum and electric charge completely specify the black hole *exterior*. This feature will turn out to play a crucial role in the late time behaviour of a stellar collapse. All the perturbations present in the initial state of the collapsing star must die off as the star radiates its hair away, a fact known as Price's theorem [10]. Part of this radiation will then fall back into the black hole with consequences described below.

Finally we give the Kerr-Newman solution which describes a rotating, electrically charged black hole. This solution, in contrast to the Schwarzschild solution, possesses an inner horizon with all its pathologies. This is most easily seen by considering the nonrotating (i.e. static) limit, the Reissner-Nordström solution. The latter has a very similar causal structure to the Kerr-Newman case which makes it an ideal model to explore the structure of the inner horizon.

Radiative tails — leftovers of the collapse and predicted by Price's theorem — get highly blue shifted as they fall towards the inner horizon. For a pure inflow situation, described by a Vaidya metric [11], this leads to a so-called whimper singularity along the inner horizon [12]. An observer crossing the inner horizon measures an infinite energy density, but all scalar quantities formed from the curvature tensors remain finite. Things change drastically once outflowing radiation is added to this setting. The cross-flow now causes a true scalar curvature singularity to form, as discussed in the following chapter.

Simple models of mass inflation

Chapter 3 gives an overview of different simple models of the inner horizon in the presence of perturbations.

As we have seen every realistic gravitational collapse is accompained by small perturbations in the form of gravitational radiation falling into the black hole. Once behind the horizon, part of this radiation will be scattered, which leads to the afore mentioned cross-flow situation. This, together with enormous blue shift effects near the inner horizon, leads to the formation of a scalar curvature singularity along the contracting Cauchy horizon. This singularity is characterized by an exponential di-

vergence of the mass function of the hole. This led Poisson and Israel [13], who first discussed this effect, to speak of a "mass inflation" singularity.

The effects of the cross-flow are probably most easily seen in a simple model due to Amos Ori [14] which treats the outflow as a thin shell of null dust. Solving Einstein's equations then reduces to the matching of two Vaidya type spacetimes along the shell. As announced, one finds the mass function diverging behind the shell as one approaches the Cauchy horizon.

The singularity, although much stronger than the original whimper singularity, is still weak in the sense that there are coordinate systems in which the metric tensor stays finite. This means that tidal distortions are small even though tidal forces diverge. This observation will be crucial when constructing approximate solutions for more realistic settings discussed in the next chapter.

Generalizing the Ori model to Kerr type solutions is difficult and so far has only been done for the slow rotation limit [15]. But how could non spherical degrees of freedom affect the mass inflation scenario? This is the main question answered in this thesis. To get an idea of what to expect, a simple model is presented which is based on work by P.R. Brady, W. Israel, S.M. Morsink and myself.

The crucial observation is that the inner horizon has a finite radius. The spatial curvature of the inner horizon therefore is negligible compared to the curvature contribution from the singularity. This allows us to approximate the spacetime near the inner horizon by plane wave spacetimes which simplifies Einstein's equations sufficiently to study the effects of shear. Being away from spherical symmetry also means that the gravitational field acquires dynamical degrees of freedom. Indeed we now don't have to model the effects of gravitational radiation by a scalar field but can just consider the self gravitating case. Imposing the right boundary conditions (the Price tail) on the shear we again recover the old mass inflation scenario, with the shear decaying as a power of advanced time, similar to the Price tail outside the black hole (which in fact was used to model the shear).

This model seems to indicate that mass inflation is a generic feature of Cauchy horizons and not only an artifact of spherical symmetry.

However all these models have shortcomings that might render them invalid. The crucial assumption is that an initial piece of the inner horizon exists. But a strong enough outflux could lead to a total contraction of spacetime into a spacelike singularity before a Cauchy horizon could form [16, 17, 18, 19, 20]. This issue needs careful

examination which deserves its own chapter.

Initial conditions for mass inflation

Chapter 4 is concerned with two things: How do perturbations evolve once they have entered a black hole and what is their effect on the inner layers? We specifically address the issue mentioned at the end of the last section, namely the possible complete destruction of the inner horizon versus the survival of an initially regular stretch of this horizon. The work in this chapter is based on work done in collaboration with A. Bonanno, S.M. Morsink and W. Israel [21].

The peculiar causal structure of the black hole interior makes this problem tractable. Descent into a black hole always means progress in time. We therefore do not need to know the (quantum) physics of the high curvature region deep inside the core of the black hole to calculate the evolution of fields through the outer layers.

Furthermore, the Price analysis gives exact initial conditions on the horizon of the hole. With this in mind we can describe the evolution of infalling perturbations, again modeled by scalar fields, as they fall towards the center of the black hole. Specifically, we do not prejudge the issue by postulating pre-existence of any segment of the inner horizon.

The gravitational barrier which is responsible for scattering part of the infalling radiation is concentrated around a fixed radius far above a potential inner horizon. This implies that the catastrophic blue shift has not yet occurred and we can safely neglect the backreaction of the infalling scalar field on the geometry. The problem then reduces to a two dimensional scattering problem on a fixed Reissner-Nordström background. One finds that the scattering does not change the qualitative features of the infalling radiation. We end up with two cross-flowing power law tails as was used in the previous analyses. But soon after the scattering region has been passed we can no longer neglect the backreaction and have to find an at least approximate solution to the full Einstein-scalar field system. For the boundary conditions obtained from the scattering analysis this is actually not too difficult to achieve. The reason for this is the fact that, as mentioned before, the metric tensor stays finite (but not its derivatives) in a suitably chosen coordinate system. Again the familiar mass inflation singularity is recovered. A careful examination of the solution now shows that this singularity gets weaker as we go back in time: The assumptions made before about

the existence of an initially regular stretch of the inner horizon are justified.

Double null dynamics for Einstein gravity

In Chapter 5 a formalism is developed which will allow us to generalize the mass inflation scenario in a concise way to include all the degrees of freedom of the gravitational field.

Our formalism is based on a foliation of spacetime into two families of lightlike surfaces, as opposed to the more traditional $3+1$ splitting of ADM. The dynamics of the spacetime is then described by the evolution of two-dimensional spacelike surfaces. This setting naturally offers itself for the description of our problem, the effects of two cross-flowing streams of radiation on the Cauchy horizon.

Of course, $2+2$ splitting of spacetime is nothing new. The novelty of our formalism is the preservation of two dimensional covariance of geometrical objects like curvatures etc.. This allows one to write Einstein's equations for a completely general spacetime in a clear and compact way. Furthermore most objects defined in this formalism possess a direct geometrical meaning. It is these features that make it possible to analyze complex problems like the structure of the inner horizon in all their generality. This will be demonstrated in the next chapter. This chapter originates from a joint publication together with P.R. Brady, W. Israel and S.M. Morsink [22].

Generic structure of the Cauchy horizon

In this last major chapter of my thesis we finally investigate the structure of the inner horizon without imposing any simplifying restrictions. We are not looking for an exact solution to specific initial data but rather trying to find the behaviour of the inner horizon for a large class of initial conditions representing various physically allowed initial states resulting from an arbitrary stellar collapse.

To get used to the $2+2$ formalism we redo the plane wave analysis presented in Chapter 3. Having gained some familiarity with this new formalism we are now ready to pursue the general case, i.e. allow all the physical degrees of freedom of the gravitational field to propagate.

We first discuss the gauge and initial conditions before solving Einstein's equations.

Clearly we cannot expect to find an analytic solution in closed form for such an arbitrary setting. But we are only interested in the dominant terms of the metric and not in the fine details, which would depend on the exact form of the initial data. It will turn out that to lowest order in curvature we nearly recover the spherical picture, with the one exception being the presence of shear. This is of course expected, as the shear describes the gravitational perturbations propagating into the black hole and then causing the inner horizon to become singular.

Even to lowest order the equations governing the shear are nonlinear and thus are extremely difficult to solve. However we will present an argument, based on the solution of the linearized equations showing that the shear stays bounded and does not alter the spherical picture qualitatively. This view is supported by a numerical computation of the graavitational field near the Cauchy horizon.

To this extent the conclusion is that the mass inflation singularity is a generic occurrence inside any realistic black hole.

The work in this chapter represents mostly my own views on the subject, though strongly influenced by discussions with P.R. Brady, W. Israel and S.M. Morsink. The numerical work was independently peformed by myself.

Credits

Most of the results presented in this thesis are based on work done in collaboration with P.R. Brady, W. Israel and S.M. Morsink. My warmest thanks to them for the enjoyable collaboration. The only exception (apart from the obvious ones in chapter 2) is the numerical work on the scattering of infalling perturbations presented in Chapter 3 which I did on my own.

Chapter 2

Review of basic black hole physics

2.1 The Schwarzschild solution

Shortly after Einstein's publication of his general theory of relativity Karl Schwarzschild[1] solved the field equations for a spherically symmetric mass distribution [8], and calculated the perihelion shift of Mercury, which Einstein had calculated before in a post-Newtonian approximation to his field equations. Einstein was quite delighted about this result:

> "... Imagine my joy at the feasibility of general covariance and the result that the equations give the perihelion motion of Mercury correctly. For a few days I was beside myself with joyous excitement."
> Albert Einstein to Paul Ehrenfest, January 17, 1916

However it took quite a few years to fully understand and anticipate the physical content and implications this solution.

The metric Schwarzschild found as a solution of the vacuum field equations is given by

$$ds^2 = -f(r)dt^2 + \frac{1}{f(r)}dr^2 + r^2 d\Omega^2, \tag{2.1}$$

where

$$f(r) = \left(1 - \frac{2m}{r}\right) \qquad \text{and} \qquad d\Omega^2 = d\theta^2 + \sin^2(\theta)\, d\varphi^2.$$

[1] Schwarzschild found his solution under quite extraordinary conditions. In 1915 he was assigned to the Eastern front, where he soon fell seriously ill. While in hospital he solved Einstein's equations for the solution which today bears his name. Shortly after he died.

The parameter m is the mass of the system, as measured far away (Note, that the metric becomes flat for $r \to \infty$). The metric (2.1) possesses a coordinate singularity at the *gravitational* or *Schwarzschild radius* $r_G = 2m$ and a physical singularity at $r = 0$. Indeed, inspecting a curvature invariant such as

$$R_{\alpha\beta\gamma\delta}R^{\alpha\beta\gamma\delta} = \frac{48m^2}{r^6}$$

shows nothing wrong at r_G, but a divergence at $r = 0$. To understand what is happening at the gravitational radius we have to introduce coordinates which are regular there. One particular set that achieves this goal are *Kruskal* coordinates [23]. To transform to these new coordinates, first introduce the *tortoise* coordinate

$$r^* = \int \frac{dr}{f(r)} = r + 2m \log\left|\frac{r}{2m} - 1\right|. \tag{2.2}$$

We can then rewrite the line element (2.1) as

$$ds^2 = f(r)\underbrace{(dr^* - dt)}_{=:-du}\underbrace{(dr^* + dt)}_{=:dv} + r^2 d\Omega^2. \tag{2.3}$$

Unfortunately the metric in these coordinates is still not regular at r_G. But we are now in a position to introduce the Kruskal coordinates

$$\begin{aligned} U = &\quad -e^{-\kappa_0 u} \\ \text{and} \qquad V = &\quad e^{\kappa_0 v}. \end{aligned} \tag{2.4}$$

Here κ_0 is a parameter, that will be determined by requiring the metric to be regular at the gravitational radius. Note that the Kruskal coordinates can be defined for an arbitrary function $f(r)$ as long as r^* is a monotonic function of r. Inserting the definition (2.4) into the metric (2.3) and requiring regularity at $r = r_G$ yields for the Schwarzschild case $\kappa_0 = 1/(4m)$ and transforms (2.3) to

$$ds^2 = -\frac{32m^3}{r}e^{-\frac{r}{2m}}dUdV + r^2 d\Omega^2, \tag{2.5}$$

which is perfectly regular at the Schwarzschild radius.

The quantity κ_0 is called the *surface gravity* of the horizon and plays a rather important role in various aspects of black hole physics (For more details see reference [5], pages 331f).

The new coordinates U and V are originally only defined in the interval $]-\infty, 0]$ and $[0, \infty[$ respectively. But there is nothing that should prevent us from extending

U and V to the whole real axis. This leads us to the *maximal extension* of the Schwarzschild spacetime. This means that the manifold covered by the coordinates U and V is geodesically complete, i.e. every geodesic is regular for all values of its affine parameter, unless it runs into the $r = 0$ singularity.

What is more important, is that the opening angle of a light cone is always $90°$, and they always point straight up (see Fig. 1) as in Minkowski space.

From figure 1 it is obvious that once behind the gravitational radius there is no escape for timelike world-lines to larger r and one has to end up in the final $r = 0$ singularity. Thus one is justified in calling the spacetime a black hole spacetime and the surface $r = 2m$ the *horizon*.

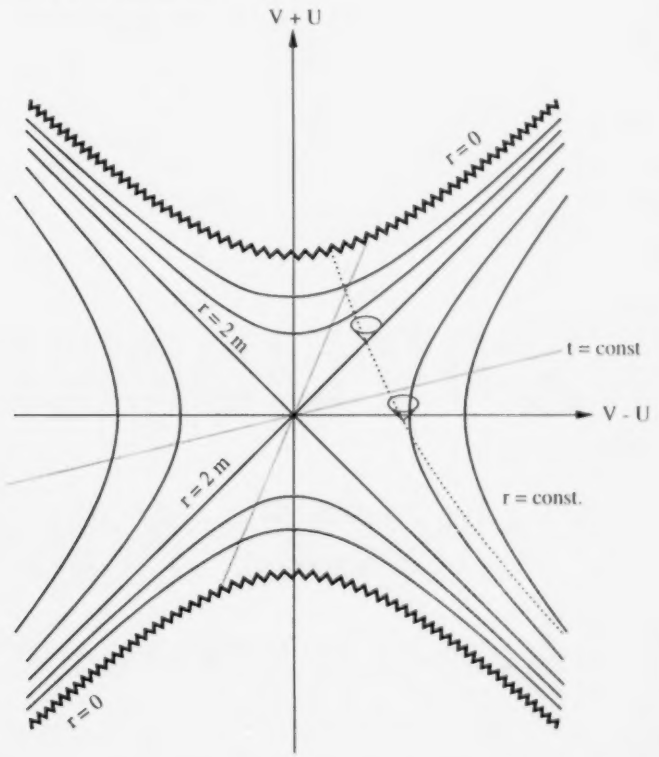

Figure 1: The maximally extended Schwarzschild manifold, plotted in terms of $V - U$ and $V + U$, with the radial coordinates suppressed. The grey lines are $t = const.$ hypersurfaces; $r = const.$ surfaces correspond to hyperbolas. The dotted line is a timelike geodesic, e.g the surface of a collapsing star. In the latter case everything to the left of this line is replaced a by different geometry representing the star's interior.

This becomes even more obvious when looking at the so-called *Penrose* or *conformal diagram*. These diagrams are an indispensable tool for examining the global properties of a spacetime manifold. To construct the Penrose diagram for the Schwarzschild spacetime we first introduce (once again) a set of new coordinates given by

$$V =: \tan(\tilde{V}) \qquad \text{and} \qquad U =: \tan(\tilde{U}). \tag{2.6}$$

Obviously $\tilde{V}$ and $\tilde{U}$ take values in $(-\pi/2, \pi/2)$. The Kruskal metric (2.5) then reads

$$ds^2 = -\frac{e^{-\frac{r}{2m}}}{r}\frac{32m^3}{\cos^2(\tilde{U})\cos^2(\tilde{V})}d\tilde{V}d\tilde{U} + r^2 d\Omega^2. \tag{2.7}$$

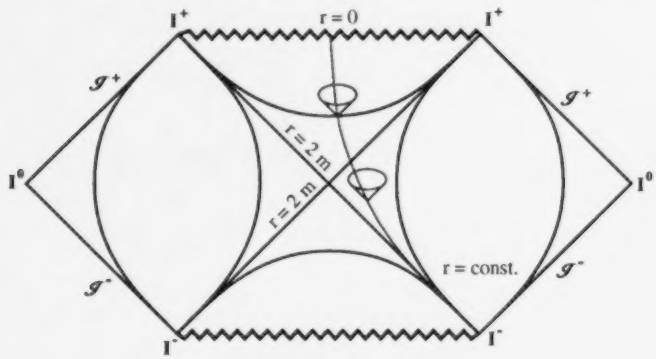

Figure 2: Penrose diagram of the Schwarzschild manifold. The dotted line is the same timelike geodesic as in Figure 1. Note that the "points" I^+ etc. are not part of the physical manifold.

Note that the transformation (2.6) preserves the form of the light cones. The compact support of the new coordinates allows us now to "zoom in" the infinitely far away boundaries of the manifold. Technically this is achieved by performing a conformal transformation to get rid of the reciprocal cosine terms. The conformal manifold then is compact, but possesses the same causal structure as the original manifold. (This is because conformal transformations do not alter the structure of the light cones.)

The different "boundaries" of the manifold are designated by the symbols:

I^+: future timelike infinity, $\mathcal{J}^+$: future lightlike infinity,
I^0: spacelike infinity,
$\mathcal{J}^-$: past lightlike infinity and I^-: past timelike infinity.

Note, that these are not part of the physical manifold. This is easily forgotten and can cause some confusion. For example the diagram in figure 2 might suggest that

the $r = 0$ singularity touches the horizon at $r = 2m$. This is, of course, nonsense, and reflects the fact that I^+ is not an actual point (or rather 2-sphere) of the spacetime. For a more detailed review of conformal diagrams see [6] and the literature cited therein.

2.2 Formation of black holes

From the discovery of the Schwarzschild metric in 1916 to the general acceptance of the idea of black holes quite some time passed. In fact the term "black hole" was only coined on December 29th 1967 by J.A. Wheeler[2].

In 1931 Chandrasekhar [25] showed that white dwarfs with masses $M > 1.4M_\odot$ are unstable and thus have to collapse. (An idea that was vehemently disputed by Eddington who did not believe that a star could exhibit such "absurd" behaviour.)

Finally, in 1939 Oppenheimer and Snyder in their classic paper [9] investigated for the first time a simple model of a collapsing star. Even today their work is still one of the most complete analyses available. Oppenheimer and Snyder considered a spherical star of initial radius R_0 whose pressure suddenly drops to zero, and thus initiates a gravitational collapse. The Birkhoff theorem [26] guarantees that the outside of the collapsing star is a patch of the Schwarzschild manifold. There is no unique solution for the interior of the star, which is dependent on the equation of state of the star's matter. A particular solution, for example, is a collapsing Friedmann spacetime, which corresponds to a homogeneous star with zero pressure.

The main features of the collapse are easily seen by realizing that due to the absence of pressure the surface of the star falls along radial geodesics of the exterior geometry. The equations of motion for a free falling particle are most easily derived from the Lagrangian

$$\mathcal{L} = \dot{x}_\mu \dot{x}^\mu = -f(r)\dot{t}^2 + \frac{\dot{r}^2}{f(r)} \equiv -1. \tag{2.8}$$

Here the $\dot{}$ denotes differentiation with respect to the proper time τ of the particle. The Killing vector ∂_t (t is a cyclic coordinate) gives rise to a conserved quantity

$$E := \frac{\partial \mathcal{L}}{\partial \dot{t}} = f(r)\dot{t}. \tag{2.9}$$

[2]In the era before, terms like "frozen star" or "collapsed star" were used to describe what today is called a black hole. For an excellent review of the history of black holes see [24].

Because $f(r) \to 1$ for $r \to \infty$ E is the particle's energy per unit rest-mass at infinity. Inserting equation (2.9) into the Lagrangian (2.8) gives

$$\dot{r}^2 = E^2 - f(r). \tag{2.10}$$

The analytic solution of this equation is easily found but not particularly interesting. The key observation is that the star's surface reaches zero radius and thus the singularity in a finite proper time, as measured by a clock on the star:

$$\tau = \int_0^{R_0} \frac{dr}{\sqrt{E^2 - f(r)}} = \frac{\pi}{2} R_0 \left(\frac{R_0}{2m}\right)^{\frac{1}{2}}. \tag{2.11}$$

For a star of solar mass-density, slightly heavier than the Chandrasekhar limit this time is about half an hour. It is important to note that equation (2.10) is regular at the Schwarzschild radius r_G. Nothing particularly interesting happens there. In fact for a massive enough star the tidal forces experienced there are perfectly tolerable.

The structure of a gravitational collapse to a black hole is best seen in Eddington-Finkelstein coordinates. The ingoing Eddington-Finkelstein coordinate is defined by $v := t + r^*$, which we already encountered in equation (2.3). The metric (2.1) then takes the form

$$ds^2 = -f(r)dv^2 + 2drdv + r^2 d\Omega^2. \tag{2.12}$$

Ingoing light rays travel along lines $v = const.$, whereas outgoing lightlike geodesics are given by $f(r)dv = 2dr$. It is more convenient to draw the spacetime diagram in terms of the coordinates r and $\tilde{t} := v - r$ rather than r and v. Infalling light rays then correspond to 45° lines as in Minkowski space. Note that, for large r, the coordinate $\tilde{t}$ becomes the proper time: $\tilde{t} \approx t$.

From figure 3 we can easily deduce the qualitative features of the collapse. A distant observer will see the surface of the star slowing down more and more (outgoing light rays are bent up) until it finally freezes as it approaches the horizon. However a clock ticking on the surface of the star will not stop, but of course just tick along while it passes the horizon. Furthermore the light that is emitted from the dying star becomes more and more red shifted. The redshift is given by

$$\begin{aligned} z = \sqrt{\frac{g_{tt}(\infty)}{g_{tt}(r)} - 1} \;&\sim\; e^{\frac{t}{4m}} \longrightarrow \infty \quad (t \longrightarrow \infty) \\ &=\; e^{\left(t \frac{m_\odot}{m} 5 \cdot 10^4 / sec\right)}. \end{aligned}$$

A far away observer sees an exponentially diverging red shift and the star disappears from sight within a fraction of a second.

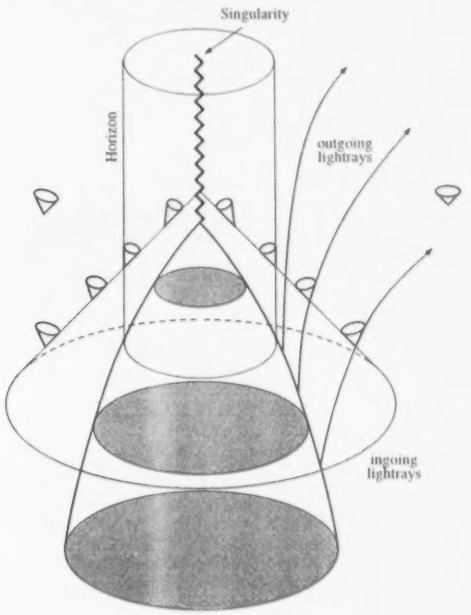

Figure 3: Gravitational collapse in Eddington-Finkelstein coordinates.

But how realistic is this simple model? Clearly one can neither neglect pressures nor asphericities. Adding either of the two ingredients makes the problem nearly intractable. The equations, that govern a realistic stellar collapse are only manageable by complicated computer codes. But we should not forget that a star above the Chandrasekhar limit *must* collapse. Imagine now a neutron star, close to that limit, accompanied by a gaseous companion. The neutron star will then gain mass until it passes over the stability limit. The star then must collapse, regardless of its internal pressures. It is also conceivable that a little rotation cannot change the scenario drastically. An analysis by Richard Price of general perturbations on a Schwarzschild background [10] shows that there are no static perturbations, and furthermore that all perturbations have to die out at late times. The black hole radiates its hair away until it is bald.

Thus it seems conceivable that black holes are really formed in Nature, and that the Oppenheimer-Snyder scenario at least catches the qualitative features of such an event.

In fact data recently obtained by the Hubble Space Telescope almost unambiguously implies the existence of large black holes in galactic nuclei [27].

2.3 Black hole uniqueness and Price's theorem

One of the most remarkable facts about black holes is their uniqueness, or as J.A. Wheeler phrased it, the fact that "Black holes have no hair". The no-hair theorem essentially states:

> Any stationary asymptotically flat, electromagnetic vacuum black hole solution of the Einstein-Maxwell system[3] is given by the Kerr–Newman solution, i.e. is fully described by the three parameters mass, angular momentum and electrical charge.

A proof and more exact formulation is given for example in [28].

The physical reason for this remarkable theorem lies in what is referred to as Price's theorem [10], which essentially states

> Everything that can be radiated away in a gravitational collapse must be radiated away.

Thus any field coupling to a collapsing star must radiate away all its dynamical degrees of freedom and only conserved quantities (hair) remain: The electric charge of the Maxwell field and the mass and angular momentum of the gravitational field. These quantities are exactly the free parameters in the Kerr-Newman metric described below.

As this radiation moves away from the collapsing star (see Figure 4) it eventually encounters a gravitational potential barrier. Part of the radiation will then be backscattered and fall into the black hole, while the remaining part will penetrate the barrier and flow towards $\mathcal{J}^+$.

Detailed calculations and numerical simulations [10, 29] show that at late times this radiation dies out in the form of radiative power-law tails. The l'th multipole moment streaming to $\mathcal{J}^+$ behaves for fixed v like

$$\psi_l(u) \sim u^{-2l-2}$$

[3]Things get much more complicated when looking at nonlinear or non-Abelian matter fields. These fields have been shown to violate the suitably generalized no hair hypothesis [30].

and similarly the back-scattered tail behaves for fixed u as

$$\psi_l(v) \sim v^{-2l-2}$$

where u and v are the standard external retarded and advanced time coordinates.

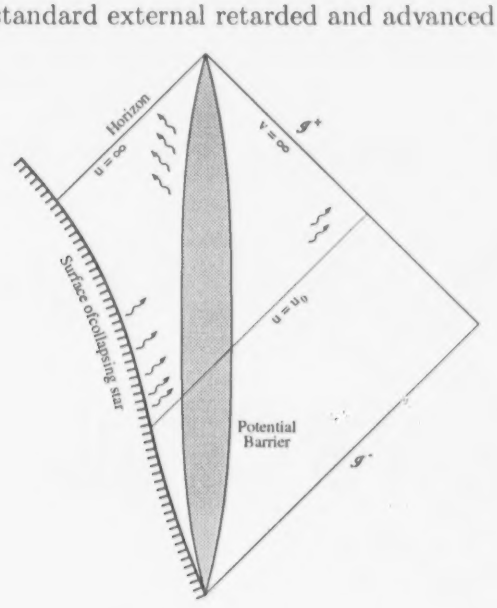

Figure 4: The exterior structure of a collapsing spacetime. The grey area is the potential barrier which back-scatters out-flowing perturbations from the star. The star starts to collapse after $u = u_0$, and the spacetime therefore is static (or at least stationary) before u_0.

These tails play an important part in the dynamics of the black hole interior as will be shown later.

2.4 The Kerr-Newman solution

So far we have only briefly touched on the effects of rotation and the presence of electrical fields on black holes. In the last section we have argued that adding angular momentum should not drastically alter the dynamics of a stellar collapse. However the slightest amount of electric charge or angular momentum changes the global structure of the Schwarzschild solution drastically, and these changes have to be taken seriously. After all most stars rotate.

The most general asymptotically flat and stationary electromagnetic vacuum solution of the Einstein-Maxwell system with a regular event horizon is the *Kerr-Newman* metric [31] given by

$$ds^2 = -\frac{\Delta}{\rho^2}\left(dt - a\sin^2\theta d\phi\right)^2 + \frac{\sin^2\theta}{\rho^2}\left((r^2+a^2)d\phi - adt\right)^2 + \frac{\rho^2}{\Delta}dr^2 + \rho^2 d\theta^2, \quad (2.13)$$

where $\Delta = r^2 - 2mr + a^2 + e^2$ and $\rho^2 = r^2 + a^2\cos^2\theta$. By expanding the metric (2.13) for large r we see that m is the mass, a the angular momentum per mass and e the electric charge of the black hole. The following limiting cases are distinguished as

	$e = 0$	the Kerr solution [32],
	$a = 0$	the Reissner-Nordström solution,
	$e = a = 0$	the Schwarzschild solution
and	$m^2 = e^2 + a^2$	an extremal black hole.

The causal structure is quite different from the simple Schwarzschild case. For $m^2 > a^2 + e^2$ the spacetime possesses two horizons, corresponding to the two solutions of $\Delta(r_\pm) = 0$. The first horizon at $r = r_+$ again is an event horizon. The inner horizon, located at $r = r_-$ is a so-called *Cauchy* horizon, a surface behind which one has a direct view onto the central singularity. Thus strong cosmic censorship is violated and the Cauchy problem is ill-defined behind this surface. Furthermore the Cauchy horizon is the entrance to a tunnel to a new universe, a fact particularly emphasized by many science-fiction writers. To study the properties of this spacetime in a little more detail we restrict our focus to the simpler Reissner-Nordstöm case. For a more detailed discussion of the full Kerr-Newman spacetime see for example reference [7], chapter 7 or [33].

For $a = 0$ the Kerr-Newman metric again takes the form (2.1)

$$ds^2 = -f(r)dt^2 + \frac{1}{f(r)}dr^2 + r^2 d\Omega^2, \quad (2.14)$$

but now

$$f(r) = \left(1 - \frac{2m}{r} + \frac{e^2}{r^2}\right). \quad (2.15)$$

This geometry still possesses two horizons, corresponding to the zeros $r_\pm$ of $f(r)$. The different coordinate systems discussed in Section 2.1 can easily be generalizd to the Reissner-Nordström spacetime. Again the apparent singularities at the horizons $r_\pm$ in (2.14) are unphysical while at $r = 0$ there is a true (timelike) curvature singularity.

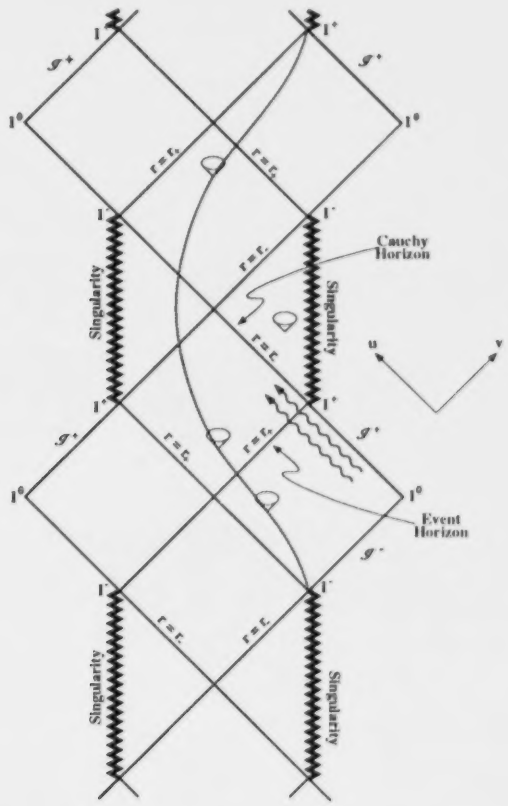

Figure 5: The Reissner-Nordström spacetime. The dotted line again is a timelike geodesic, which could be the surface of a collapsing star in an Oppenheimer-Snyder type of collapse. Unlike before, the star re-emerges from a white hole. The wiggly arrows represent infalling radiation (travelling along $v = const.$ lines), which is present in every collapse. This radiation causes an instability of the Cauchy horizon.

Furthermore, timelike geodesics don't hit the singularity, but have a turning point after which they start to expand again to emerge through a "white hole" into a new universe (see Fig. 5). The geodesic equation for a radially infalling particle becomes $\dot{r}^2 = E^2 - f(r)$, and thus $\dot{r} = 0$ at $r_{\min} = (\sqrt{m^2 - (E^2-1)e^2} - m)/(E^2-1)$. The maximal extension of the Reissner-Nordström spacetime is a grid of such black hole-white hole pairs patched together. It is important to note that the Reissner-Nordström solution has a similar causal structure as the more realistic Kerr solution. This justifies investigating this much easier spacetime, instead of the rather complicated Kerr

spacetime.

So far, no one has ever seen a "white hole" spontanously exploding into a star and it thus seems unlikely that a real black hole possesses such a structure.

In fact it is quite easy to see and was already noted more than 25 years ago by Roger Penrose [2] that the Cauchy horizon is unstable. Consider some radiation — which is always present — falling into the black hole at late times. This could, for example, be some gravitational radiation, left over from the collapse, or some electromagnetic waves etc.. Looking at Figure 5 it is evident, that this radiation gets enormously blue shifted at the Cauchy horizon. An observer passing through that region of the spacetime gets hit by an enormously amplified flash of radiation. For a pure inflow which was first considered by William Hiscock [12] the stress tensor is of the form $T_{\mu\nu} = (L(v)/(4\pi r^2))\partial_\mu v \partial_\nu v$.

The spacetime is described by the *Vaidya* metric

$$ds^2 = 2dr dv - f(r,v)dv^2 + r^2 d\Omega^2,$$

where $f(r,v) = 1 - 2m(v)/r + e^2/r^2$. Einstein's equations in this case reduce to the simple equation $L(v) = \dot{m}$. In view of Price's work [10], $L(v) \propto v^{-p}$ where $p \geq 12$. A radially infalling observer with an energy E measures an energy flux given by

$$u^\mu u^\nu T_{\mu\nu} = \frac{\dot{m}}{4\pi r^2}\left(\frac{\partial v}{\partial \tau}\right)^2.$$

Now $\partial v/\partial\tau = \partial v/\partial r \cdot \partial r/\partial\tau$. But as the Cauchy horizon is reached in a finite proper time and lies at a finite radius r_- the term $\partial r/\partial\tau$ stays finite. On the other hand for an observer with energy $E > 0$ we find

$$\frac{\partial v}{\partial r} = \frac{1}{f}\left(1 + \sqrt{1 + fE}\right)$$

and thus $v \sim r^* + O(1/v)$, where $r^* = \int dr/f(r)|_{v=\infty}$ is the familiar tortoise coordinate. Note that for large v the function f hardly differs from the corresponding function for the Reissner Nordström case. Thus $v \sim -\log(r - r_-)$ and $f \sim -\kappa_-(r - r_-)/2$ where κ_- is the surface gravity of the inner horizon. Putting all this together we find for the energy flux

$$u^\mu u^\nu T_{\mu\nu} \sim \left(\log(r - r_-)^p (r - r_-)^2\right)^{-1} \to \infty \quad \text{as} \quad r \to r_-$$

which is diverging.

However all the curvature invariants stay finite as the Cauchy horizon is approached. This type of behaviour is known as a *whimper* singularity, and is expected to be generically unstable [2, 3, 34, 35].

It is the goal of this thesis to examine and describe the structure of the inner horizon instablity in detail for a generic collapse.

Chapter 3

Simple models of mass inflation

We have seen in the last chapter that generic black holes possess an inner horizon, which seems to open a gateway to unknown lands, where one faces such bizarre things as naked singularities and new universes.

However those spacetimes are not stable under perturbations. Neglecting perturbations is permissible for the exterior of the black hole. Once a black hole has formed, Price's theorem suggests that these perturbations have to die off with time. Ultimately, the spacetime has to settle down to the Kerr-Newman solution.

On the other hand, we expect that generic perturbations falling into the hole cause more dramatic effects inside the black hole due to the large blue shift they experience as they approach the inner horizon. But it is not a priori clear what type of singularity will form.

It is generally believed that the final $r = 0$ singularity is of an oscillatory BKL [36] or Mixmaster type. But it is not obvious that infalling perturbations should completely destroy the Cauchy horizon. In fact, general considerations [35] as well as specific models suggest that this is not the case. The first to consider a more realistic setting were Eric Poisson and Werner Israel in their 1989 paper [13]. They showed, that once one looks at the full nonlinear equations for cross-flowing radiation a true scalar curvature singularity develops at the inner horizon. This singularity, which is characterized by an exponential blow up of the mass function m of the hole (and hence is called a mass inflation singularity) is lightlike.

In this chapter we would like to present some simple models of the mass inflation scenario to set the framework for the remaining parts of this thesis.

3.1 The Ori model

We have seen that pure infalling radiation causes a whimper singularity to form at the Cauchy horizon. This singularity is unstable, and the slightest outflowing perturbation crossing the Cauchy horizon (see Figure 6) will cause the formation of a true curvature singularity (The term "outflowing" is somewhat a misnomer as radiation in the interior of the hole is always flowing to smaller radii. However we will continue using this terminology for the lack of a better one.) This outflowing radiation has various sources. The collapsing star will still emit radiation after it crossed the event horizon. We expect this radiation to be weak towards the past end of the Cauchy horizon, in order not to get singularities along the event horizon. Another much stronger source near the past end is infalling radiation which gets scattered at the inner gravitational potential barrier. These sources will be discussed in more detail in the next chapter.

The full cross-flow problem was solved by Poisson and Israel [37]. They assumed a stress tensor of the form

$$T_{\mu\nu} = \frac{1}{4\pi r^2}\left(L_{\rm out} n_\nu n_\mu + L_{\rm in} l_\nu l_\mu\right), \tag{3.1}$$

where $l_\mu = -\partial_\mu v$ and $n_\mu = -\partial_\mu u$ are in- and outgoing null vectors and for the interior we have redefined the coordinate u as $u = r^* - t$, so that u increases towards the future. The conservation equations $T^\mu_{\nu;\mu} = 0$ then demand that $L_{\rm out}$ and $L_{\rm in}$ are functions only of u and v respectively. Even though no closed form solution is known for this particular stress tensor, Poisson and Israel [37] were able to show that the resulting spacetime possesses a curvature singularity at the Cauchy horizon.

We will not repeat this analysis, but instead present a simpler model due to Amos Ori [14] that still catches the essential results.

The form of the outflow is not of particular importance [37], as long as it is not too strong to cause an immediate collapse of the Cauchy horizon. (We will discuss this issue in greater detail in the next chapter.) We thus model the outflux by a thin shell Σ of outflowing null matter. The outflowing matter is described by a stress tensor of the form (3.1) with $L_{\rm out} = \delta(u - u_0)$.

The shell splits the spacetime into two parts $\oplus$ and $\ominus$ each described by a Vaidya metric (See fig. 6)

$$ds^2 = -f_\pm dv_\pm^2 + 2dv_\pm dr + r^2 d\Omega^2.$$

The coordinates $v_\pm$ denote the standard advanced time coordinates in their respective regions. Note that the radial coordinate r is continuous across the shell because of its geometrical significance as the proper radius of the two-spheres with metric $r^2 d\Omega^2$.

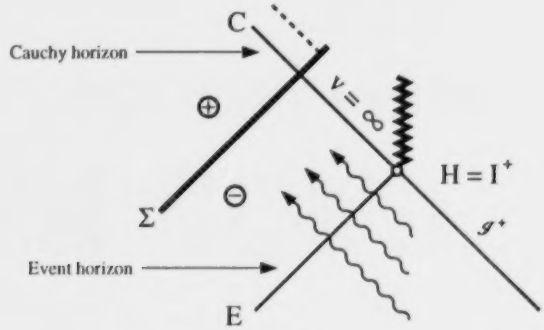

Figure 6: The contraction of the inner horizon caused by "outfalling" radiation, here modeled by a thin shell Σ, allows the infalling blue shifted radiation to create a curvature singularity at the portion of the Cauchy horizon in $\oplus$ behind the shell. The dashed line is the inner apparent horizon behind the shell.

The stress tensor now becomes $T^{\pm}_{\mu\nu} = L_\pm l_\mu l_\nu$ in the respective regions. Therefore Einstein's equations in the two regions reduce to

$$\frac{dm_\pm}{dv_\pm} = L_\pm(v_\pm). \tag{3.2}$$

The influx in the $\ominus$-region is nothing but the Price tail discussed in the last section. Thus we readily find $m_- = m_0 - av^{-p+1}$, for $p = 4l + 4$.

The behaviour in the $\oplus$-region behind the shell is then found by matching the two metrics along Σ. First define the vector n^α tangential to Σ, i.e. $n^\alpha n_\alpha = 0$ and $n^\alpha l_\alpha \neq 0$. We conveniently choose r as a parameter and thus find

$$n^\alpha = \frac{\partial x^\alpha}{\partial r} = \left(\frac{2}{f_\pm}, 1, 0, 0\right). \tag{3.3}$$

Continuity of the influx across the shell implies

$$\left(T^+_{\mu\nu} - T^-_{\mu\nu}\right) n^\mu n^\nu = 0 \implies \frac{L_+}{f_+^2} = \frac{L_-}{f_-^2}. \tag{3.4}$$

The relation between v_- and v_+ derives from the fact that Σ is null, i.e.

$$-f_\pm dv_\pm + 2dr = 0 \Longrightarrow f_+ dv_+ = f_- dv_-. \tag{3.5}$$

Combining equations (3.2-3.5) gives the key equation for the behaviour of m_+ along the shell Σ:

$$\frac{\partial m_+}{\partial v} = \frac{f_+}{f_-}\frac{\partial m_-}{\partial v}, \tag{3.6}$$

where we dropped the subscript $-$ from v_-. It is already clear from this equation that the function m_+ diverges at the Cauchy horizon. As $v \to \infty$ the function f_- approaches zero whereas f_+ stays nonzero, because the mass of the shell dislocates the inner apparent horizon behind Σ a bit ($r_- \to r_-(1 - \delta m/\sqrt{m^2 - e^2} + O(\delta m^2))$ where δm denotes the mass of the shell). Thus the combination f_+/f_- blows up to cause the singular behaviour of m_+.

Let us now solve equation (3.6) asymptotically. We first determine $r(v)$ along the shell from equation (3.5): $\dot{r} = 2/f_-(r, v)$. For large values of v we find

$$r = r_0 + \frac{a}{v^{p-1}\kappa_0 r_0}\left(1 + \frac{p-1}{v\kappa_0} + \frac{p(p-1)}{v^2\kappa_0^2} + \frac{(p+1)p(p-1)}{v^3\kappa_0^3} + \ldots\right) \tag{3.7}$$

where $r_0 = m_0 - \sqrt{m_0^2 - e^2}$ is the initial radius of the inner horizon and $\kappa_0 = -f_{,r}(r_0)/2$ its surface gravity.

Inserting this result into equation (3.6) finally gives an ordinary differential equation for m_+:

$$\frac{\partial m_+}{\partial v} = m_+\left(\kappa_0 - \frac{p}{v} + O\left(\frac{1}{v^2}\right)\right).$$

Integrating for m_+ gives

$$m_+(v) = m_i e^{\kappa_0 v} v^{-p}\left(1 + O\left(\frac{1}{v}\right)\right) \tag{3.8}$$

where m_i is an integration constant. Thus the mass function diverges behind the shell Σ as we approach the Cauchy horizon. This phenomenon has been dubbed *mass inflation*.

The mass inflation singularity, as opposed to a whimper singularity, is a true curvature singularity. The only nonvanishing Weyl curvature invariant in spherical symmetry is the Coulomb component

$$\Psi_2 = -\frac{1}{2}C^{\vartheta\varphi}{}_{\vartheta\varphi} = \frac{\left(\frac{e^2}{r} - m\right)}{r^3}$$

which now diverges exponentially because m does.

The singularity, which is much stronger than a whimper singularity, is still weak in the sense that there are coordinate systems in which the metric stays finite. In $\oplus$ we have

$$ds^2 = dv_+ (2dr - f_+ dv_+) + r^2 d\Omega^2 = \frac{2dv_+}{r}(rdr + m_+ dv_+) - \left(1 + \frac{e^2}{r^2}\right) dv_+^2 + r^2 d\Omega^2.$$

We now define a new coordinate

$$U := (r^2 - r_0^2) + 2\int_{v_0}^{v} dv_+ m_+(v) = (r^2 - r_0^2) + 2m_i \int_{v_0}^{v} dv v^{-p} \left(1 + O\left(\frac{1}{v}\right)\right)$$

which is regular at the Cauchy horizon. In terms of U and dv_+ the line element becomes

$$ds^2 = dv_+ \left(\frac{2}{r} dU - \left(1 + \frac{e^2}{r^2}\right) dv_+\right) + r^2 d\Omega^2$$

which is perfectly regular at the horizon. This means that even though tidal forces diverge, tidal distortions stay bounded. This leads to the speculation that one might survive a crash through the mass inflation singularity [38], but see also [39].

3.2 Plane mass inflation

The work by Poisson and Israel as well as the Ori model presented in the last section relied heavily on spherical symmetry. Furthermore, to get an inner horizon within the framework of spherical symmetry, we had to electrically charge the black hole. However stars generally are not electrically charged, and furthermore pair production processes might discharge the core before the Cauchy horizon forms [40]. On the technical side the presence of an electrostatic contribution unnecessarily complicates the analysis.

It is therefore desirable to have a model that circumvents the above obstacles to get a better understanding of the inner structure of a black hole.

The key observation, that leads to such a model is the fact that the inner horizon has a *finite* radius r_0. Thus the contribution to the total curvature from the two-spheres $r^2 d\Omega^2$ is of the order $1/r_0^2$, which is finite and therefore negligible if the curvature diverges due to gravitational effects. We thus can "flatten out" the two-spheres: to a nearby observer the Cauchy horizon seems flat.

Mathematically this amounts to approximating the spacetime locally by plane waves. A simple metric with these properties is

$$ds^2 = -2\frac{e^{2\sigma}}{r}dudv + r^2\left(e^{2\beta}dx^2 + e^{-2\beta}dy^2\right). \tag{3.9}$$

The quantities σ, r and β are for the moment functions of u and v only.

For a pure lightlike cross-flow the field equations $R_{\mu\nu} = 8\pi T_{\mu\nu}$ with a stress tensor of the form (3.1) become

$$(r^2)_{,uv} + 4r^2\left(\sigma_{,uv} + \beta_{,u}\beta_{,v}\right) = 0, \tag{3.10}$$

$$(r^2)_{,uv} = 0, \tag{3.11}$$

$$2\beta_{,uv} + \beta_{,u}(\log r^2)_{,v} + \beta_{,v}(\log r^2)_{,u} = 0, \tag{3.12}$$

$$2\sigma_{,v}(r^2)_{,v} - 2r^2\left(\beta_{,v}\right)^2 - (r^2)_{,vv} = L_{\text{in}}(v) \tag{3.13}$$

and

$$2\sigma_{,u}(r^2)_{,u} - 2r^2\left(\beta_{,u}\right)^2 - (r^2)_{,uu} = L_{\text{out}}(u). \tag{3.14}$$

The absence of an electrostatic contribution makes equation (3.11) for r^2 particularly simple:

$$r^2 = r_0^2 + f(v) + g(u).$$

The two functions f and g are pure gauge but can't normally be gauged to zero. For standard advanced time a comparison with the Ori model suggests $f(v) \sim v^{-p+1}$.

Let us now turn our attention to the shear β. First note that (3.12) for β is the same as the wave equation $\Box\beta = 0$.

The question is whether the presence of the shear β changes the spherical scenario drastically. If not, we have some reason to believe that mass inflation is a generic feature of Cauchy horizons. Let us now analyze the equation for β in more detail.

The simple form of r^2 allows us to introduce new coordinates $R := r^2$ and $\chi = f(v) - g(u)$. Equation (3.12) then becomes

$$\beta_{,RR} - \beta_{,\chi\chi} + \frac{\beta_{,R}}{R} = 0. \tag{3.15}$$

This equation can be solved in terms of Fourier Bessel transforms

$$\beta = \beta_0 + \int dk e^{ik\chi}\left(C(k)Y_0(|k|R) + D(k)J_0(|k|R)\right),$$

where $C(k)$ and $D(k)$ are functions determined by the boundary conditions. The function Y_0 diverges at the origin, but since the Cauchy horizon has a finite radius

there is no need to worry. But nevertheless it is difficult to extract the behaviour of β near the Cauchy horizon from the above solution.

We can write the general solution of (3.15) as a series

$$\beta = \beta_0 + \sum_{i\geq 0} A_i R^{-i} \left(F^{(-i)}(R+\chi) + G^{(-i)}(R-\chi) \right). \tag{3.16}$$

Here F and G are arbitrary functions, and the notation $F^{(-i)}$ means the i-th integral of F. One finds for coefficients $A_i = A_0 2^i (i!)^3/(2i)!$, which diverge as $i \to \infty$. Let us now choose the functions F and G to be of the form $F(x) = (x - x_0)^q$ for some q, and similarly for G (with possibly a different q, depending on the boundary data). Inserting this into (3.16) we find after a little algebra

$$A_i F^{(-i)}(x) =: B_i (x - x_0)^{i+q} = \frac{2^i (i!)^3}{(2i!)\Gamma(i+q+1)} (x - x_0)^{i+q}.$$

Even though the A_i's diverge, the B_i's decay faster than exponentially. Using the Stirling formula we get $B_i \sim (i+q+1)^{-i}$ for large i's. We conclude that in this case the series (3.16) is convergent.

The Ori analysis suggests $f(v) \sim v^{-p+1}$. The boundary conditions for β on a $u = const.$ surface is $\beta \sim v^{-p/2+1}$. Therefore q takes the value $q = (p-2)/(2p-2)$ and $x_0 = r_0^2$. For this choice of F the dominant contribution comes from the $i = 0$ term. As expected the shear β decays as a power law tail at late times along $u = const.$ geodesics.

Similarly we expect G to stay regular for regular boundary conditions. However the limit $u \to -\infty$ is problematic. If we already are on the Cauchy horizon, i.e. for $v = \infty$ we will stay on the Cauchy horizon forever. If we are at a finite value for v, we will eventually end up on the event horizon. Therefore the respective limits for u and v don't commute. This results from the fact, that $H = I^+$ in Figure 6 is *not* part of the spacetime (The event horizon does not touch the Cauchy horizon, see Figure 7 in the next Chapter). However we don't expect any problems for finite values of u.

Knowing β and r^2 we can now integrate equation (3.10) for

$$\sigma = a(u) + b(v) - \int du \int dv \beta_{,u} \beta_{,v}. \tag{3.17}$$

The two functions $a(u)$ and $b(v)$ are pure gauge. Because β and its derivatives decay like a power law in u and v we expect the integral in (3.17) to be finite. For a given choice of coordinates (standard retarded and advanced time in our case) the functions

a and b have to satisfy the constraint equations (3.14) and (3.13). Inserting σ into (3.13) gives

$$2\sigma_{,v} = \frac{L_{\rm in}(v)}{(r^2)_{,v}} + 2r^2\frac{(\beta_{,v})^2}{(r^2)_{,v}} + \left(\log((r^2)_{,v})\right)_{,v}.$$

As we have seen before $L(v)/(r^2)_{,v} \sim const$, and so is (by construction) $(\beta_{,v})^2/(r^2)_{,v}$. The last term decays as $1/v$ and can thus be neglected. Again we find $b(v)$ diverging as $-b_0 v$ for some positive b_0 ($(r^2)_{,v} < 0$). With β present this is even true for $L_{\rm in} \equiv 0$. This is not too surprising. The influx is supposed to model gravitational perturbations emerging from a collapse. As the gravitational field has no dynamics in spherical symmetry we had to put these in by hand in that case. Here it already arises in vacuo due to the shear. Analyzing the other constraint (3.14) gives $a(u) = a_0 u$. Therefore near the Cauchy horizon

$$\sigma = -(b_0 v + a_0 u) + O(\log(u), \log(v)).$$

The curvature is now more complicated than before. For the tetrad

$$\begin{aligned} l_\mu dx^\mu &= \frac{e^\sigma}{\sqrt{r}}dv, \\ n_\mu dx^\mu &= \frac{e^\sigma}{\sqrt{r}}du \\ \text{and} \qquad m_\mu dx^\mu &= \frac{r}{\sqrt{2}}\left(e^\beta dx + ie^{-\beta}dy\right) \end{aligned}$$

we find the following nonzero tetrad components of the Weyl curvature

$$\begin{aligned} \Psi_0 &= -C_{\alpha\beta\mu\nu}l^\alpha m^\beta l^\mu m^\nu = -re^{-2\sigma}\left(2\beta_{,u}\sigma_{,u} - r^{-3}(\beta_{,u}r^3)_{,u}\right), \\ \Psi_2 &= -C_{\alpha\beta\mu\nu}l^\alpha m^\beta \bar{m}^\mu n^\nu - \frac{re^{-2\sigma}}{6}\left(4\frac{\beta_{,u}\beta_{,v}}{r^2} - (2\sigma - 3\log(r))_{,uv}\right) \\ \text{and} \qquad \Psi_4 &= -C_{\alpha\beta\mu\nu}n^\alpha \bar{m}^\beta n^\mu \bar{m}^\nu = -re^{-2\sigma}\left(2\beta_{,v}\sigma_{,v} - r^{-3}(\beta_{,v}r^3)_{,v}\right). \end{aligned}$$

Therefore $R_{\mu\nu\rho\delta}R^{\mu\nu\rho\delta} \sim e^{-4\sigma}$ which diverges in the limit $v \to \infty$. The spacetime is now asymptotically of Petrov Type N, with n_μ being the (only) principal null direction, indicating the buildup of a gravitational shock wave traveling along the Cauchy horizon (See e.g. [41] for a definition of the Petrov types).

This rather simple model will turn out to capture all the essential features of a generic nonspherical Cauchy horizon singularity.

Chapter 4

Initial conditions for mass inflation

We have argued in the last chapter that small perturbations present in a stellar collapse cause the formation of a lightlike curvature singularity along the Cauchy horizon. This view has been challenged by other studies. Yurtsever [16] — based on the behaviour of plane wave spacetimes — argues that a spacelike singularity should develop before a Cauchy horizon can form. However his arguments are vague and not very conclusive with regard to just how the interior corresponds to a plane wave spacetime. Yurtsever's point of view finds support from two numerical simulations of a collapsing scalar field performed by Gnedin and Gnedin [17, 18]. This work clearly shows the formation of a spacelike $r = 0$ singularity as the endpoint of the collapse. But the simulation does not touch the region of interest to us, namely the very late time regime of the collapse (the "corner" H in figure 8). The existence of the Cauchy horizon is left in the dark despite the author's claims of its nonexistence.

Nevertheless the above possibilities have to be investigated before one can go on to discuss the structure of the inner horizon. The models presented in the last section avoided this question by simply assuming the existence of an initially regular piece of the Cauchy horizon. The Ori model as well as Poisson and Israel's continuous cross-flow scenario only switch the outflux on after a finite retarded time $u = u_0$, and the plane wave model just assumes the existence of the limit $r \to r_-$ (by choosing the appropriate boundary conditions for r^2).

For a spherical metric

$$ds^2 = g_{ab}dx^a dx^b + r^2 d\Omega^2$$

the behaviour of the Cauchy horizon is governed by Raychauduri's equation (derivable

from equation (A.10) in appendix A):

$$\frac{d^2r}{d\lambda^2} = -4\pi r T_{\mu\nu} l^\mu l^\nu \equiv -4\pi r T_{\lambda\lambda}, \tag{4.1}$$

$$l^\mu = \frac{\partial x^\mu}{\partial \lambda} = g^{\mu\nu}\partial_\nu V, \tag{4.2}$$

where λ is an affine parameter. Inspecting equation (4.1) shows that a solution with finite r for $\lambda \to \infty$ does not exist unless

$$\lim_{\lambda \to -\infty} \lambda^2 T_{\lambda\lambda} = 0. \tag{4.3}$$

Either a diverging $T_{\lambda\lambda}$ or g^{ab} could lead to a violation of this condition.

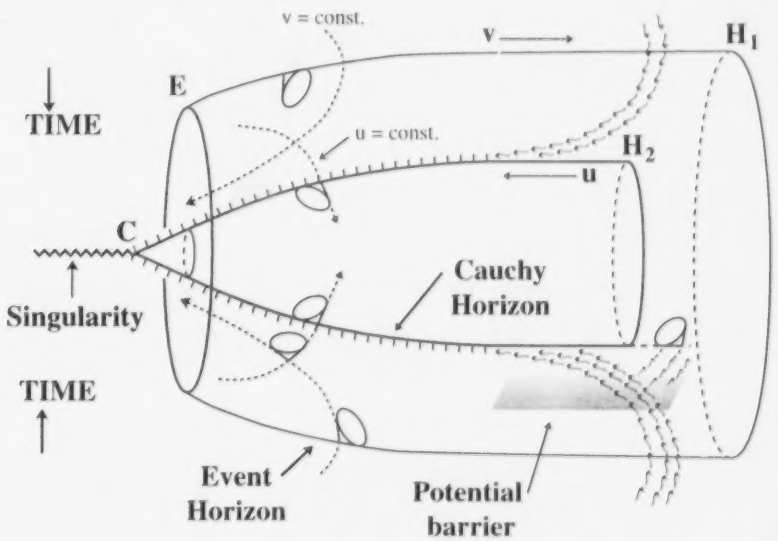

Figure 7: A spacetime diagram of the interior of a black hole with one angular coordinate suppressed. Infalling radiation traveling along $v = const.$ lines gets partly backscattered off the internal potential barrier. The transmitted radiation piles up along the inner horizon making it singular. The scattered radiation traveling along $u = const.$ lines leads to a slow contraction of the Cauchy horizon which initially is static (at H_2).

The analysis of this problem fortunately splits into two nearly independent parts. The important point to note is that descent into the black hole is always a progress in time. We can therefore start with what we know, the initial data on the surface

of the collapsing star and the event horizon. The latter is – thanks to the no hair property – exactly known. (Contrast this to the case of cosmology.) The structure of deeper layers is then determined by evolving these data in time, and does not depend on the unknown (quantum) physics of the Planckian curvature region in the core of the hole. For simplicity let us describe the matter again by a scalar field ϕ. The initial conditions on the event horizon are given by the Price tail $\phi \sim v^{-p}$ for some p. The evolution of ϕ is determined by the wave equation $\Box\phi = 0$. Infalling radiation will partly be scattered off the inner gravitational potential barrier into outflowing radiation. This barrier is concentrated at a radius far above the troublesome high blue shift region. This allows us to treat the scattering problem on a fixed Reissner-Nordström background without having to worry about the much more complicated back reaction problem.

Once the potential has been left behind the radiation again streams nearly freely. Only now will it experience the catastrophic blue shift that ultimately leads to the destruction of the Cauchy horizon. At this stage the field ϕ can be modeled as a stream of high energy particles described by the Isaacson [42] stress tensor. This allows us to finally get a handle on the back-reaction of the scalar field on the metric, which at this stage cannot be neglected anymore.

4.1 The scattering problem

Let us now analyze the scattering of the infalling perturbations in more detail. Our goal is to determine the strength of the radiation crossing the Cauchy horizon. There are two sources for this radiation, the matter emitted from the surface of the star and the back scattered parts of the infalling Price tail.

The first contribution is weak, in fact exponentially weak in terms of the retarded time u. To see this consider a pure out-flow of radiation along the event horizon, described by the Vaidya metric

$$ds^2 = -2drdu - f(r,u)du^2 + r^2 d\Omega^2,$$

where f is of the same form as in equation (2.15) but with the mass function now depending on u. This metric satisfies Einstein's equations for an energy momentum tensor of the form $T_{\mu\nu} = [L(u)/(4\pi r^2)]\partial_\mu u \partial_\nu u$.

For a Kruskalized coordinate U the metric is regular at the horizon. Thus m is of the form

$$m \sim m_0 + m_1 U + O(U^2) = m_0 + m_1 e^{-\kappa_0 u} + \ldots,$$

and we find $L(u) = \dot{m} \approx e^{-\kappa_0 u} \sim (\Phi_{,u})^2$ as $u \to +\infty$. Thus in the standard retarded time coordinate u the luminosity decays exponentially fast.

Calculating the strength of the backscattered part requires a little more effort. As explained before, we can treat the scattering problem on a fixed Reissner-Nordström background. The spherical symmetry once again allows one to decompose the scalar field ϕ into its multipole components: $\phi = \sum \psi_{lm} Y_{lm}/r$. The wave equation then separates into the equation

$$\psi_{,tt} - \psi_{r^*r^*} + V_l(r)\psi = 0, \tag{4.4}$$

where we have dropped the indices l and m. r^* is now the inner tortoise coordinate given by

$$r^* = r + \frac{1}{2\kappa_+} \log \kappa_+ (r_+ - r) + \frac{1}{2\kappa_-} \log \kappa_- (r_- - r)$$

where $\kappa_\pm$ are the surface gravities of the inner and outer horizon respectively. Note that $\kappa_- < 0$ so that $r^* \to +\infty$ at the inner horizon. V is the before mentioned gravitational potential and takes the form

$$V = f(r) \left(\frac{l(l+1)}{r^2} + \frac{f'(r)}{r} \right). \tag{4.5}$$

It is concentrated around the zero of $r^*(r)$ at $r = e^2/m_0$ and falls off exponentially fast for $r^* \to \pm\infty$. Near the horizons we find

$$f(r) \cong \frac{1}{2}\kappa_\pm (r - r_\pm) \tag{4.6}$$

and therefore

$$V(r^*) \sim e^{\kappa_\pm r^*/2}$$

which goes to zero at the respective horizons $r_\pm$.

Equation (4.4) describes a one dimensional scattering problem for the (localized) potential V:

$$\widehat{\psi}_{,r^*r^*} + (\omega^2 - V(r^*))\widehat{\psi} = 0. \tag{4.7}$$

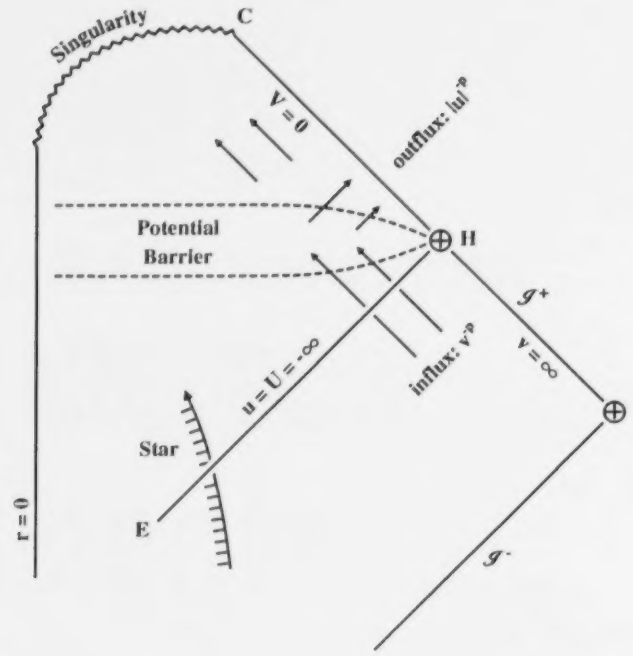

Figure 8: A conformal or Penrose diagram of the interior of a black hole. Note that the points H_1 and H_2 in figure 7 are now merged into one point H. The region below the potential barrier is characterized by two streams of cross flowing radiation, which will ultimately cause the Cauchy horizon to become singular.

Following [34, 19, 20] we are looking for solutions of equation (4.7) with an asymptotic behaviour

$$\widehat{\psi} \sim \begin{cases} \widehat{\psi}_0(\omega) e^{-i\omega r^*} & r^* \longrightarrow -\infty \\ \widehat{\psi}_0(\omega) \left(r(\omega) e^{i\omega r^*} + t(\omega) e^{-i\omega r^*} \right) & r^* \longrightarrow +\infty, \end{cases}$$

where $r(\omega)$ and $t(\omega)$ are the reflection and transmission coefficients of the potential V. The initial condition for $\widehat{\psi}$ – posed on the event horizon, i.e. for $r^* \longrightarrow -\infty$ is the Fourier transform of the Price tail:

$$e^{-i\omega r^*} \widehat{\psi}_0(\omega) = \frac{e^{-i\omega r^*}}{\sqrt{2\pi}} \int dt e^{i\omega(t+r^*)} \psi_0(v) = \frac{e^{-i\omega r^*}}{\sqrt{2\pi}} \int dv \theta(v - v_0) v^{-p} e^{i\omega v} = a_0 \omega^{p-1}$$

where a_0 is the constant depending on v_0 and p. The solution of the wave equation (4.4) behind the potential, i.e. for $r^* \to +\infty$ is given by $\psi = X(v) + Y(u) =$

$\int d\omega e^{-i\omega t}\widehat{\psi}$ so that

$$X(v) = \frac{1}{\sqrt{2\pi}}\int d\omega \widehat{\psi}_0(\omega)t(\omega)\omega^{p-1}e^{-i\omega v} \tag{4.8}$$

$$\text{and} \qquad Y(u) = \frac{1}{\sqrt{2\pi}}\int d\omega \widehat{\psi}_0(\omega)r(\omega)\omega^{p-1}e^{i\omega u}. \tag{4.9}$$

The functions $r(\omega)$ and $t(\omega)$ for the potential (4.5) can only be calculated numerically. We are however only interested in $X(v)$ and $Y(u)$ for large values of v and u, that is their asymptotic behaviour near the "point" H in figure 8. But for large u and v only the low frequencies contribute to the integrals (4.8) and (4.9). For low frequencies we expect r and t to behave as

$$r = 1 + O(\omega^2) \qquad \text{and} \qquad t = t_0\omega + O(\omega^2). \tag{4.10}$$

This is indeed confirmed by a numerical calculation of r and t. (See figure 9.) Inserting equations (4.10) into the integrals (4.8) and (4.9) then gives

$$X(v) = \frac{t_0 a_0}{\sqrt{2\pi}}\int d\omega\, \omega^p(1+O(\omega))e^{-i\omega v} = \beta_0 v^{-p-1}\left(1+O\left(\frac{1}{v}\right)\right) \tag{4.11}$$

$$\text{and} \qquad Y(u) = \frac{a_0}{\sqrt{2\pi}}\int d\omega\, \omega^{p-1}\left(1+O\left(\omega^2\right)\right)e^{i\omega u} = \alpha_0 u^{-p}\left(1+O\left(\frac{1}{u^2}\right)\right) \tag{4.12}$$

where α_0 and β_0 are some numerical constants.

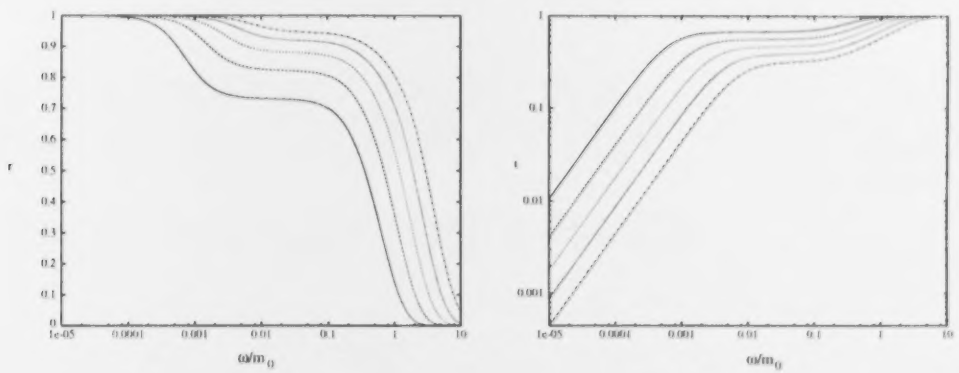

Figure 9: A plot of the scattering (left) and the transmission coefficients of the potential (4.5) for $l = 0$ and different values of e^2/m_0^2.

In summary we have seen that inside a black hole the Price tail gets scattered a second time to form the dominant source of the outflowing radiation irradiating the

Cauchy horizon. The scattering does not alter the character of the infalling radiation; the scattered radiation still decays as a — for late times, characteristic — power law tail, although with a larger power in the case of the transmitted radiation. In the next section we will investigate the effects of the two radiation tails on the geometry of the Cauchy horizon without the assumptions made in the previous models.

4.2 Effects on the Cauchy horizon

As a first model of the Cauchy horizon we consider a spherical spacetime. The high blue shift of the scalar field behind the potential barrier should make the Isaacson effective stress tensor [42]

$$T_{\mu\nu} = (L_{\rm out} n_\mu n_\nu + L_{\rm in} l_\mu l_\nu)/4\pi r^2.$$

a good description of the scalar radiation there (See Figure 8). In fact only the last term, i.e. the term $L_{\rm in} l_\mu l_\nu$) experiences a blue shift and will dominate over the other terms in the stress tensor. The exact form of the other terms is not important and the outflux is merely needed as a catalyst to initiate mass inflation, whereas the cross term $\propto l_{(\nu} n_{\mu)}$ can be completely neglected. (We shall treat the full scalar field case below.) From equations (4.11) and (4.12) we conclude

$$\begin{aligned} L_{\rm in} &= a v^{-2p+1} \sim (\phi_{,v})^2 \\ L_{\rm out} &= b u^{-2p} \sim (\phi_{,u})^2, \end{aligned} \tag{4.13}$$

where a and b are some constants. As before the vectors l and n are defined as $l_\mu = -\partial_\mu V$ and $n_\mu = -\partial_\mu U$, where V and U denote Kruskalized coordinates with respect to the inner horizon. The relation between these koordinates and the coordinates u and v used in the last section is $U = -e^{-u}/\kappa_0$ and $V = -e^{-v}/\kappa_0$. Here we have set $\kappa_0 = -\kappa_- > 0$.

We can choose the metric as

$$ds^2 = -2\frac{e^{2\sigma}}{r} dU dV + r^2 d\Omega^2. \tag{4.14}$$

In terms of the Kruskal coordinates U and V the luminosity functions in (4.13) become

$$L_{\rm in}(V) = \frac{a}{(\kappa_0 V)^2 (-\log(-V)/\kappa_0)^{2p+2}} \tag{4.15}$$

$$\text{and} \qquad L_{\rm out}(U) = \frac{b}{(\kappa_0 U)^2 (-\log(-U)/\kappa_0)^{2p}}. \tag{4.16}$$

Using the expressions derived in appendix A for the Ricci tensor we find the following field equations:

$$\partial_U \left(e^{-2\sigma}(r^2)_{,U}\right) = -2e^{2\sigma}L_{\text{out}}(U), \tag{4.17}$$

$$\partial_V \left(e^{-2\sigma}(r^2)_{,V}\right) = -2e^{2\sigma}L_{\text{in}}(V), \tag{4.18}$$

$$2\sigma_{,UV} = \frac{e^{2\sigma}}{2r^3}\left(1-3\frac{e^2}{r^2}\right) \tag{4.19}$$

$$\text{and} \qquad (r^2)_{,UV} = \frac{e^{2\sigma}}{r}\left(\frac{e^2}{r^2}-1\right). \tag{4.20}$$

Note that the two wave equations (4.19) and (4.20) have finite source terms, provided $e^{2\sigma}$ and r stay finite. In particular, these two equations contain no contributions from the cross-flow. (This results from the lightlike structure of the stress tensor.) Under these circumstances there is, in fact, hope that r and σ behave regularly near the Cauchy horizon. This particular form of the stress tensor suggests that the dominant correction due to the cross-flowing radiation to σ is of the form $A(U)+B(V)$ for some functions A and B. It is therefore possible to choose coordinates in which the metric is finite and only derivatives diverge. This is precisely the behaviour we expect of a mass inflation singularity. Let us now proceed to show that this is indeed the case.

To start we define the two functions $A(U)$ and $B(V)$ by setting $A''(U) := L_{\text{out}}(U)$ and $B''(V) := L_{\text{in}}(V)$. In the region near point H in figure 8, that is for the limits $U \to -\infty$ and $V \to -0$ we find $A'' \ll A' \ll A \to 0$ but $A'' \gg A'^2$ and similarly $B'' \gg B' \to \infty$; $B \to 0$ and $B'' \gg B'^2$. These relations can be derived by integrating and calculating limits like $\lim_{V\to 0} A''/A' = 0$.

By defining the function $\chi := e^{-2\sigma}$ the constraint equations (4.17) and (4.18) take the simple form

$$\partial_U \left(\chi(r^2)_{,U}\right) = -2\chi A''(U) \tag{4.21}$$

$$\text{and} \qquad \partial_V \left(\chi(r^2)_{,V}\right) = -2\chi B''(V). \tag{4.22}$$

We can now solve the field equations iteratively by taking the static solution (denoted by a subscript s) as the zeroth order. This still is a formidable task. But we are only interested in an approximation that is valid for the limiting values of $U \to -\infty$ and $UV \to 0$.

The metric functions and its derivatives are easily calculated in Kruskal coordi-

nates. With $f = 1 - 2m_0/r + e^2/r^2$ one finds, for example,

$$(r_s^2)_{,U} = 2r\frac{\partial r}{\partial r^*}\frac{\partial r^*}{\partial U} = -\frac{rf}{2\kappa_0 U} \qquad \text{and} \quad (r_s^2)_{,V} = \ldots = -\frac{rf}{2\kappa_0 V}.$$

Similarly one deduces

$$\chi_s = -\frac{2\kappa_0^2 UV}{r_s f},$$

$$\chi_{s,U} = -\frac{\kappa_0 V}{r_s^2}\left[1 + 2\kappa_0 r_s\left(\frac{\kappa_0 - \kappa}{f}\right)\right]$$

and $\chi_{s,V}$ is obtained by exchanging U and V in the last equation. Here we have set $\kappa := -\frac{1}{2}\partial f(r)/\partial r$ so that $\kappa_0 = \kappa(r_-)$.

These expressions now allow us to determine the asymptotic behaviour of the static solution. From the definition of U and V and equation (4.6) it follows that $f \cong -2UV$. The behaviour of $r_{s,U}$ etc. now follow trivially except for the derivatives of χ which require a little more care. To evaluate the latter we have to perform the limit

$$\lim_{r\to r_-}\frac{\kappa_0 - \kappa}{f(r)} = 2\lim_{r\to r_-}\frac{\partial^2 f}{\partial r^2}\Big/\frac{\partial f}{\partial r} = 2\frac{\tilde{\kappa_0}}{\kappa_0}$$

where we defined $\tilde{\kappa_0} = -\frac{1}{2}\partial^2 f(r)/\partial r^2|_{r=r_-}$. The second equality follows from the rule of Bernoulli-de l'Hôspital. Inserting these formulae into the expressions for χ_s and r_s we finally get

$$\begin{array}{lllll} r_s^2 & \sim & r_-^2, & \chi_s & \sim & \frac{\kappa_0^2}{r_-}, \\ r_{s,U}^2 & \sim & -2\frac{r_- V}{\kappa_0}, & \chi_{s,U} & \sim & -\frac{\kappa_0}{r_-^2}(1 + 4\,\tilde{\kappa})V, \\ r_{s,V}^2 & \sim & -2\frac{r_- U}{\kappa_0}, & \chi_{s,V} & \sim & -\frac{\kappa_0}{r_-^2}(1 + 4\,\tilde{\kappa})U. \end{array} \tag{4.23}$$

We can now formally integrate equations (4.21) and (4.22) to find

$$r^2 = r_s^2 - 2\int\frac{dU}{\chi}\int dU\chi A''(U) - 2\int\frac{dV}{\chi}\int dV\chi B''(V).$$

As explained before to a first approximation we can set $\chi \equiv \chi_s$. After a partial integration we obtain the result

$$r^2 = r_s^2 - 2(A(U) + B(V)) + \epsilon. \tag{4.24}$$

The error ϵ we make by discarding the remaining integrals is vanishingly small compared to the term $2(A + B)$:

$$\epsilon \sim U\int B(V)dV + V\int A(U)dU \ll A(U) + B(V) \to 0.$$

We can now substitute r^2 into equation (4.20) and solve for χ. The result, after expanding in $A+B$, is

$$\chi - \chi_s \cong (A(U)+B(V))\frac{1}{r^2_{s,UV}r^2_s} \to 0. \tag{4.25}$$

Equations (4.24) and (4.25) show that our approximation scheme is excellent in the region of interest. However the fact that the metric functions approach the static solution does not mean that we deal with essentially the static metric. This is best seen by calculating the mass function as defined in appendix A equation (A.6). We find

$$m = \frac{1}{4}(r^2)_{,U}(r^2)_{,V}\chi + \frac{r}{2}\left[1-\frac{e^2}{r^2}\right] \cong m_0 + \chi_s A'(U)B'(V) + m_{\mathbf{in}} + m_{\mathbf{out}} + O(A+B), \tag{4.26}$$

where the terms $m_{\mathbf{in}}(U)$ and $m_{\mathbf{out}}(V)$ denote the "Vaidya" contribution to the mass and m_0 is the mass associated with the static solution. In the limit $V \to 0$ we have

$$B'(V) \sim \frac{1}{-\kappa_0 V(-log(-V)/\kappa_0)^{2p+2}} = \frac{e^{\kappa_0 v}v^{-2p-2}}{\kappa_0} \to \infty,$$

so that the mass function behaves as predicted by the earlier models of mass inflation. It is important to note that $A'(U)$ shows the opposite behaviour, i.e. as we go back along the Cauchy horizon the singularity becomes weaker. This is the reason the old models of mass inflation accurately predicted the behaviour near the Cauchy horizon.

We are now in the position to check the validity of condition (4.3). The relation between the affine parameter λ and the coordinate U is given by equation (4.2) which for our approximate solution reduces to

$$\frac{\partial U}{\partial \lambda} = r\chi \sim const. + O(A+B),$$

so that $\lambda \propto U$. Therefore the condition

$$\lim_{U\to-\infty} \lambda^2 T_{\lambda\lambda} \sim \lim_{U\to-\infty} (\log(-U))^{-2p} \to 0$$

is satisfied and we conclude that the Cauchy horizon exists and shows the expected behaviour. Furthermore, as $U \to -\infty$ the singularity gets weaker. This is of course expected from the physical picture presented in figure 7: the longer we wait, the more blue shifted radiation piles up on the inner horizon and makes it singular.

So far we have not considered the true back-reaction problem between the gravitational and scalar field. The latter was modeled as a stream of radiation propagating on a *fixed* Reissner-Nordström background. While the results of the last section suggest that this is indeed a good approximation, it is certainly desirable to have an approximate solution which takes the full back-reaction into account. It is not very difficult to extend our previous analysis to include the full scalar field.

The equations governing a minimally coupled scalar field $\phi := \psi/r$ (with Lagrangian $\mathcal{L} = \frac{1}{16\pi}\sqrt{-g}\partial_\mu\phi\partial^\mu\phi$) for the same metric (4.14) as before are the Einstein equations

$$\partial_U\left(\chi(r^2)_{,U}\right) = -r^2\chi\left(\left(\frac{\psi}{r}\right)_{,U}\right)^2, \tag{4.27}$$

$$\partial_V\left(\chi(r^2)_{,V}\right) = -r^2\chi\left(\left(\frac{\psi}{r}\right)_{,V}\right)^2, \tag{4.28}$$

$$2\sigma_{,UV} = \frac{1}{2\chi r^3}\left(1-3\frac{e^2}{r^2}\right) - \frac{1}{2}\left(\frac{\psi}{r}\right)_{,V}\left(\frac{\psi}{r}\right)_{,U}, \tag{4.29}$$

$$\text{and} \qquad (r^2)_{,UV} = \frac{1}{\chi r}\left(\frac{e^2}{r^2}-1\right) \tag{4.30}$$

and the wave equation

$$\psi_{,UV} - \psi\frac{r_{,UV}}{r} = 0. \tag{4.31}$$

What makes matters more difficult than before is the fact that the right hand sides of equations (4.27) and (4.28) are not known anymore. Note that, as before, the source term for the wave equation (4.30) contains no diverging terms if χ and r stay finite.

Guided by our previous result, we now make the Ansatz

$$r^2 = r_s^2 - 2(A(U) + B(V))$$

where A and B are two unknown functions and are assumed to be small for $U \to -\infty$, and $V \to 0$. In the same spirit we can write for the scalar field

$$\psi = a(U) + b(V) + g(U,V) \tag{4.32}$$

with unknown functions a, b and g. The only assumption we make is that $g \ll a, b$, which is justified by the fact that in the limit $r \to r_s$ we get $g \to 0$. Inserting ψ into the wave equation, and only keeping the dominant terms, gives the equation

$$g_{,UV} \cong \frac{a+b}{r_s^3}\left(A'(U)r_{s,V} + B'(v)r_{s,U}\right)$$

and thus

$$g \cong \frac{a+b}{r_s^2}(A+B) + \text{smaller terms},$$

so that g indeed is much smaller than a and b.

The functions a and b are then fully determined by the boundary conditions which we pose right after the potential barrier. Comparing equation (4.32) with the results of the scattering analysis (4.11) and (4.12) gives

$$a(U) = \alpha_0 \log(-U)^{-p} \qquad \text{and} \qquad b(V) = \beta_0(-\log(-V))^{-p-1}, \tag{4.33}$$

which confirms our assumptions about the relative size of a, b and its derivatives. The constraint equations (4.27) and (4.28) can now be used to determine A and B. To leading order we find

$$2A''(U) = a'(U)^2 + 4\frac{a'(U)A'(U)}{r_s^2} + 4\frac{A'(U)^2}{r_s^4} \simeq a'(U)^2,$$

provided that $a'(U) \gg A'(U) = \frac{1}{2}\int dU a'(U)^2$. This last condition is easily verified by looking at the expression (4.33) for a. The same analysis for b shows that $B''(V) = \frac{1}{2}b'(V)^2$.

Let us now integrate the wave equation (4.29) for σ. Contrary to equation (4.19) there is now a diverging source term. To leading order, σ has to obey

$$\sigma_{,UV} \cong \frac{1}{2\chi_s r_s^2}\left[1 - 3\frac{e^2}{r_s^2}\right] - \frac{1}{2}\frac{a'b'}{r_s^2}.$$

Fortunately the divergence is integrable and we find

$$\sigma \cong \sigma_s - \frac{1}{2}\frac{a(U)b(V)}{r_s^2}.$$

At this point we have recovered the *same* quantitative behaviour as in the cross-flow case.

In summary, we have shown that perturbations falling into a black hole at late times (i.e the Price tail) form decaying tails of radiation even after having been scattered again off the interior potential barrier. These tails then disturb the inner horizon in a manner that leads to a mass inflation type singularity, that is to a null curvature singularity along the former inner horizon. The tails however are not strong enough to cause a complete collapse of the inner horizon to zero radius before the

mass inflation singularity occurs. In fact as we go back along the Cauchy horizon the singularity becomes weaker.

We thus do not see the formation of an all-encompassing $r = 0$ spacelike singularity as suggested by [16, 17, 18]. Our conclusions indeed have been confirmed by a numerical study recently performed by Brady and Smith [43].

Chapter 5

Double null dynamics of Einstein gravity

5.1 Introduction

The classic analysis of Arnowitt, Deser and Misner (ADM) [44] formulates gravitational dynamics in terms of the evolution of a spatial 3-geometry. The geometrical framework is the imbedding formalism of Gauss and Codazzi for the foliation of spacetime by spacelike hypersurfaces [6].

Quite often, however, one encounters circumstances where a lightlike foliation is especially suitable. Because of the degeneracies that arise in the lightlike case the imbedding relations are very different and the situation not quite so familiar and under control. To bypass the degeneracies, one is forced to fall back to a foliation of codimension 2, by spacelike 2-surfaces. It is our aim in this chapter to develop a simple $(2+2)$-imbedding formalism of this kind.

Several $(2+2)$-formalisms are extant [45], the earliest and best known being the generalized spin-coefficient formalism of Geroch, Held and Penrose (GHP) [46]. Basically, of course, all such formalisms have the same content, but they take very different forms.

The essential feature of the present approach is that it maintains manifest two-dimensional covariance while operating with objects having direct geometrical meaning. Two-dimensional covariance permits reduction of the Einstein field equations to an especially concise and transparent form: the ten Ricci components are embraced

in a set of just three compact, two-dimensionally covariant expressions.

There is a limitation, at least in the version presented here. (It applies to most of the formalisms we have listed [45].) The two independent normals to an imbedded 2-surface—conveniently taken as a pair of lightlike vectors, since their directions are uniquely defined—are assumed from the beginning to be hypersurface-orthogonal. This precludes choosing them as principal null vectors of the Weyl tensor for a twisting geometry like Kerr. In this respect, the formalism is less flexible than GHP, and not as well tailored for the study of algebraically special metrics.

(2+2) formalisms have a wide range of applications: to the analysis of the characteristic initial-value problem [47], the dynamics of strings [48] and of real and apparent horizons [49] and light-cone quantization [50] and gravitational interactions in ultra-high energy collisions [51]. Last but not least we will employ this formalism in the next Chapter to analyse the generic structure of the inner horizon.

We conclude this Introduction by briefly outlining the contents of this chapter. The basic metrical notions (adapted co-ordinates, basis vectors and form of the metric) are defined in Sec. 5.2. In Sec. 5.3, we introduce in two-dimensionally covariant form the geometrical information encoded in first derivatives of the metric: the extrinsic curvatures and "twist," as well as the invariant operators which perform differentiation along the two lightlike normals. This comprises the basic formal machinery needed in Sec. 5.4, which presents the central result of this chapter, the tetrad components of the Ricci tensor as three concise equations (5.27)–(5.29). (To make direct access to these results easy, their derivation is deferred to the second half of the chapter (Secs. 9–12), which also provides (Sec. 5.13) the tetrad components of the full Riemann tensor.)

The contracted Bianchi identities (Sec. 5.5) are applied in Sec. 5.7 to analyze the structure of the characteristic initial-value problem. In Sec. 5.8 we sketch the Lagrangian formulation of covariant double-null dynamics.

The Ricci and Riemann components result from the commutation relations for four-dimensional covariant differentiation. Their most efficient derivation calls for a formalism that is both four- and two-dimensionally covariant. Unfortunately, these two requirements do not mesh easily. Four-dimensional covariance tends to clutter the formulae by treating subsidiary two-dimensional quantities, like shift vectors and the two-dimensional connection, as 4-scalars on a par with the primary geometrical properties, extrinsic curvature and twist. Those properties, for their part, are corre-

lated, not with four-dimensional covariant derivatives, but with Lie derivatives, which are non-metric and have no direct link to curvature. To patch up these differences, and thus streamline the derivations, seems to need a certain degree of artifice. In Sec. 5.10 we address this (purely technical) problem by temporarily working with a "rationalized" covariant derivative which exhibits both four-dimensional and restricted ("rigid") two-dimensional covariance.

Some brief remarks (Sec. 5.14) conclude the chapter.

5.2 $(2+2)$-split of the metric

We shall suppose that we are given a foliation of spacetime by lightlike hypersurfaces Σ^0 with normal generators $\ell^{(0)}_\alpha$, and a second, independent foliation by lightlike hypersurfaces Σ^1 with generators $\ell^{(1)}_\alpha$ nowhere parallel to $\ell^{(0)}_\alpha$. The intersections of $\{\Sigma^0\}$ and $\{\Sigma^1\}$ define a foliation of codimension 2 by spacelike 2-surfaces S. (The topology of S is unspecified. All our considerations are local.) S has exactly two lightlike normals at each of its points, co-directed with $\ell^{(0)}$ and $\ell^{(1)}$.

In terms of local charts, the foliation is described by the imbedding relations

$$x^\alpha = x^\alpha(u^A, \theta^a). \tag{5.1}$$

Here, x^α are four-dimensional spacetime co-ordinates (assumed admissible in the sense of Lichnerowicz [52]); u^0 and u^1 are a pair of scalar fields constant over each of the hypersurfaces Σ^0 and Σ^1 respectively; and θ^2, θ^3 are intrinsic co-ordinates of the 2-spaces S, each characterized by a fixed pair of values (u^0, u^1).

Notation: Our conventions are: Greek indices $\alpha, \beta, \ldots$ run from 0 to 3; upper-case Latin indices $A, B, \ldots$ take values $(0, 1)$; and lower-case Latin indices $a, b, \ldots$ take values $(2, 3)$. We adopt MTW curvature conventions [6] with signature $(-+++)$ for the spacetime metric $g_{\alpha\beta}$. When there is no risk of confusion we shall often omit the Greek indices on 4-vectors like $\ell^{(A)}_\alpha$ and $e^\alpha_{(a)}$: they are easily identifiable as 4-vectors by their parenthesized labels. Four-dimensional covariant differentiation is indicated either by ∇_α or a vertical stroke: $\nabla_\beta A_\alpha \equiv A_{\alpha|\beta}$. Four-dimensional scalar products are often indicated by a dot: thus, $\ell_{(A)} \cdot \ell_{(B)} \equiv g_{\alpha\beta}\, \ell^\alpha_{(A)}\, \ell^\beta_{(B)}$. Further conventions will be introduced as the need arises.

Without essential loss of generality we may assume the functions $x^\alpha(u^A, \theta^a)$ to be smooth (at least thrice differentiable). (We are always free to make the co-ordinate

choice $x^A = u^A$, $x^a = \theta^a$, but at the cost of losing manifest four-dimensional and two-dimensional covariance.)

The lightlike character of the hypersurfaces Σ^A is encoded in

$$\nabla u^A \cdot \nabla u^B \equiv g^{\alpha\beta}(\partial_\alpha u^A)(\partial_\beta u^B) = e^{-\lambda}\eta^{AB} \tag{5.2}$$

for some scalar field $\lambda(x^\alpha)$, where

$$\eta^{AB} = \text{anti-diag}\,(-1,-1) = \eta_{AB}; \tag{5.3}$$

η^{AB} and its inverse η_{AB} are employed to raise and lower upper-case Latin indices, e.g., $\ell_{(0)} = -\ell^{(1)}$.

The generators $\ell^{(A)}$ of Σ^A are parallel to the gradients of $u^A(x^\alpha)$. It is symmetrical and convenient to define $\ell_{(A)} = e^\lambda \nabla u^A$, i.e.,

$$\ell^{(A)}_\alpha = e^\lambda \partial_\alpha u^A. \tag{5.4}$$

Then

$$\ell_{(A)} \cdot \ell^{(B)} = e^\lambda \delta^B_A. \tag{5.5}$$

The pair of vectors $e_{(a)}$, defined from (5.1) by

$$e^\alpha_{(a)} = \partial x^\alpha / \partial \theta^a, \tag{5.6}$$

are holonomic basis vectors tangent to S. The intrinsic metric $g_{ab}\, d\theta^a\, d\theta^b$ of S is determined by their scalar products:

$$g_{ab} = e_{(a)} \cdot e_{(b)}. \tag{5.7}$$

Lower-case Latin indices are lowered and raised with g_{ab} and its inverse g^{ab}; thus $e^{(a)} \equiv g^{ab} e_{(b)}$ are the dual basis vectors tangent to S, with $e^{(a)} \cdot e_{(b)} = \delta^a_b$. Since $\ell^{(A)}$ is normal to every vector in Σ^A, we have

$$\ell^{(A)} \cdot e_{(a)} = 0. \tag{5.8}$$

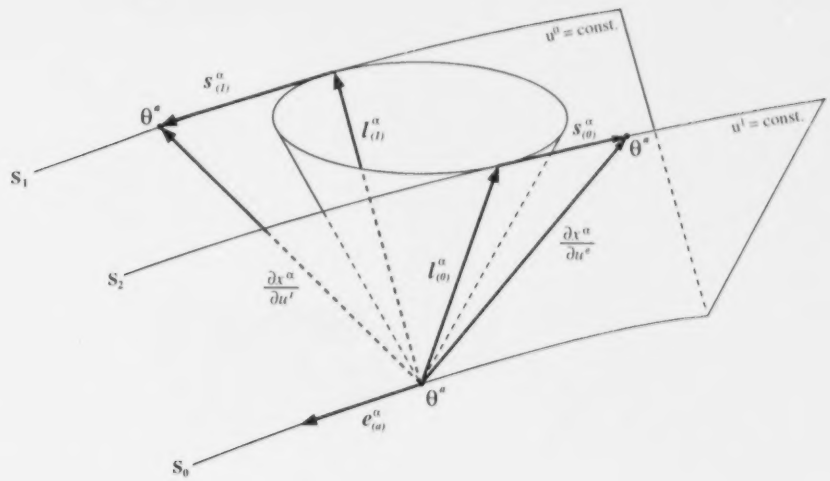

Figure 10: The 2 + 2 splitting of the four dimensional spacetime into a foliation of intersecting null surfaces $u^0 = const.$ and $u^1 = const.$.

In general, θ^a cannot be chosen so as to remain constant along *both* sets of generators $\ell^{(A)}$. They are convected (Lie-transported) along the pair of vector fields $\partial x^\alpha / \partial u^A$ (in general, non-lightlike).

From (5.4) and (5.5) one finds that $\partial x^\alpha / \partial u^A - \ell^\alpha_{(A)}$ is orthogonal to $\ell_{(B)}$, i.e., tangent to S. This validates the decomposition

$$\frac{\partial x^\alpha}{\partial u^A} = \ell^\alpha_{(A)} + s^a_A \, e^\alpha_{(a)}, \tag{5.9}$$

thus defining a pair of "shift vectors" s^α_A tangent to S (see Fig. 10).

An arbitrary displacement dx^α in spacetime is, according to (5.6) and (5.9), decomposable as

$$dx^\alpha = \ell^\alpha_{(A)} \, du^A + e^\alpha_{(a)} (d\theta^a + s^a_A \, du^A). \tag{5.10}$$

From (5.5), (5.7) and (5.8) we read off the completeness relation

$$g_{\alpha\beta} = e^{-\lambda} \eta_{AB} \ell^{(A)}_\alpha \ell^{(B)}_\beta + g_{ab} e^{(a)}_\alpha \, e^{(b)}_\beta . \tag{5.11}$$

Combining (5.10) and (5.11) shows that the spacetime metric is decomposable as

$$g_{\alpha\beta} dx^\alpha \, dx^\beta = e^\lambda \eta_{AB} \, du^A \, du^B + g_{ab} (d\theta^a + s^a_A \, du^A)(d\theta^b + s^b_B \, du^B). \tag{5.12}$$

5.3 Two-dimensionally covariant objects embodying first derivatives of the metric: extrinsic curvatures K_{Aab}, twist ω^a and normal Lie derivatives D_A

Absolute derivatives of four-dimensional tensor fields with respect to u^A and θ^a are projections of the four-dimensional covariant derivative ∇_α, and denoted by

$$\frac{\delta}{\delta u^A} = \frac{\partial x^\alpha}{\partial u^A}\,\nabla_\alpha, \qquad \frac{\delta}{\delta \theta^a} = e_{(a)} \cdot \nabla. \tag{5.13}$$

From (5.6) and the symmetry of the mixed partial derivatives and the affine connection,

$$\frac{\delta e^\alpha_{(a)}}{\delta u^A} = \frac{\delta}{\delta \theta^a}\left(\frac{\partial x^\alpha}{\partial u^A}\right), \qquad \frac{\delta e_{(a)}}{\delta \theta^b} = \frac{\delta e_{(b)}}{\delta \theta^a}. \tag{5.14}$$

The object

$$\Gamma^c_{ab} = e^{(c)} \cdot \delta e_{(a)}/\delta\theta^b \tag{5.15}$$

is, as the notation suggests, the Christoffel symbol associated with g_{ab}, as is easily verified by forming $\partial_c g_{ab}$, recalling (5.7) and applying Leibnitz's rule.

Associated with its two normals $\ell_{(A)}$, S has two extrinsic curvatures K_{Aab}, defined by

$$K_{Aab} = e_{(a)} \cdot \delta \ell_{(A)}/\delta\theta^b = \ell_{(A)\alpha|\beta}\, e^\alpha_{(a)}\, e^\beta_{(b)}. \tag{5.16}$$

(Since we are free to rescale the null vectors $\ell_{(A)}$, a certain scale-arbitrariness is inherent in this definition.) Because of (5.8), we can rewrite

$$K_{Aab} = -\ell_{(A)} \cdot \delta e_{(a)}/\delta\theta^b, \tag{5.17}$$

which exhibits the symmetry in a, b.

A further basic geometrical property of the double foliation is given by the Lie bracket of $\ell_{(B)}$ and $\ell_{(A)}$, i.e., the 4-vector

$$[\ell_{(B)}, \ell_{(A)}]^\alpha = 2(\ell_{[(B)} \cdot \nabla)\ell^\alpha_{(A)]}. \tag{5.18}$$

Noting (5.9) and the fact that the Lie bracket of the vectors $\partial x^\alpha/\partial u^B$ and $\partial x^\alpha/\partial u^A$ vanishes identically, and recalling (5.14), we find

$$[\ell_{(B)}, \ell_{(A)}] = \epsilon_{AB}\, \omega^a\, e_{(a)}, \tag{5.19}$$

where the 2-vector ω^a is given by

$$\omega^a = \epsilon^{AB}(\partial_B s^a_A - s^b_B s^a_{A;b}), \tag{5.20}$$

the semicolon indicates two-dimensional covariant differentiation associated with metric g_{ab}, and ϵ_{AB} is the two-dimensional permutation symbol, with $\epsilon_{01} = +1$. (Note that raising indices with η^{AB} to form ϵ^{AB} yields $\epsilon^{10} = +1$.)

The geometrical significance of the "twist" ω^a can be read off from (5.19): the curves tangent to the generators $\ell_{(0)}$, $\ell_{(1)}$ mesh together to form 2-surfaces (orthogonal to the surfaces S) if and only if $\omega^a = 0$. In this case, it would be consistent to allow the co-ordinates θ^a to be dragged along both sets of generators, and thus to gauge both shift vectors to zero.

We denote by D_A the two-dimensionally invariant operator associated with differentiation along the normal direction $\ell_{(A)}$. Acting on any two-dimensional geometrical object $X^{a\ldots}_{b\ldots}$, D_A is formally defined by

$$D_A X^{a\ldots}_{b\ldots} = (\partial_A - \mathcal{L}_{s^d_A}) X^{a\ldots}_{b\ldots}. \tag{5.21}$$

Here, ∂_A is the partial derivative with respect to u^A and $\mathcal{L}_{s^d_A}$ the Lie derivative with respect to the 2-vector s^d_A.

As examples of (5.21), we have for a 2-scalar f (this includes any object bearing upper-case, but no lower-case, Latin indices):

$$D_A f = (\partial_A - s^a_A \partial_a) f = \ell^\alpha_{(A)} \partial_\alpha f \tag{5.22}$$

(in which the second equality follows at once from (5.9)); and for the 2-metric g_{ab}:

$$D_A g_{ab} = \partial_A g_{ab} - 2 s_{A(a;b)} = 2K_{Aab}, \tag{5.23}$$

in which the second equality is derivable from (5.7), (5.14) and (5.9). (For the detailed derivation, see (5.75) below, or Appendix C.)

The geometrical meaning of D_A is quite generally the following (see Appendix C): $D_A X^{a\ldots}_{b\ldots}$ is the projection onto S of the Lie derivative of the equivalent tangential 4-tensor

$$X^{\alpha\ldots}_{\beta\ldots} \equiv X^{a\ldots}_{b\ldots} e^\alpha_{(a)} e^{(b)}_\beta \ldots$$

with respect to the 4-vector $\ell^\mu_{(A)}$:

$$D_A X^{a\ldots}_{b\ldots} = e^{(a)}_\alpha e^\beta_{(b)} \cdot \mathcal{L}_{\ell^\mu_{(A)}} X^{\alpha\ldots}_{\beta\ldots}. \tag{5.24}$$

The objects K_{Aab}, ω^a and D_A comprise all the geometrical structure that is needed for a succinct two-dimensionally covariant expression of the Riemann and Ricci curvatures of spacetime. According to (5.16), (5.19) and (5.24), all are simple projections onto S of four-dimensional geometrical objects. Consequently, they transform very simply under two-dimensional co-ordinate transformations. Under the arbitrary reparametrization

$$\theta^a \to \theta^{a'} = f^a(\theta^b, u^A) \tag{5.25}$$

(which leaves u^A and hence the surfaces Σ^A and S unchanged), ω_a and K_{Aab} transform cogrediently with

$$e_{(a)} \to e'_{(a)} = e_{(b)}\partial\theta^b/\partial\theta^{a'} \tag{5.26}$$

(see (5.6)), and D_A is invariant. By contrast, $\partial x^\alpha/\partial u^A$ and hence the shift vectors s^a_A (see (5.9)) undergo a more complicated gauge-like transformation, arising from the u-dependence in (5.25).

5.4 Ricci tensor

The geometrical and notational groundwork laid in the previous sections allows us now to simply display the components of the Ricci tensor, deferring derivations to Secs. 9–12. Our notation for the tetrad components is typified by

$${}^{(4)}R_{ab} = R_{\alpha\beta}e^\alpha_{(a)}e^\beta_{(b)}, \qquad R_{aA} = R_{\alpha\beta}e^\alpha_{(a)}\ell^\beta_{(A)}.$$

The results are

$$\begin{aligned}
{}^{(4)}R_{ab} &= \frac{1}{2}\,{}^{(2)}Rg_{ab} - e^{-\lambda}\left(D_A + K_A\right)K^A_{ab} \\
&\quad +2e^{-\lambda}K_{A(a}{}^{d}K^A_{b)d} - \frac{1}{2}e^{-2\lambda}\,\omega_a\omega_b - \lambda_{;ab} - \frac{1}{2}\lambda_{,a}\lambda_{,b} \qquad (5.27)\\
R_{AB} &= -D_{(A}K_{B)} - K_{Aab}K_B{}^{ab} + K_{(A}D_{B)}\lambda \\
&\quad -\frac{1}{2}\eta_{AB}\left[\left(D^E + K^E\right)D_E\lambda - e^{-\lambda}\omega^a\omega_a + \left(e^\lambda\right)^{;a}{}_a\right] \qquad (5.28)\\
R_{Aa} &= K^b_{Aa;b} - \partial_a K_A - \frac{1}{2}\partial_a D_A\lambda + \frac{1}{2}K_A\partial_a\lambda \\
&\quad +\frac{1}{2}\epsilon_{AB}e^{-\lambda}\left[\left(D^B + K^B\right)\omega_a - \omega_a D^B\lambda\right], \qquad (5.29)
\end{aligned}$$

where ${}^{(2)}R$ is the curvature scalar associated with the 2-metric g_{ab}, and $K_A \equiv K_A{}^a{}_a$.

5.5 Bianchi identities. Bondi's lemma

The Ricci components are linked by four differential identities, the contracted Bianchi identities

$$\nabla_\beta R^\beta{}_\alpha = \frac{1}{2}\partial_\alpha R, \tag{5.30}$$

where the four-dimensional curvature scalar $R = R^\alpha{}_\alpha$ is given by

$$R = e^{-\lambda} R^A{}_A + R^a{}_a, \tag{5.31}$$

according to (5.11).

As we show in Sec. 5.12, projecting (5.30) onto $e_{(a)}$ leads to

$$(D_A + K_A)\, R^A{}_a = \frac{1}{2}\partial_a R^A{}_A + \frac{1}{2}e^\lambda \partial_a {}^{(4)}R^b{}_b - \left(e^\lambda {}^{(4)}R^b{}_a\right)_{;b}. \tag{5.32}$$

Projection of (5.30) onto $\ell_{(A)}$ similarly yields

$$\begin{aligned} &D_B\left(R^B{}_A - \frac{1}{2}\delta^B_A R^D{}_D\right) - \frac{1}{2}e^\lambda D_A\, {}^{(4)}R^a{}_a \\ &\quad = e^\lambda {}^{(4)}R_{ab} K_A{}^{ab} - R^B{}_A K_B - \left(e^\lambda R^a{}_A\right)_{;a} + \epsilon_{AB}\omega^a R^B{}_a. \end{aligned} \tag{5.33}$$

Equations (5.32) and (5.33) express the four Bianchi identities in terms of the tetrad components of the Ricci tensor.

We now look at the general structure of these equations.

For $A = 0$ in (5.33), R^0_0 does not contribute to the first (parenthesized) term, since

$$-R_{01} = R^0_0 = R^1_1 = \frac{1}{2}R^A_A. \tag{5.34}$$

This equation therefore takes the form

$$D_1 R_{00} + \frac{1}{2}e^\lambda D_0\, {}^{(4)}R^a_a = -K_0 R_{01} + \mathcal{L}({}^{(4)}R_{ab}, R_{00}, R_{0a}, \partial_a), \tag{5.35}$$

in which the schematic notation $\mathcal{L}$ implies that the expression is linear homogeneous in the indicated Ricci components and their two-dimensional spatial derivatives ∂_a.

The other ($A = 1$) component of (5.33) has the analogous structure

$$D_0 R_{11} + \frac{1}{2}e^\lambda D_1\, {}^{(4)}R^a_a = -K_1 R_{01} + \mathcal{L}({}^{(4)}R_{ab}, R_{11}, R_{1a}, \partial_a). \tag{5.36}$$

The form of the remaining two Bianchi identities (5.32) is

$$D_0 R_{1a} + D_1 R_{0a} = \mathcal{L}({}^{(4)}R_{ab}, R_{01}, R_{Aa}, \partial_a). \tag{5.37}$$

It is noteworthy that the appearance of R_{01} in (5.35) and (5.36) is purely algebraic: its vanishing would be a direct consequence of the vanishing of just six of the other components. Bondi et al [54] and Sachs [47] therefore refer to the R_{01} field equation as the "trivial equation."

The structure of (5.35)–(5.37) provides insight into how the field equations propagate initial data given on a lightlike hypersurface. Let us (arbitrarily) single out u^0 as "time," and suppose that the six "evolutionary" vacuum equations

$$ {}^{(4)}R_{ab} = 0, \qquad R_{00} = R_{0a} = 0 \tag{5.38} $$

are satisfied everywhere in the neighbourhood of a hypersurface $u^0 = \text{const}$. (Bondi and Sachs refer to ${}^{(4)}R_{ab}$ as the "main equations" and to R_{00}, R_{0a} as "hypersurface equations." R_{00} is, in fact, the Raychaudhuri focusing equation [53], governing the expansion of the lightlike normal $\ell_{(0)} = -\ell^{(1)}$ to the *transverse* hypersurface $u^1 = \text{const.}$, and R_{0a} similarly governs its shear.)

Then (5.35) shows that the trivial equation $R_{01} = 0$ is satisfied automatically. From (5.36) and (5.37) it can be further inferred that if R_{11} and R_{1a} vanish on one hypersurface $u^0 = \text{const.}$, then they will vanish everywhere as a consequence of the six evolutionary equations (5.38). This is the content of the Bondi-Sachs lemma [54, 47], which identifies the three conditions $R_{11} = R_{1a} = 0$ as constraints—on the expansion and shear of the generators $\ell_{(1)}$ of an initial hypersurface $u^0 = \text{const.}$—which are respected by the evolution.

5.6 Co-ordinate conditions and gauge-fixing

The characteristic initial-value problem [47] involves specifying initial data on a given pair of lightlike hypersurfaces Σ^0, Σ^1 intersecting in a 2-surface S_0.

It is natural to choose our parameters u^A so that $u^0 = 0$ on Σ^0 and $u^1 = 0$ on Σ^1. The requirement (5.2) that u^A be *globally* lightlike already imposes two co-ordinate conditions on (u^A, θ^a), considered as co-ordinates of spacetime. Two further global conditions may be imposed. We may, for instance, demand that θ^a be convected (Lie-propagated) along the lightlike curves tangent to $\ell^\alpha_{(0)}$ from values assigned arbitrarily on Σ^0. According to (5.9), this means the corresponding shift vector is zero everywhere:

$$ s^a_{(0)} = -\ell^\alpha_{(0)}\, \partial_\alpha \theta^a = 0. \tag{5.39} $$

In this case, (5.20) shows that

$$\omega^a = \partial_0 s_1^a \tag{5.40}$$

is just the "time"-derivative of the single remaining shift vector.

These global co-ordinate conditions can still be supplemented by appropriate initial conditions. We are still free to require that θ^a be convected along generators of Σ^0 from assigned values on S_0; then

$$s_1^a = 0 \qquad (u^0 = 0) \tag{5.41}$$

in addition to (5.39).

In addition to (or independently of) (5.39) and (5.41), we are free to choose u^1 along Σ^0 and u^0 along Σ^1 to be *affine* parameters of their generators. On Σ^0, for instance, this means, by virtue of (5.9) and (5.4),

$$\ell^\alpha_{(1)} = \left(\frac{dx^\alpha}{du^1}\right)_{\text{gen.}} = -g^{\alpha\beta}\partial_\beta u^0 = -e^{-\lambda} g^{\alpha\beta}\ell^{(0)}_\beta$$

so that λ vanishes over Σ^0. There is a similar argument for Σ^1. Thus, we can arrange

$$\lambda = 0 \qquad (\Sigma^0 \quad \text{and} \quad \Sigma^1). \tag{5.42}$$

Alternatively, in place of (5.42), the co-ordinate condition

$$D_1\lambda = \frac{1}{2}K_1 \quad \text{on} \quad \Sigma^0 \tag{5.43}$$

could be imposed to normalize u^1. (A corresponding condition on Σ^1 would normalize u^0.) The Raychaudhuri equation (5.28) for R_{11} on Σ^0 would then become linear in the expansion rate $\overline{K}_1 = \partial_1 \ln g^{\frac{1}{2}}$, and that facilitates its integration (cf Hayward [45], Brady and Chambers [49]).

5.7 Characteristic initial-value problem

We are now ready to address the question of what initial data are needed to prescribe a unique vacuum solution of the Einstein equations in a neighbourhood of two lightlike hypersurfaces Σ^0 and Σ^1 intersecting in a 2-surface S_0 [47].

We arbitrarily designate u^0 as "time," and shall refer to Σ^0 $(u^0 = 0)$ as the "initial" hypersurface and to Σ^1 $(u^1 = 0)$ as the "boundary."

We impose the co-ordinate conditions (5.39), (5.41) and (5.42) to tie down θ^a and u^A. While (5.39) and (5.41) control the way θ^a are carried off S_0, onto Σ^0 and into spacetime, the choice of θ^a on S_0 itself is unrestricted. Thus, our procedure retains covariance under the group of two-dimensional transformations $\theta^a \to \theta^{a'} = f^a(\theta^b)$.

In the 4-metric $g_{\alpha\beta}$, given by (5.12), the following six functions of four variables are then left undetermined:

$$g_{ab}, \quad \lambda, \quad s_1^a. \tag{5.44}$$

(In place of s_1^a, it is completely equivalent to specify $\omega^a = \partial_0 s_1^a$, since the "initial" value of s_1^a is pegged by (5.41).)

We shall formally verify that a vacuum 4-metric is uniquely determined by the following initial data:

(a). On S_0, seven functions of two variables θ^a:

$$g_{ab}, \quad \omega^a, \quad \overline{K}_A = \partial_A \ln g^{\frac{1}{2}} \qquad (S_0); \tag{5.45}$$

(b). on Σ^0 and Σ^1, two independent functions of three variables which specify the intrinsic conformal 2-metric:

$$g^{-\frac{1}{2}} g_{ab} \qquad (\Sigma^0 \text{ and } \Sigma^1). \tag{5.46}$$

Instead of (5.46), it is equivalent to give the shear rates of the respective generators,

$$\sigma_{1a}^{\ b} \text{ on } \Sigma^0, \quad \sigma_{0a}^{\ b} \text{ on } \Sigma^1, \tag{5.47}$$

defined as the trace-free extrinsic curvatures:

$$\sigma_{Aab} = \overline{K}_{Aab} - \frac{1}{2} g_{ab} \overline{K}_A = \frac{1}{2} g^{\frac{1}{2}} \partial_A (g^{-\frac{1}{2}} g_{ab}). \tag{5.48}$$

These two functions correspond to the physical degrees of freedom ('radiation modes') of the gravitational field [47, 55].

To build a vacuum solution from the initial data (5.45), (5.47), we begin by noting that (5.39) implies that $D_0 = \partial_0$, $K_{0ab} = \overline{K}_{0ab}$ everywhere. Hence the general expression (5.28) for R_{00} reduces here to

$$-R_{00} = \left(\partial_0 + \frac{1}{2} K_0 - \lambda_{,0}\right) K_0 + \sigma_{0ab} \sigma_0^{ab}. \tag{5.49}$$

On Σ^1, we have $\lambda = \lambda_{,0} = 0$ by (5.42). Thus, (5.49) becomes an ordinary differential equation for

$$K_0 = \overline{K}_0 = \partial_0 \ln g^{\frac{1}{2}}$$

as a function of u^0. This can be integrated along the generators, using the given data for $\sigma_{0a}^{\ b}$ on Σ^1, and the initial value of $\overline{K}_0$ on S_0, to obtain $g^{\frac{1}{2}}$, hence the full 2-metric g_{ab} (hence also $K_{0\,ab}$) over Σ^1.

Expression (5.29) for R_{0a} reduces similarly to

$$R_{0a} = -\frac{1}{2}e^{-\lambda}\left(\partial_0 + K_0 - \lambda_{,0}\right)\omega_a - \frac{1}{2}(\partial_0 - K_0)\lambda_{,a} + K_{0a;b}^{\ \ b} - \partial_a K_0 \tag{5.50}$$

in a spacetime neighbourhood of Σ^0 and Σ^1. On Σ^1, since $K_{0\,ab}$ is now known, and $\lambda = \lambda_{,a} = \lambda_{,0} = 0$, (5.50) is a linear ordinary differential equation for ω_a which may be integrated along generators, with initial condition (5.45), to find ω_a (hence s_1^a).

Thus, our knowledge of the six metric functions (5.44) has been extended to all of Σ^1 with the aid of the evolutionary equations $R_{00} = R_{0a} = 0$.

A similar procedure, applied to the constraint equations $R_{11} = R_{1a} = 0$, determines the functions (5.44) (hence also K_{1ab}) over the initial hypersurface Σ^0. (Here we exploit (5.41)—implying $D_1 = \partial_1$—which holds on Σ^0 only. This limitation is of little practical consequence, since the Bianchi identities (Sec. 5.7) relieve us of the need to recheck the constraints off Σ^0.)

Thus, the data (5.44), together with their tangential derivatives ∂_1, ∂_a—which we denote schematically by

$$\mathcal{D} = \{g_{ab},\ \lambda,\ \omega_a,\ s_1^a,\ \partial_1,\ \partial_a\} \tag{5.51}$$

—are now known all over the initial hypersurface Σ^0 $u^0 = 0$. (Note that $\mathcal{D}$ includes K_{1ab}.)

We now proceed recursively. Suppose that $\mathcal{D}$ is known over some hypersurface Σ : $u^0 = \text{const}$. We show that the six evolutionary equations ${}^{(4)}R_{ab} = 0$, $R_{00} = R_{0a} = 0$, together with the known boundary values of g_{ab}, K_{0ab}, ω_a and s_1^a on Σ^1, determine all first-order time-derivatives ∂_0 of $\mathcal{D}$, and hence the complete evolution of $\mathcal{D}$.

Expression (5.27) for the evolutionary equations ${}^{(4)}R_{ab} = 0$ can be written more explicitly, with the aid of the identity

$$D_A K_{ab}^A - 2K_{A(a}^{\ \ d} K_{b)d}^A = -2D_1 K_{0ab} + 4K_{0(a}^{\ \ d} K_{1b)d} + \omega_{(a;b)}, \tag{5.52}$$

which is rooted in the symmetry

$$\partial_{[B}\overline{K}_{A]ab} = 0, \qquad \overline{K}_{Aab} \equiv K_{Aab} + s_{A(a;b)} \tag{5.53}$$

(see (5.23) and Appendix C).

The equations ${}^{(4)}R_{ab} = 0$ are thus seen to reduce to a system of three linear ordinary differential equations for K_{0ab} as functions of u^1 on Σ, whose coefficients are concomitants of the known data $\mathcal{D}$ on Σ. Together with the boundary conditions on K_{0ab} at $u^1 = 0$ (i.e., the intersection of Σ with Σ^1), they determine a unique solution for K_{0ab} on Σ.

We next turn to (5.49) and (5.50) to read off the values of $\partial_0\lambda$ and $\partial_0\omega_a$ on Σ. Since the remaining time-derivatives are known trivially from

$$\partial_0 s_1^a = \omega^a, \qquad \frac{1}{2}\partial_0 g_{ab} = \overline{K}_{0ab} = K_{0ab},$$

we are now in possession of the first time-derivatives of all the data $\mathcal{D}$ on Σ.

This completes our formal demonstration that the initial conditions (5.45) and (5.46), or (5.45) and (5.47), determine (at least locally) a unique vacuum spacetime.

5.8 Lagrangian

According to (5.12) and (5.31), the Einstein-Hilbert Lagrangian density $\mathcal{L} = \sqrt{-{}^4g}R^\alpha_\alpha$ decomposes as

$$\mathcal{L} = g^{\frac{1}{2}}e^\lambda(e^{-\lambda}R^A_A + {}^{(4)}R^a_a), \tag{5.54}$$

in which $g^{\frac{1}{2}}$ refers to the determinant of g_{ab}. Substitution from (5.27) and (5.28) yields the explicit form

$$\begin{aligned} g^{-\frac{1}{2}}\mathcal{L} = {} & e^\lambda\,{}^{(2)}R - D_A(2K^A + D^A\lambda) - K_AK^A - K^{ab}_AK^A_{ab} \\ & + \frac{1}{2}e^{-\lambda}\omega^a\omega_a - e^\lambda\left(2\lambda^{;a}{}_{;a} + \frac{3}{2}\lambda_{,a}\lambda^{,a}\right). \end{aligned} \tag{5.55}$$

Second derivatives of the metric in (5.55) can be isolated in the form of a pure divergence by calling on the identities

$$g^{\frac{1}{2}}D_AX^A = \partial_\alpha\left[(-{}^4g)^{\frac{1}{2}}e^{-\lambda}X^A\ell^\alpha_{(A)}\right] - g^{\frac{1}{2}}X^AK_A, \tag{5.56}$$

$$A^a{}_{;a} + A^a\lambda_{,a} = \nabla_\alpha(A^ae^\alpha_{(a)}), \tag{5.57}$$

which follow from (5.102) below, and hold for any scalars X^A and 2-vector A^a. We thus obtain

$$\mathcal{L} = -\partial_\alpha \left[\left(-{}^4g\right)^{\frac{1}{2}} e^\lambda \left(2K^A + D^A\lambda\right) \ell^\alpha_{(A)} + 2\left(-{}^4g\right)^{\frac{1}{2}} \lambda^{,a} e^\alpha_{(a)} \right]$$
$$+ g^{\frac{1}{2}} \left[e^{\lambda\,(2)}R + K_A K^A - K^{ab}_A K^A_{ab} + \frac{1}{2} e^{-\lambda} \omega^a \omega_a + K^A D_A \lambda + \frac{1}{2} e^\lambda \lambda_{,a} \lambda^{,a} \right]. \quad (5.58)$$

The divergence term integrates as usual to a surface term in the action $S = \int \mathcal{L}\, d^4x$, and has no influence on the classical equations of motion.

Variation of S with respect to

$$-e^\lambda = g_{(0)(1)} \equiv \ell_{(0)} \cdot \ell_{(1)}$$

reproduces the expression obtained from (5.27) for $G^{01} = \frac{1}{2} e^\lambda R^a_a$. Similarly, variation with respect to s^a_A yields the expression (5.29) for $G_{Aa} = R_{Aa}$, if we take account of the implicit dependence of K_{Aab}, D_A and ω^a on s^a_A through

$$K_{Aab} = \frac{1}{2} \partial_A g_{ab} - s_{A(a;b)}, \quad (5.59)$$

(5.22) and (5.20). Finally, variation with respect to g_{ab} yields ${}^{(4)}G^{ab}$, if we note the identity

$$g^{-\frac{1}{2}} \frac{\delta}{\delta g^{ab}} \int \varphi\, {}^{(2)}R g^{\frac{1}{2}}\, d^2\theta = g_{ab}\, \varphi^{;c}{}_{c} - \varphi_{;ab}. \quad (5.60)$$

Thus, variation of the action (5.58) yields eight of the ten Einstein equations. The remaining two equations—the Raychaudhuri equations for R_{00} and R_{11}—cannot be retrieved directly from (5.58), because the a priori conditions $\eta^{00} = \eta^{11} = 0$ (expressing the lightlike character of u^0 and u^1) which is built into (5.58), precludes us from varying with respect to these "variables." The two Raychaudhuri equations can, however, be effectively recovered from the other eight equations via the Bianchi idendities.

The Hamiltonian formulation of the dynamics has been discussed in detail by Torre [45]. We hope to pursue this topic elsewhere.

5.9 Gauss-Weingarten (first order) relations

In this second half of this chapter, we return to the beginning and to the task of laying a more complete geometrical foundation for the Ricci and Bianchi formulas which we

quoted without derivation in (5.27)–(5.29) and (5.32), (5.33). We begin with the first-order imbedding relations for the 2-surface S as a subspace of spacetime.

(5.15) and (5.17) allow us to decompose the 4-vector $\delta e^{\alpha}_{(a)}/\delta\theta^b$ in terms of the basis $(\ell_{(A)}, e_{(a)})$. Recalling (5.5), we find

$$\frac{\delta e_{(a)}}{\delta\theta^b} = -e^{-\lambda}K^A_{ab}\ell_{(A)} + \Gamma^c_{ab}e_{(c)}. \tag{5.61}$$

Similarly, in view of (5.16), we may decompose

$$\frac{\delta\ell_{(A)}}{\delta\theta^a} = L_{ABa}\ell^{(B)} + K_{Aab}e_{(b)} \tag{5.62}$$

where the first coefficient is given by

$$L_{ABa} = e^{-\lambda}\ell_{(B)}\cdot\delta\ell_{(A)}/\delta\theta^a. \tag{5.63}$$

This coefficient can be reduced to a much simpler form. Its symmetric part is

$$L_{(AB)a} = \frac{1}{2}e^{-\lambda}\partial_a(\ell_{(A)}\cdot\ell_{(B)}) = \frac{1}{2}\eta_{AB}\partial_a\lambda. \tag{5.64}$$

To obtain the skew part, we note first that

$$e^{\alpha}_{(a)}\,\ell^{\beta}_{[(B)}\ell_{(A)][\alpha|\beta]} = 0. \tag{5.65}$$

since $\ell_{(A)}$ is proportional to a lightlike gradient (see (5.4)). With the aid of (5.65) and (5.19) we now easily derive

$$\begin{aligned} L_{[AB]a} &= e^{-\lambda}\ell^{\beta}_{[(B)}\ell_{(A)]\beta|\alpha}e^{\alpha}_{(a)} = \frac{1}{2}e^{-\lambda}[\ell_{(B)},\ell_{(A)}]^{\alpha}\,e_{(a)\alpha} \\ &= \frac{1}{2}\epsilon_{AB}\omega_a e^{-\lambda}, \end{aligned} \tag{5.66}$$

Combining (5.64) and (5.66), we arrive at the simple expression

$$2L_{ABa} = \eta_{AB}\partial_a\lambda + e^{-\lambda}\epsilon_{AB}\omega_a \tag{5.67}$$

for the first coefficient in (5.62).

The Gauss-Weingarten equations (5.61) and (5.62) govern the variation of the 4-vectors $\ell_{(A)}$ and $e_{(a)}$ along directions tangent to S. We now turn to their variation along the two normals.

We have from (5.4),

$$\nabla_\beta\ell_{(A)\alpha} = 2\ell_{(A)[\alpha}\partial_{\beta]}\lambda + \nabla_\alpha\,\ell_{(A)\beta}. \tag{5.68}$$

Multiplying by $\ell^{\beta}_{(B)}$ and symmetrizing in A, B gives

$$(\ell_{(B)} \cdot \nabla)\ell_{(A)} + (\ell_{(A)} \cdot \nabla)\ell_{(B)} = 2\ell_{((A)}D_{B)}\lambda - \eta_{AB}e^{\lambda}\nabla\lambda \tag{5.69}$$

where $D_A\lambda$ is defined as in (5.22). It follows that

$$\nabla\lambda = e^{-\lambda}\ell^{(A)}D_A\lambda + e^{(a)}\partial_a\lambda. \tag{5.70}$$

On the other hand, the *difference* of the two terms on the left of (5.69) is given by (5.19) as $\epsilon_{AB}\omega_a e^{(a)}$. Adding finally yields

$$(\ell_{(B)} \cdot \nabla)\ell_{(A)} = N_{ABC}\ell^{(C)} - e^{\lambda}L_{BAa}e^{(a)}, \tag{5.71}$$

where

$$N_{ABC} = D_{(A}\lambda\eta_{B)C} - \frac{1}{2}\eta_{AB}D_C\lambda, \tag{5.72}$$

and L was defined in (5.67).

Proceeding finally to the transverse variation of $e_{(a)}$, we have from (5.14) and (5.9),

$$\frac{\delta e_{(a)}}{\delta u^A} = \frac{\delta}{\delta\theta^a}\left(\ell_{(A)} + s^b_A e_{(b)}\right).$$

Substituting from (5.61) and (5.62), it is straightforward to reduce this to

$$\frac{\delta e_{(a)}}{\delta u^A} = (L_{ABa} - s^b_A e^{-\lambda}K_{Bab})\ell^{(B)} + \widetilde{K}_{Aa}{}^b\, e_{(b)} \tag{5.73}$$

where

$$\widetilde{K}_{Aab} = K_{Aab} + s_{Ab;a}. \tag{5.74}$$

Applying Leibnitz's rule to

$$\partial_A g_{ab} = \frac{\delta}{\delta u^A}(e_{(a)} \cdot e_{(b)}),$$

we read off from (5.73) the result

$$\frac{1}{2}\partial_A g_{ab} = \overline{K}_{Aab} \equiv \widetilde{K}_{A(ab)}, \tag{5.75}$$

which gives direct geometrical meaning to the extrinsic curvature in terms of transverse variation of the 2-metric.

The normal absolute derivatives of $e_{(a)}$ are given by (recalling (5.9) and (5.13))

$$(\ell_{(A)} \cdot \nabla)e_{(a)} = \frac{\delta e_{(a)}}{\delta u^A} - s_A{}^b\frac{\delta e_{(a)}}{\delta\theta^b}.$$

With the help of (5.73) and (5.61) this reduces to

$$(\ell_{(A)} \cdot \nabla) e_{(a)} = L_{ABa} \ell^{(B)} + (\widetilde{K}_{Aa}{}^{b} - s_A{}^{c} \Gamma^{b}_{ac}) e_{(b)} \tag{5.76}$$

Correspondingly, the two normal derivatives of g_{ab} are

$$(\ell_{(A)} \cdot \nabla) g_{ab} = 2\overline{K}_{Aab} - s^{c}_{A} \partial_c g_{ab}. \tag{5.77}$$

The two-dimensionally noncovariant terms which appear in (5.76) and (5.77) are not a mistake. They arise because the normal gradient $\ell_{(A)} \cdot \nabla$, applied to objects carrying lower-case Latin indices—let us say g_{ab}—does not preserve manifest two-dimensional covariance, since it contains (see (5.22)) a piece $-s^{c}_{A} \partial_c g_{ab}$ involving ordinary (rather than two-dimensional covariant) derivatives with respect to θ^c. Although not incorrect, this is a formal impediment: it threatens to clutter our formulae with terms in the shift vectors s^{a}_{A} which are, to boot, noncovariant. In the following section, we explain how this can be remedied by introducing a "rationalized" gradient operator $\widetilde{\nabla}$.

5.10 Rationalized operators $\widetilde{\nabla}$, $\widetilde{D}_A$, ∇_a

The rationalized operator $\widetilde{\nabla}_\alpha$ avoids the two-dimensionally noncovariant terms which appear when ∇_α is applied to objects bearing lower-case Latin indices, as in (5.61), (5.76) and (5.77).

Applied to scalar fields or to 4-tensors not bearing lower-case Latin indices, $\widetilde{\nabla}$ is identical with ∇. If the object does carry such indices, there are supplementary terms involving the two-dimensional connection Γ^{a}_{bc}.

Specifically, we define

$$\widetilde{\nabla}_\alpha = \nabla_\alpha + p^{(a)}_{\alpha} (\nabla_a - e_{(a)} \cdot \nabla) \tag{5.78}$$

in which $e_{(a)} \cdot \nabla \equiv \delta / \delta \theta^a$ is the absolute derivative introduced in (5.13), and the operator ∇_a will be specified in a moment. We have introduced the pair of 4-vectors $p^{(a)} = \nabla \theta^a$, i.e.,

$$p^{(a)}_{\alpha} = \partial \theta^a / \partial x^\alpha. \tag{5.79}$$

Their projections onto the basis vectors are, according to (5.6) and (5.9),

$$p^{(a)} \cdot e_{(b)} = \delta^{a}_{b}, \qquad p^{(a)} \cdot \ell_{(A)} = -s^{a}_{A}, \tag{5.80}$$

from which follows the identity

$$\delta^\beta_\alpha - p^{(a)}_\alpha e^\beta_{(a)} = e^{-\lambda}\ell^{(A)}_\alpha \partial x^\beta/\partial u^A. \tag{5.81}$$

Hence (5.78) can be recast in terms of the absolute derivative $\delta/\delta u^A$:

$$\widetilde{\nabla} = e^{-\lambda}\ell^{(A)}\partial/\partial u^A + p^{(a)}\nabla_a. \tag{5.82}$$

We next introduce the differential operator

$$\widetilde{D}_A \equiv \ell_{(A)}\cdot\widetilde{\nabla} = \ell_{(A)}\cdot\nabla - s^a_A(\nabla_a - \delta/\delta\theta^a). \tag{5.83}$$

An alternative form

$$\widetilde{D}_A = \delta/\delta u^A - s^a_A\nabla_a \tag{5.84}$$

follows from (5.82).

Since $e_{(a)}\cdot\widetilde{\nabla} = \nabla_a$, we can reconstruct $\widetilde{\nabla}$ from (5.83) in yet another form:

$$\widetilde{\nabla} = e^{-\lambda}\ell^{(A)}\widetilde{D}_A + e^{(a)}\nabla_a. \tag{5.85}$$

We now specify the operator ∇_a. It is defined so as to act as a two-dimensional covariant derivative on all lower-case Latin indices (including parenthesized ones), and at the same time as an absolute derivative $\delta/\delta\theta^a$ on Greek indices. Upper-case Latin indices are treated as inert.

As an example,

$$\nabla_b e_{(a)} = \delta e_{(a)}/\delta\theta^b - \Gamma^c_{ab}e_{(c)}. \tag{5.86}$$

It is evident that, quite generally, the "correction" $\nabla_a - \delta/\delta\theta^a$ in (5.83) and (5.78) is linear and homogeneous in the two-dimensional connection Γ^c_{ab}.

Examples of how ∇_a and $\widetilde{D}_A$ act on scalars and 2-tensors are

$$\begin{array}{ll} \nabla_a f = \partial_a f, & \widetilde{D}_A f = (\partial_A - s^a_A\partial_a)f = D_A f, \\ \nabla_a X^{b\ldots}_{c\ldots} = X^{b\ldots}_{c\ldots;a}, \widetilde{D} & \widetilde{D}_A X^{b\ldots}_{c\ldots} = (\partial_A - s^a_A\nabla_a)X^{b\ldots}_{c\ldots}. \end{array} \tag{5.87}$$

For the 2-metric g_{ab}, we have from (5.84),

$$\widetilde{D}_A g_{ab} = \partial_A g_{ab}, \tag{5.88}$$

since $\nabla_c g_{ab} \equiv g_{ab;c} = 0$. Thus, (5.75) can be expressed as

$$\frac{1}{2}\widetilde{D}_A g_{ab} = \overline{K}_{Aab}, \tag{5.89}$$

which should be contrasted with (5.77).

Similarly, with the aid of (5.86) and (5.83), the noncovariant expressions (5.61) and (5.76) become

$$\nabla_b e_{(a)} = \nabla_a e_{(b)} = -e^{-\lambda} K_{Aab} \ell^{(A)}, \tag{5.90}$$

$$\widetilde{D}_A e_{(a)} = L_{ABa} \ell^{(B)} + \widetilde{K}_{Aab} e^{(b)}. \tag{5.91}$$

Quite generally, $\widetilde{D}_A$, ∇_a and $\widetilde{\nabla}$ preserve both four-dimensional covariance and covariance under "rigid" two-dimensional co-ordinate transformations $\theta^a \to \theta^{a'} = f^a(\theta^b)$, with no dependence on u^A. (u-dependence of f^a would induce "gauge" transformations of the shift vectors s^a_A, see the remarks following (5.26).)

With the aid of (5.85), the last two results can be put together to form the rationalized covariant derivative of $e_{(a)}$:

$$e^{\lambda} \widetilde{\nabla}_\beta e_{(a)\alpha} = (L_{BAa} \ell^{(A)}_\alpha + \widetilde{K}_{Bab} e^{(b)}_\alpha) \ell^{(B)}_\beta - K_{Aab} \ell^{(A)}_\alpha e^{(b)}_\beta. \tag{5.92}$$

Equations (5.62) and (5.71) similarly combine to produce

$$\nabla_\beta \ell_{(A)\alpha} = (e^{-\lambda} N_{ABC} \ell^{(C)}_\alpha - L_{BAa} e^{(a)}_\alpha) \ell^{(B)}_\beta + (L_{ABb} \ell^{(B)}_\alpha + K_{Aab} e^{(a)}_\alpha) e^{(b)}_\beta. \tag{5.93}$$

(No distinction here between $\widetilde{\nabla}$ and ∇, since $\ell_{(A)}$ carries no lower-case Latin indices.)

To sum up: equations (5.92) and (5.93) encapsulate the full set of first-order (Gauss-Weingarten) equations, which control tangential and normal variations of the basis vectors $e_{(a)}$, $\ell_{(A)}$. The coefficients in these equations are given by (5.16), (5.67), (5.20), (5.72) and (5.74). Their geometrical meaning emerges from (5.75), (5.19) and remarks following those equations.

5.11 Rationalized Ricci commutation rules

The usual commutation relations need to be modified for $\widetilde{\nabla}_\alpha$. To derive the modified form, consider the action of $\widetilde{\nabla}$ on any field object X_a bearing just one lower-case Latin and an arbitrary set of other indices.

From (5.78) and (5.86),

$$\widetilde{\nabla}_\gamma \widetilde{\nabla}_\beta X_a = (\delta^c_a \nabla_\gamma - p^{(n)}_\gamma \Gamma^c_{na})(\delta^b_c \nabla_\beta - p^{(m)}_\beta \Gamma^b_{mc}) X_b.$$

Skew-symmetrizing with respect to β and γ, and noting from (5.79) that $\nabla_{[\gamma} p^{(m)}_{\beta]} = 0$ leads to

$$\widetilde{\nabla}_{[\gamma}\widetilde{\nabla}_{\beta]}X_a = \nabla_{[\gamma}\nabla_{\beta]}X_a + p^{(m)}_{[\beta}\{p^{(n)}_{\gamma]}\frac{1}{2}R^b{}_{amn} - e^{-\lambda}\ell^{(A)}_{\gamma]}\partial_A\Gamma^b_{ma}\}X_b, \tag{5.94}$$

in which $\partial_\gamma\Gamma^b_{ma}$ has been expanded using

$$\partial_\gamma = e^{-\lambda}\ell^{(A)}_\gamma\partial_A + p^{(n)}_\gamma\partial_n, \tag{5.95}$$

which is a special case of (5.82).

The right-hand side of (5.94) can be further reduced: $\partial_A\Gamma^b_{ma}$ is a 2-tensor, given by

$$\partial_A\Gamma^b_{ma} = 2\overline{K}^b_{A(a;m)} - \overline{K}_{Ama}{}^{;b} \tag{5.96}$$

according to (5.75); and in two dimensions we have

$$R^b{}_{amn} = {}^{(2)}R\delta^b_{[m}g_{n]a}. \tag{5.97}$$

If $e^\alpha_{(a)}$ is substituted for X_a, (5.94), (5.92) and (5.93) can be used to express the projection onto $e_{(a)}$ of the four-dimensional Riemann tensor in terms of the first-order Gauss-Weingarten variables K, L, N and their derivatives. If our interest is primarily in the Ricci tensor, the contracted form ($\gamma = \alpha$) of (5.94) suffices:

$$(\widetilde{\nabla}_\alpha\widetilde{\nabla}_\beta - \widetilde{\nabla}_\beta\widetilde{\nabla}_\alpha)e^\alpha_{(a)} = e^\alpha_{(a)}R_{\alpha\beta} - \frac{1}{2}{}^{(2)}Rp_{(a)\beta} + e^{-\lambda}(\partial_a\overline{K}_A)\ell^{(A)}_\beta \tag{5.98}$$

where

$$\overline{K}_A \equiv \overline{K}^a_{Aa} = \partial_A \ln g^{\frac{1}{2}} \tag{5.99}$$

and $g \equiv \det g_{ab}$.

5.12 Contracted Gauss-Codazzi (second order) relations. Ricci tensor

The Gauss-Codazzi relations are the integrability conditions of the system of first order (Gauss-Weingarten) differential equations (5.92), (5.93). As just noted, they express projections of the four-dimensional Riemann tensor in terms of K, L, N and their first derivatives.

Contraction of these equations gives frame components of the Ricci tensor. The most concise way of deriving these components in practice is through recourse to a generalized form of Raychaudhuri's equation [53].

Let A^α be an arbitrary 4-vector (which may bear arbitrary label indices) and B^α a second vector free of lower-case Latin indices, so that $\widetilde{\nabla}_\beta B^\alpha = \nabla_\beta B^\alpha$ and the standard commutation rules apply. Then it is easy to check the identity

$$R_{\alpha\beta}A^\alpha B^\beta = \widetilde{\nabla}_\beta(A^\alpha \nabla_\alpha B^\beta) - A^\alpha \nabla_\alpha(\nabla_\beta B^\beta) - (\widetilde{\nabla}_\beta A^\alpha)(\nabla_\alpha B^\beta). \tag{5.100}$$

If, on the other hand, B is replaced by $e_{(b)}$, then we call upon the commutation law (5.98) for $\widetilde{\nabla}$, with the result

$$\begin{aligned} R_{\alpha\beta}A^\alpha e^\beta_{(b)} &= \widetilde{\nabla}_\beta(A^\alpha \widetilde{\nabla}_\alpha e^\beta_{(b)}) - A^\alpha \widetilde{\nabla}_\alpha(\widetilde{\nabla}_\beta e^\beta_{(b)}) - (\widetilde{\nabla}_\beta A^\alpha)(\widetilde{\nabla}_\alpha e^\beta_{(b)}) \\ &\quad + \frac{1}{2}\,{}^{(2)}R(A\cdot p_{(b)}) - e^{-\lambda}(\partial_b \overline{K}_B)(A\cdot \ell^{(B)}). \end{aligned} \tag{5.101}$$

With the choices $A = \ell_{(A)}$ and $e_{(a)}$, $B = \ell_{(B)}$ we can recover all frame components of the Ricci tensor from these equations in tandem with (5.92) and (5.93).

Some details of these calculations are recorded in Appendix B. The final results have already been listed in (5.27)–(5.29).

We next turn to the contracted Bianchi identities. The projection of (5.30) onto $e_{(a)}$ yields

$$\widetilde{\nabla}_\beta(R^\beta_\alpha e^\alpha_{(a)}) - R^\beta_\alpha \widetilde{\nabla}_\beta\, e^\alpha_{(a)} = \frac{1}{2}\partial_a R.$$

The second term is evaluated with the aid of (5.92). In the first term, we expand

$$e^\alpha_{(a)} R^\beta_\alpha = R^b_a e^\beta_{(b)} + e^{-\lambda} R^A_a \ell^\beta_{(A)},$$

and note the (often used) results

$$\widetilde{\nabla}_\beta\, e^\beta_{(b)} = \partial_b \lambda, \qquad \nabla_\beta\, \ell^\beta_{(A)} = K_A + D_A \lambda, \tag{5.102}$$

which follow from (5.92) and (5.93). The result is (5.32), and (5.33) is obtained similarly.

5.13 Riemann tensor

We list here the tetrad components of the Riemann tensor, obtainable from the uncontracted Ricci commutation rules (see, e.g., (5.94)). The notation for the tetrad

components is as in Sec. 5.4.

$$
\begin{aligned}
{}^{(4)}R^{ab}{}_{cd} &= {}^{(2)}R\,\delta^a_{[c}\delta^b_{d]} - 2e^{-\lambda}K^{\ a}_{A[c}K^{Ab}_{d]} \\
R_{ABCD} &= \frac{1}{4}\,\epsilon_{AB}\,\epsilon_{CD}(2e^{\lambda}D^E D_E\lambda - 3\omega^a\,\omega_a + e^{2\lambda}\lambda^{,a}\lambda_{,a}) \\
R_{Aabc} &= 2K_{Aa[b;c]} - K_{Aa[b}\lambda_{,c]} - e^{-\lambda}\,\epsilon_{AB}K^B_{a[b}\omega_{c]} \\
R_{aABC} &= \frac{1}{2}\,\epsilon_{BC}\{D_A\omega_a + K_{Aab}\,\omega^b - e^{\lambda}\,\epsilon_{AE}(D^E\partial_a\lambda - K^E_{ab}\lambda^{,b}) - \omega_a D_A\lambda\} \\
R^{A\ B}_{\ a\ b} &= -D^{(A}K^{B)}_{ab} + K^A_{bd}K^{Bd}_a + D^{(A}\lambda\,K^{B)}_{ab} - \frac{1}{2}\eta^{AB}D_E\lambda\,K^E_{ab} \\
&\qquad -\frac{1}{4}\eta^{AB}(e^{-\lambda}\omega_a\omega_b + e^{\lambda}\lambda_{,a}\lambda_{,b} + 2e^{\lambda}\lambda_{;ab}) - \frac{1}{4}\epsilon^{AB}g^{\frac{1}{2}}\,\epsilon_{ab}\tau.
\end{aligned}
$$

We have here defined

$$e^{-\lambda}\tau = g^{-\frac{1}{2}}\,\epsilon^{ab}\,\partial_a(e^{-\lambda}\omega_b)$$

5.14 Concluding remarks

The (2+2) double-null imbedding formalism developed in this chapter leads to simple and geometrically transparent expressions for the Einstein field equations (5.27)–(5.29) and the Einstein-Hilbert action (5.96). It should find ready application in a variety of areas, as indicated in the Introduction.

(2+2) formalisms are certainly not new [45, 46], but they have languished on the relativist's back-burner. We hope that this exposition will play a role in promoting these versatile methods from the realm of esoterica into an everyday working tool.

Chapter 6

Generic structure of the Cauchy horizon

In this final chapter we will apply the double null formalism developed in the last chapter to explore the generic structure of the Cauchy horizon. By generic we mean that there are no assumptions made about the initial data except that they should originate from a realistic gravitational collapse, i.e. they should exhibit the Price behaviour. In mathematical terms this means we can, once the gauge is fixed, specify two arbitrary functions of three variables on each of the characteristic initial surfaces. (A somewhat different definition of a generic singularity is given in [56].) In this sense the mass inflation singularity offers an alternative to the BKL [36] singularity which was thought to be the only generic singularity.

The analysis of the field equations is tricky but not impossible. What we attempt to find is a self-consistent approximation to the true solution of Einstein's equations for a given class of initial conditions. We construct this approximation by making use of our insider knowledge: Choosing a convenient gauge we expect certain quantities (the mass function, or more precisely the conformal curvature) to diverge. Thus it makes sense to expand in inverse powers of this diverging quantity to obtain a set of zeroth order equations. It should not come as a surprise that these equations are very similar to the ones discussed in Chapter 3.

To begin we review the plane wave model presented in section 3.2 which fits naturally into this framework. The insight gained in this warm-up exercise will then guide us through the treatment of the more complicated generic case. To start this we first discuss the gauge and boundary conditions before solving the full set of

Einstein's equations. At the end of the chapter we will briefly describe the results of some numerical work.

6.1 Plane wave mass-inflation revisited

In accordance with the notation introduced in Chapter 5 we rewrite the metric (3.9) as

$$ds^2 = -2e^{\lambda} du dv + r^2 \left(e^{2\beta} dx^2 + e^{-2\beta} dy^2 \right),$$

where the relation between λ and σ is given by $\lambda = 2\sigma - \log r$. To keep matters simple we restrict the functions λ, β and r to depend only on the null coordinates u and v.

The initial data will be posed on the two characteristic initial surfaces $\Sigma^u : u = u_0 = const.$ behind the event horizon and $\Sigma^v : v = v_0 = const.$ before the Cauchy horizon. Note that we cannot choose Σ^u to coincide with the event horizon. This is for two reasons. First it is not clear that any asymptotic expansion around the Cauchy horizon still gives valid results near the event horizon. (Remember from Figure 7 that the event horizon is never "near" the Cauchy horizon.) But more importantly we don't expect our approximation to be good near the event horizon. The curvature (or mass function) is finite and small near the event horizon. Thus expanding in inverse curvatures would be a rather bad idea near the event horizon. Furthermore we don't want to deal, in this part of the analysis, with the scattering process inside the black hole because it already is well handled by the perturbation analysis on the Reissner Nordström background performed in Chapter 4. Thus we want to set boundary data which are a result of scattered radiation falling into the hole. From all this we conclude that the two characteristic initial surfaces should lie behind, i.e. to the future, of the internal potential barrier.

Let us now specify the gauge and initial conditions. In view of Chapters 3 and 4 it is most convenient to choose u and v such that

$$\begin{aligned} (r^2)_{,u} &= -(\alpha_u)^2 |u|^{-p} \quad \text{on } \Sigma^v \\ (r^2)_{,v} &= -(\alpha_v)^2 v^{-q} \quad \text{on } \Sigma^u, \end{aligned}$$

so that $u \to -\infty$ leads towards the event horizon and $v \to \infty$ towards the Cauchy horizon. (Another possible choice would be $(r^2)_{,v} = 1$ and $(r^2)_{,u} = -1$ on the respective initial surfaces.)

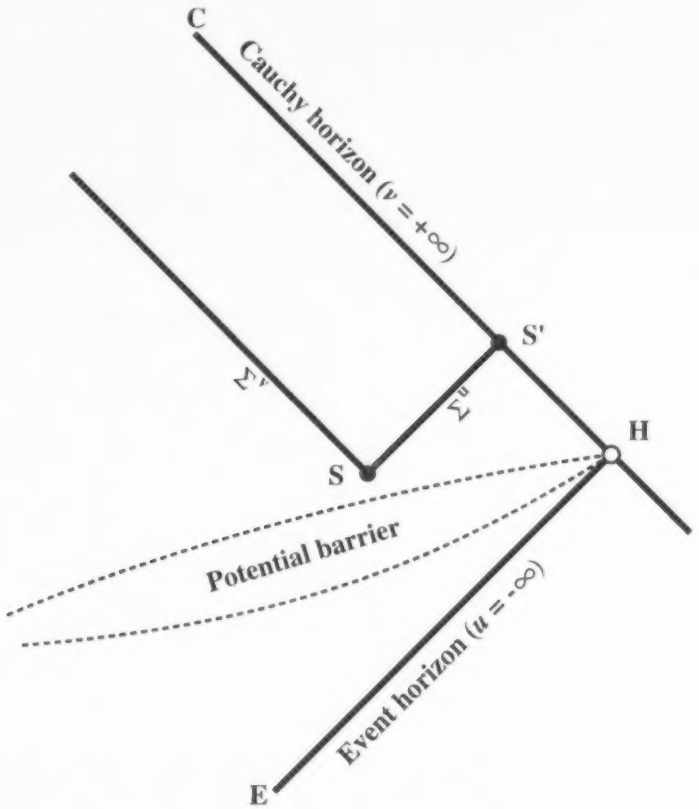

Figure 11: The conformal diagram representing the interior of a general black hole. The initial data are given on the two characteristics Σ^u and Σ^v which intersect in the two-space S. The surface Σ^u is located behind the event horizon and intersects the Cauchy horizon in a two-surface S'.

The scalar field analysis of section 4.1 suggests initial data of the form

$$\begin{aligned} \beta_{,u} &= |u|^{-p/2} f_u(u) \quad \text{on } \Sigma^v \\ \beta_{,v} &= v^{-q/2} f_v(v) \quad \text{on } \Sigma^u. \end{aligned}$$

The functions f_A $(A = u, v)$ are arbitrary except for the requirement that they shall not vanish anywhere and that the $\beta_{,u}$ and $\beta_{,v}$ have finite limits as $u \to -\infty$ and $v \to \infty$ respectively. These requirements certainly make sense for $b_{,v}$. But one might ask what meaning this has for $\beta_{,u}$ as Σ^v lies at a finite value $u = u_0$. However we can choose u_0 as small as we want and the limit $u \to -\infty$ is understood in this sense. These restrictions are not very severe. They even allow for mildly divergent f_A's.

Lastly we have to specify λ on the two-surface S. As we have excluded any θ^a dependence of our metric functions, λ is just constant on S.

Clearly, for the above metric the shifts s^a_A, and thus also the twist ω^a, vanish. Therefore $K_{Aab} = \overline{K}_{Aab}$ and we drop the bar for the remainder of this section.

The only nontrivial tetrad components of the Ricci tensor then read

$$\begin{aligned} {}^{(4)}R_{ab} &= -e^{\lambda}\left[(\partial_A + K_A)K^A{}_{ab} - 2K_{Ad(a}K^{Ad}{}_{b)}\right] = 0 \\ R_{AB} &= -\partial_{(A}K_{B)} - K_{Aab}K_B{}^{ab} + K_{(A}\partial_{B)}\lambda - \frac{1}{2}\eta_{AB}\left(\partial_D + K_D\right)\partial^D\lambda = 0. \end{aligned}$$

Using equations (5.45) and (5.48) for the expansion and the shear we find

$$\sigma_{Aba} = r^2\beta_{,A}\mathrm{diag}(e^{2\beta}, e^{-2\beta}) \text{ and } K_A = (\log r^2)_{,A}.$$

Using these expressions, the $R_{AA} = 0$ equation becomes

$$\left(\lambda + \log r^2\right)_{,A} = \frac{1}{(r^2)_{,A}}\left((r^2)_{,AA} + 2\left(\beta_{,A}\right)^2 r^2\right)$$

which we can easily integrate for λ on the initial surfaces Σ^B $(B \neq A)$. Doing so for $u^A = v$ on Σ^u we find asymptotically for large values of v

$$\lambda + \log r^2 \simeq -\int_{v_o}^{v} dv f_v^2(v) r_0^2 - q\log v + O(1/v) \tag{6.1}$$

where r_0 is the value of r on the Cauchy horizon (i.e. the value of r on S' in Figure 11). Because the integrand is strictly positive we see that $\lambda \to -\infty$ as $v \to \infty$.

In a similar fashion one shows that on Σ^v

$$\lambda + \log r^2 \simeq +\int_{u_0}^{|u|} du f_u^2(u)\overline{r}_0^2 - p\log u + O(1/u) \tag{6.2}$$

where $\overline{r}_0$ is the value of r on S. Thus $\lambda \to +\infty$ as $u \to -\infty$.

We are now ready to solve for the functions r^2, λ and β in the region enclosed by the characteristics Σ^A.

The trace $g^{ab\,(4)}R_{ab} = 0$ gives the wave equation for r^2

$$\partial_A K^A + K_A K^A = -2\frac{(r^2)_{,uv}}{r^2} = 0.$$

It has a solution

$$r^2 = r_0^2 + \frac{\alpha_v^2}{q-1}v^{1-q} - \frac{\alpha_u^2}{p-1}|u|^{1-p}$$

which satisfies the boundary conditions and is well-behaved for all the interesting values of u and v.

The wave equation for λ derives from $R_{uv} = 0$ and is

$$\lambda_{,uv} = \frac{1}{2}\frac{(r^2)_{,u}(r^2)_{,v}}{r^2} - 2\beta_{,u}\beta_{,v} = 0. \tag{6.3}$$

If $\beta_{,A}$ is regular the right hand side of equation (6.3) is well behaved and finite. The solution to (6.3) is thus

$$\lambda = \int dudv \left(\frac{1}{2}\frac{(r^2)_{,u}(r^2)_{,v}}{r^2} - 2\beta_{,u}\beta_{,v}\right) + F_u(u) + F_v(v). \tag{6.4}$$

The two functions F_A are determined by the boundary values for λ on the initial surfaces Σ^A. Comparing (6.4) with equations (6.1) and (6.2) we find

$$\begin{aligned} F_v(v) &\simeq -\int_{v_o}^{v} dv f_v^2(v) r_0^2 - q\log v + O(1/v) \\ F_u(u) &\simeq +\int_{u_o}^{|u|} du f_u^2(u) \overline{r}_0^2 - p\log u + O(1/u) \end{aligned}$$

which, of course, agrees with the result of Chapter 3.

The wave equation for β is the same as in Chapter 3:

$$2\beta_{,uv} + \beta_{,u}(\log r^2)_{,v} + \beta_{,u}(\log r^2)_{,v} = 0. \tag{6.5}$$

The same comments as in Section 3.2 apply, and (6.5) has a series solution which exhibits the power law fall-off imposed by the boundary data.

Thus, naturally, the double null formalism yields the same results as before. The important points to keep in mind though are that we expect the shear σ_{Aab} to stay finite, but λ to diverge in the described manner. To treat the full case, i.e. allow for a θ^a dependence as well as the existence of a nonvanishing shift s_u^a (we can always gauge one of the shift vectors s_A^a to zero), we will use this behaviour of λ. In a first approximation we neglect all the terms that are suppressed by a factor e^λ. This is where the double null formalism comes in handy. All the equations are already ordered in powers of e^λ. Again we stress the point that we perform a *self-consistent* analysis. The results of our approximations should not contradict these very approximations, i.e. terms assumed to be small should not be forced to become large by some equation, etc. With this in mind let us now proceed to uncover the generic structure of the Cauchy horizon.

6.2 The generic structure of the Cauchy horizon

6.2.1 Gauge and initial conditions

The setup for the general characteristic initial value problem treated in this section is much the same as in the plane wave case. We start with two characteristic initial surfaces Σ^u and Σ^v, as shown in Figure 11, on which we give the initial data.

As mentioned before we are free to choose one of the shift vectors s^a_A to vanish globally. It seems natural to choose $s^a_v = 0$, as we are mainly interested in the limit $v \to \infty$. We are still free to choose s^a_u on one hypersurface $v = const.$ The most convenient choice is that s^a_u vanishes on the Cauchy horizon, i.e. in the limit $v \to \infty$. If we were to choose a "large" s^a_u we would be choosing a coordinate system that would twist near the Cauchy horizon, and thus artificially make certain quantities behave singularly, which otherwise would be small for a better choice of coordinates.

As before we now have to specify the null coordinates u and v. But rather than giving the derivatives of $r^2 = \sqrt{det(g_{ab})}$ we choose to set

$$K_v = -\alpha_v^2(\theta^a)v^{-q} \text{ on } \Sigma^u \tag{6.6}$$

$$K_u = -\alpha_u^2(\theta^a)|u|^{-p} \text{ on } \Sigma^v \tag{6.7}$$

for some yet unspecified functions $\alpha_u(\theta^a)$.

The initial data are encoded in the shear σ_{Aab} and are, as argued before, of the form

$$\sigma_{vab} = v^{-q/2} f_{vab}(v, \theta^a) \text{ on } \Sigma^u \tag{6.8}$$

$$\sigma_{uab} = |u|^{-q/2} f_{uab}(u, \theta^a) \text{ on } \Sigma^v. \tag{6.9}$$

The two functions f_A of the last section have now been promoted to two matrix valued functions $f_{Aab}(u^A, \theta^a)$. As before, we require $\sigma_{Aab} \to 0$ in the respective limits $|u|^A \to \infty$, and $f_{Aab} f_A{}^{ab} \neq 0$ for large enough values of $|u^A|$. Note that the functions f_{Aab} and α_A are not always independent . If $\omega^a = 0$ then we have, on say Σ^u, the two equations

$$R_{vv} = -K_{v,v} - \frac{1}{2}(K_v)^2 - \sigma_{vab}\sigma_v{}^{ab} + K_v\lambda_{,v} = 0$$

$$R_{va} = \sigma_{va;b}{}^{b} - \frac{1}{2}\lambda_{,va} + \frac{1}{2}K_v\lambda_{,v} = 0.$$

From these equations we can eliminate λ and its derivatives to obtain a complicated relation between K_v and σ_{vab}, and similarly for K_u and σ_{uab} on Σ^v. This fact will have some physical consequences, as we will shall see below.

Finally we have to give $\omega^a(\theta^b)$ and $\lambda(\theta^b)$ on the two surface $S = \Sigma^u \cap \Sigma^v$. This fully specifies the characteristic initial value problem describing the neighbourhood of the Cauchy horizon.

6.2.2 Integration of Einstein's equations

In the first step we have to determine the functions λ and ω^a on the entire characteristics Σ^A from their initial values on S. Let us start with the $R_{vv} = 0$ equation for λ. On Σ^u we find

$$\lambda_{,v} = (\log K_v)_{,v} + \frac{1}{2} K_v + \sigma_{vab}\sigma_v{}^{ab}.$$

Thus, using equations (6.6) and (6.8) we get

$$\lambda = -q \log v - \alpha_v^2(\theta^a) v^{-q/2} - \int_{v_0}^{v} dv f_{vab}(\theta^a) f_v{}^{ab}(\theta^a)/\alpha_v^2(\theta^a) + \lambda_0(\theta^a) \tag{6.10}$$

where λ_0 is determined by the boundary data for λ on S. Note that the integrand is a positive and nonzero function so that the integral must diverge as $v \to \infty$. Indeed we can bound the integral from below. Let $\kappa_v^2 = \min f_{vab} f_v{}^{ab}/\alpha_v^2$ for all v, θ^a. Because $f_{vab} f_v{}^{ab} \neq 0$ it follows that $\kappa_v^2 > 0$ and thus $\lambda < -p \log v - \kappa_v^2 v + const.$ as $v \to \infty$. Thus, at least on Σ^u, λ diverges on the Cauchy horizon.

The next step is to determine the twist ω^a on Σ^u. The leading order of the equation $e^\lambda R_{va} = 0$ is rather simple, as $s_v^a = 0$:

$$(\partial_v + K_v - \lambda_{,v})\, \omega_a = 0$$

which has the solution

$$\omega_a = \omega_0 e^{\lambda - \int_{v_0}^{v} K_v dv}.$$

Using the fact that $K_v = (\log r^2)_{,v}$ we get

$$\omega_a = \omega_0 e^\lambda / r^2 \tag{6.11}$$

where ω_0 is determined by the initial data on S. Because of our choice for the asymptotic behaviour of s_u^a we find that $s_u^a \sim e^\lambda$ because for $s_v^a = 0$ we have $\omega^a = -\partial_v s_u^a$. On first sight the integration for ω^a seems a little more tricky on Σ^v as $s_u^a \neq 0$. However ω_a is always of the form (6.11) on any $u = const.$ surface but with a different ω_0. Thus we expect $s_u^a \sim e^\lambda$ everywhere. To keep the analysis consistent we therefore have to set $D_u = \partial_u + O(e^\lambda)$. To our approximation we then find

$$(\partial_u + K_u - \lambda_{,u})\, \omega_a = 0$$

which is satisfied by (6.11). Here we have used the fact that now $K_u = \overline{K}_u + O(e^\lambda)$.

Now that we have s^a_u "out of the way", i.e. exponentially small, we can analyze the $R_{uu} = 0$ equation

$$\lambda_{,u} = (\log K_u)_{,u} + \frac{1}{2} K_u + \sigma_{uab}\sigma_u{}^{ab}$$

so that on Σ^v

$$\lambda = -p \log u - \alpha_u^2 u^{-p/2} + \int_{u_0}^{|u|} du f_{uab}(\theta^a) f_u^{ab}(\theta^a)/\alpha_u^2(\theta^a) + \tilde{\lambda}_0(\theta^a). \tag{6.12}$$

Again $\tilde{\lambda}_0$ is a function determined by the boundary data on S. Note the sign difference of the integral compared to (6.10). Thus in the limit of large negative u, λ goes to $+\infty$.

So far our analysis of λ has been confined to the two characteristics Σ^A. The behaviour of λ on two intersecting null surfaces has been analyzed before by Brady and Chambers [57] with the same result. In fact these authors set Σ^v on the Cauchy horizon and showed that the Weyl curvature there is singular.

However it is now possible to solve, at least to leading order, the full set of wave equations describing the gravitational field near the Cauchy horizon. The fact that e^λ is expected to go to zero (and does so at least on Σ^u) makes this analysis possible. Let us first look at

$$e^\lambda g^{ab(4)} R_{ab} = 2\frac{(r^2)_{,uv}}{r^2} = 0.$$

Again we have used the fact that to our approximation $K_A \simeq (\log r^2)_{,A}$. Thus we find

$$r^2 = r_0^2 + g_v(v, \theta^a) + g_u(u, \theta^a).$$

Comparing this expression to the boundary data (6.6) and (6.7) we find

$$\begin{aligned} g_v(v, \theta^a) &\sim v^{1-q} \\ g_u(u, \theta^a) &\sim |u|^{1-p}. \end{aligned}$$

Again the expansion K_A decays as an inverse power law in u (respectively v) for the respective limits. The key point is that r^2 does not go to zero as $v \to \infty$ but to a finite value. If this were not the case our approximation would break down (because $1/r^2$ would be large) and we would be dealing with an $r = 0$ type singularity which has a very different structure from the mass-inflation singularity.

Next we look at the wave equation $R_{uv} = 0$, for λ which to lowest order reads

$$\lambda_{,uv} = \partial_{(u}K_{v)} + \frac{1}{2}K_u K_v + \sigma_{uab}\sigma_v{}^{ab}.$$

We can formally integrate this equation for λ

$$\lambda = \int dudv \left(\partial_{(u}K_{v)} + \frac{1}{2}K_u K_v + \sigma_{uab}\sigma_v{}^{ab}\right) + F_u(u,\theta^a) + F_v(v,\theta^a). \tag{6.13}$$

The two functions F_A are determined by the boundary data on Σ^B. We will argue below that the shear σ_{Aab} does not diverge but in fact decays as an inverse power of u and v. Thus the source term over which we integrate exhibits an inverse power law decay from which it follows that the integral itself should stay finite. From the boundary values (6.10) and (6.12) for λ it is clear on the other hand that $F_v(v,\theta^a) \to -\infty$ as $v \to \infty$ and $F_u(u,\theta^a) \to +\infty$ as $u \to -\infty$.

Let us now look at the $R_{Aa} = 0$ equations again. Inserting equation (6.11) we are left with

$$2\sigma_{Aa}{}^{b}{}_{;b} - \lambda_{,Aa} + K_A\lambda_{,a} = O(e^{\lambda}) \simeq 0$$

or after a little algebra,

$$\left(\partial_A - (\log r^2)_{,A}\right)\lambda_{,a} = 2\sigma_{Aa}{}^{b}{}_{;b}. \tag{6.14}$$

This is an equation on surfaces of constant u^B for $\lambda_{,a}$. For $u^B = v$ we can formally integrate (6.14) for $\lambda_{,a}$

$$\lambda_{,a} = 2r^2 \int_{v_0}^{v} dv \frac{\sigma_{Aa}{}^{b}{}_{;b}}{r^2} + h_a(u,\theta^b).$$

The function h_a is determined by the boundary data on Σ^v for $\lambda_{,a}$. These data are regular on the initial surface Σ^v and because the integral is finite (σ_{Aab} is) $\lambda_{,a}$ is finite as $v \to \infty$. This means that the diverging function $F_v(v,\theta^a)$ in (6.13) must be independent of θ^a, i.e. F_v is a function of v only. The same reasoning applied to $\lambda_{,au}$ then tells us that $F_u(u,\theta^a)$ must be independent of θ^a. Thus a pure rescaling of the coordinates u and v can make the metric function e^{λ} a well behaved finite function. (Of course this coordinate transformation would make derivatives of metric functions like g_{ab} diverge. After all we are dealing with a curvature singularity.)

Finally the shear is governed by the traceless part of $R_{ab} = 0$

$$\partial_A \sigma^A_{ab} - 2\sigma_{Ada}\sigma^{Ad}{}_{b} = 0, \tag{6.15}$$

which is the equivalent of (3.12). For nondiagonal g_{ab}, equation (6.15) is nonlinear, which makes its analysis much more difficult than that of equation (3.12).

To see this we write the two-metric as

$$g_{ab} = r^2 \begin{bmatrix} e^{2\beta}\cosh(\gamma) & \sinh(\gamma) \\ \sinh(\gamma) & e^{-2\beta}\cosh(\gamma) \end{bmatrix}, \tag{6.16}$$

so that $\det(g_{ab}) = r^4$. Inserting this into equation (5.45) and (5.48) and simplifying gives

$$\begin{aligned} 2r^2\beta_{,uv} + (r^2)_{,u}\beta_{,v} + (r^2)_{,v}\beta_{,u} + r^2\tanh\gamma\,(\gamma_{,u}\beta_{,v} + \gamma_{,v}\beta_{,u}) &= 0 \\ 2r^2\gamma_{,uv} + (r^2)_{,u}\gamma_{,v} + (r^2)_{,v}\gamma_{,u} - 4\,r^2\sinh(2\gamma)\beta_{,u}\beta_{,v} &= 0. \end{aligned} \tag{6.17}$$

Clearly if $\gamma = 0$ we get equation (3.12) back. However for $\gamma \neq 0$ these two equations are nonlinear and cannot be solved analytically. We therefore have to resort to either perturbative or numerical methods to solve these equations.

Let us first solve these equations perturbatively. There is still the freedom to perform a rigid gauge transformation in the θ^a coordinates so that g_{ab} becomes diagonal at one instant, $u = const.$ and $v = const.$, which we can choose to be S. We can now proceed to show that the shear indeed is bounded.

To zeroth order we can neglect the nonlinear terms in equations (6.17). This is admissible because we have chosen a gauge where γ is small in the region of interest, i.e. near the Cauchy horizon. The resulting equations are again of the form (3.12) and can thus be solved by series of the form (3.16) which indeed decays near the Cauchy horizon.

To get a better approximation we now insert this zeroth order solution into the nonlinear parts and treat the latter as source terms j^0 for the linear equations. The solution to this new system of equations then is a sum of a particular solution to the inhomogeneous equations plus a solution to the homogeneous equations. The latter will be chosen so as to satisfy the boundary data. Let us now proceed to show that a solution obtained in this manner stays bounded and does not diverge near the Cauchy horizon.

Because $(r^2)_{,uv} = 0$ we can, as in Section 3.2, rewrite these equations as

$$\Box\beta^{(1)} := 2\left(\beta^{(1)}_{,XX} - \beta^{(1)}_{,RR} - \frac{\beta^{(1)}_{,R}}{R}\right) = j^0_\beta, \quad \text{and} \quad \Box\gamma^{(1)} = j^0_\gamma,$$

where R and χ are defined in much the same way as in Section 3.2. Note that R and χ in general depend on θ^a. But this dependence affects the solutions of these equations only implicitly through their dependence on R and χ.

In Appendix D we show that these solutions have a formal solution given by equation[1](D.5):

$$\beta^{(1)} = (2\pi)^2 \int dR d\chi \Theta(R - R') j^0_\beta(R', \chi') R' \int dk \, (\alpha_k(R, \chi) \alpha^*_k(R', \chi') + c.c.) \quad (6.18)$$

and similarly for $\gamma^{(1)}$. The functions α_k are the mode solutions to the homogeneous equation $\Box \alpha_k = 0$ and are normalized with respect to the inner product (D.4).

A short calculation shows that these modes are given by

$$\alpha_k = \sqrt{\frac{\pi}{8}} e^{\pm i\chi k} H^{(2)}_0(kR)$$

where $H^{(2)}_0(kR)$ are the second Hankel functions of order zero.

We claim that $\beta^{(1)}$ and $\gamma^{(1)}$ are not diverging. The only potential danger in equation (6.18) comes from the divergence of the Hankel functions as $k \to 0$. However, as is well known $H^{(2)}_0(kR) \propto \log(kR)$ as $k \to 0$. The integral $\int dk \log(kR)^2$ is *not* divergent in this limit. Furthermore, as the source term decays towards the Cauchy horizon we expect the R' and χ' integrals not to diverge either. Thus $\beta^{(1)}$ and $\gamma^{(1)}$ are finite (but not necessarily small) functions near the Cauchy horizon. To satisfy the boundary condition we now have to add appropriate solutions of the homogeneous equations to $\beta^{(1)}$ and $\gamma^{(1)}$. These additions then will ensure that the final result is indeed small near the inner horizon: because the initial data are small there, so that, at least near the initial surfaces, the full solution must be small too.

We can now iterate the shear equations in the described manner to get better and better approximations. But these approximations will always decay, by construction, in the way expected from the boundary data. Thus the shear σ_{Aab} indeed decays as assumed previously.

Even though a perturbative analysis gives a good qualitative picture of the behaviour of the shear, only a numerical solution of equations (6.17) can yield a more

[1]Note that the variables x and y which are used in Appendix D in the derivation of equation (D.5) are in no way related to the coordinates θ^a. While the latter are coordinates of a physical spacetime the former are merely a mathematical construct, used in the derivation of the final result, in which they no longer appear.

quantitative picture of the solution. The lowest order equations (6.17) for the shear and $R_{AA} = 0$ for λ, which now reads

$$\left(\lambda + \frac{1}{2}\log r^2\right)_{,A} = \frac{1}{(r^2)_{,A}}\left((r^2)_{,AA} + 2r^2\beta_{,A}^2\cosh^2\gamma + \frac{r^2}{2}\gamma_{,A}^2\right), \tag{6.19}$$

are sufficiently simple to make a numerical analysis possible. To this order none of the functions β, γ and λ depend on θ^a.

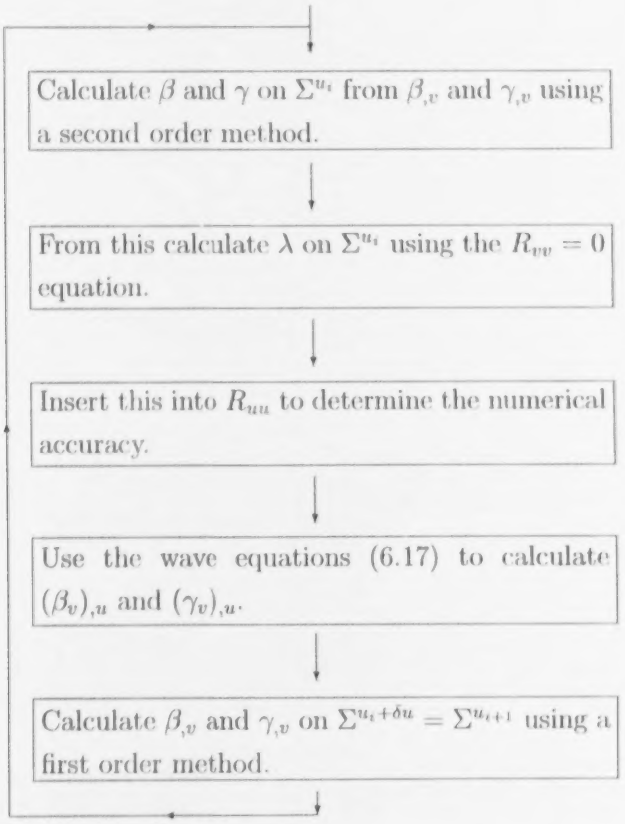
Calculate β and γ on Σ^{u_i} from $\beta_{,v}$ and $\gamma_{,v}$ using a second order method.
From this calculate λ on Σ^{u_i} using the $R_{vv} = 0$ equation.
Insert this into R_{uu} to determine the numerical accuracy.
Use the wave equations (6.17) to calculate $(\beta_v)_{,u}$ and $(\gamma_v)_{,u}$.
Calculate $\beta_{,v}$ and $\gamma_{,v}$ on $\Sigma^{u_i+\delta u} = \Sigma^{u_{i+1}}$ using a first order method.

Figure 12: This flow chart shows the principal workings of the program used to integrate the shear equations (6.17) and the constraints (6.19). Only the main loop of the program is shown. Σ^{u_i} denotes surfaces of constant $u = u_0 + i\delta u$, where δu is the "time" step of the numerical grid.

The coordinates used for the numerical integration are the same u and v coordinates as defined in equations (6.6). We first solve the coupled wave equations for β

and γ and then integrate the $R_{vv} = 0$ for λ. The $R_{uu} = 0$ equation is monitored to keep track of the numerical accuracy. (Another way to solve for λ would have been to solve the wave equation $R_{uv} = 0$ for λ and then use both constraints $R_{AA} = 0$ to check the numerical accuracy.) Figure 12 shows a simplified flow chart of the program.

In a first run we investigated the behaviour of the shear for the Price power law boundary conditions used in the text before. The results of a typical run are shown in Figure 13. Clearly the shear components β and γ show the expected power law behaviour, whereas λ "mass inflates", i.e. behaves as predicted by the approximate solution (6.13) for λ. The Ricci component R_{uu}, shown in the lower right of Figure 13, does not vanish as it should, due to numerical errors. However as we increase the number of grid points R_{uu} becomes smaller.

To see how sensitive mass inflation is to the exact form of the boundary conditions we performed a second set of numerical integrations in which we replaced the Price tail initial data for $\gamma_{,A}$ by a Gaussian wave packet. While the quantitative features clearly change, espcially for λ, the qualitative features of mass inflation remain. The larger derivative term of $\gamma_{,A}$ in equation (6.19) in fact drives λ towards large negative values even faster. Note that the difference between the u and v dependence, which was symmetric before, is not too surprising. While before we had symmetric boundary conditions on Σ^u and Σ^v this is no longer the case here. Were we to switch the position of the Gaussians, we would discover a fast decay in the v direction.

Also the asymmetry in the R_{uu} constraint is no mystery. It comes from the fact that λ is calculated using the equation $R_{vv} = 0$, which is integrated from v_0 towards large values of v. As mentioned before, the R_{uu} constraint is increasingly well satisfied with an increasing number of grid points.

Overall it can be said that the numerical solutions of equations (6.17) and (6.19) confirm the predictions made by the perturbative analysis of these equations.

This concludes our analysis of the generic black hole interior. The results of this Chapter indeed seem to confirm the predictions made by the simpler models treated earlier. On top of that, it suggests that the mass inflation scenario is generic in the sense that it allows 2×2 independent functions of three variables each (two on each Σ^A). It is therefore not just an artefact of some special symmetries or boundary conditions.

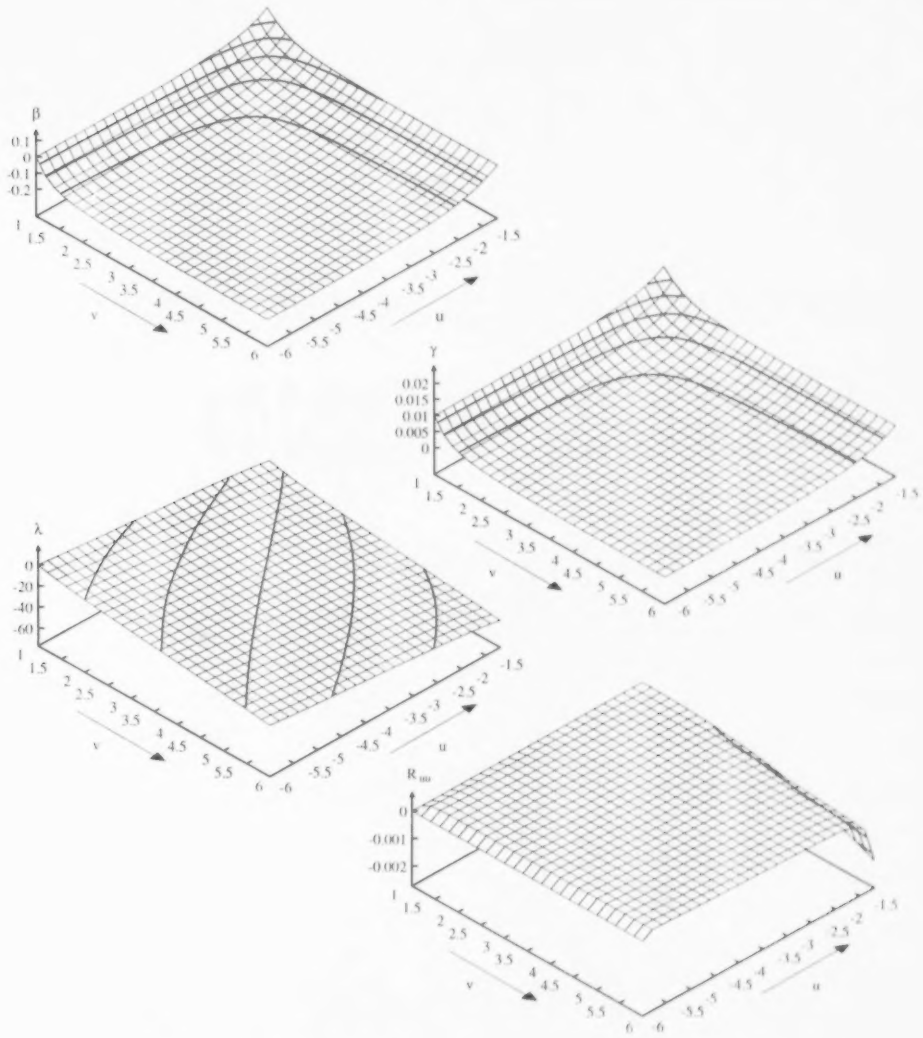

Figure 13: Numerical results for Price power law initial conditions. In this particular simulation we have choosen $q = 12$ and $p = 10$ where p and q are defined in the text. The initial data are set on the lines $u = -6$ and $v = 1$. Increasing v means approaching the Cauchy horizon whereas decreasing u (i.e. going to larger negative values) leads towards the event horizon.

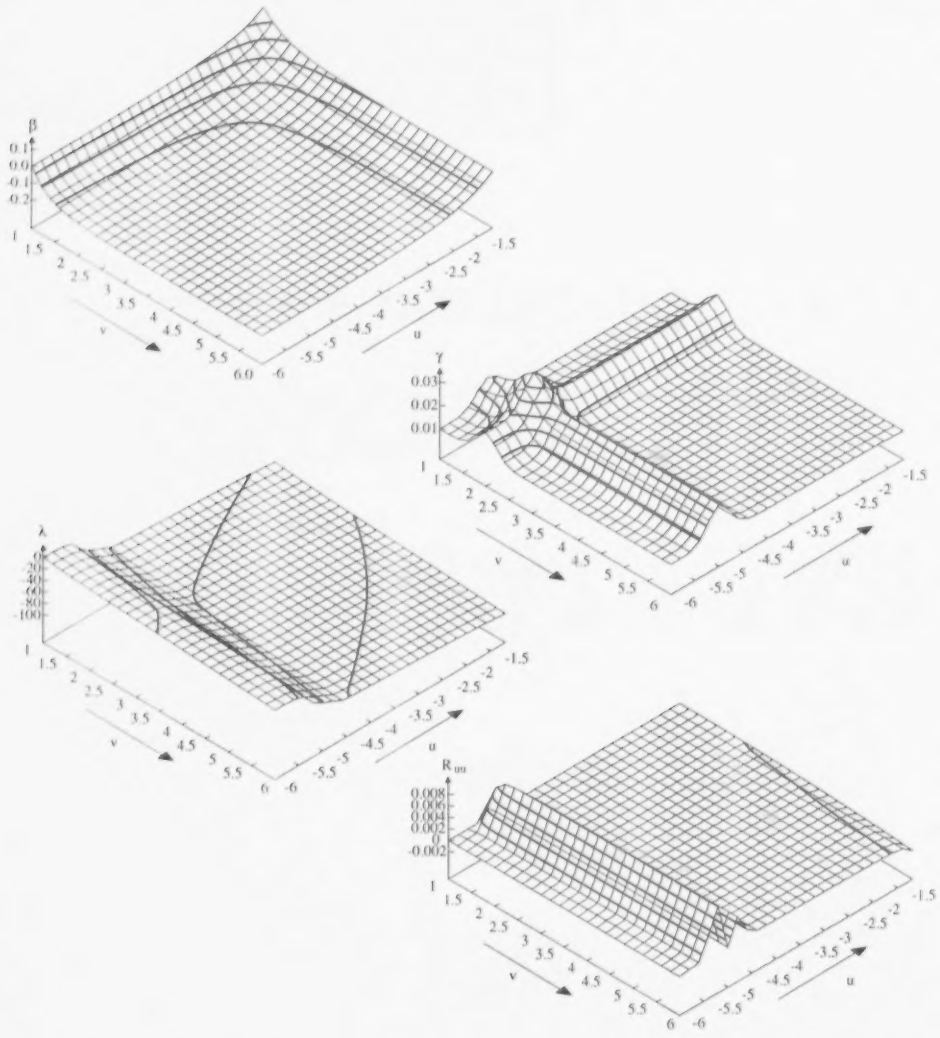

Figure 14: Numerical results for Gaussian initial conditions. The values for p and q are the same as in Figure 13 and so are the boundary conditions for β. Note the much faster falloff of λ compared to Figure 13.

Chapter 7

Conclusions

As we have seen in the introduction, black hole physics has made enormous progress since its difficult birth 80 years ago. This is even more true for the physics of black hole interiors which only really started less than 30 years ago with Penrose's [2] speculations about the instabilities of the inner horizon of a realistic black hole.

It took more than 20 years since these first steps were taken to fully understand the nature of this singularity, first by analyzing Hiscock's pure inflow model [12] and then later by looking at the more realistic cross-flow model of Poisson and Israel [13, 37]. Only now are we at a point where at least the classical aspects of the Cauchy horizon singularity are fully understood.

The analysis presented in Chapters 3, 4 and 6 suggests that the comparatively simple model of Poisson and Israel indeed gives the correct picture: Radiative tails, expected to be present in any stellar collapse fall back into the black hole. Part of these perturbations are then scattered off the internal gravitational potential barrier and start irradiating the initially static inner horizon, which as a result starts to slowly contract.

It is important to note that the scattered tail is far too weak to cause an immediate destruction of the inner horizon, as was suggested by several authors [16, 17, 18]. Indeed the analysis in Chapter 4 shows that initially the inner horizon is static and coincides with the Cauchy horizon of the unperturbed hole.

The contraction of the inner horizon, together with the catastrophic blue shift of the infalling radiation then causes a scalar curvature singularity to form along the inner horizon. This singularity, dubbed mass inflation singularity because of the exponential blow up of the (only in spherical symmetry well-defined) mass function

of the black hole has a rather simple structure, even in the generic case.

While the final $r = 0$ singularity is believed to be of the BKL type [36] (which exhibits chaotic behaviour) the mass inflation singularity seems to be "smooth" in the sense that, at least to leading order in curvatures, all the initial irregularities are damped out exponentially. This behaviour does not change in the presence of shear, as was initially feared [58], and one is tempted to speak of a no-hair theorem for the Cauchy horizon singularity.

What changes from the spherical picture is the presence of nonvanishing Weyl curvature tetrad components besides the Coulomb component Ψ_2. Analyzing their structure shows that the spacetime asymptotically is of Petrov type N [41, 59], indicating the presence of a gravitational shock wave traveling along the contracting Cauchy horizon.

This picture, supported by a recent numerical calculation [43], seems to be fairly robust and earlier doubts about the mass inflation scenario by now are hopefully settled.

Despite this optimistic scenario, there are still open questions. Once curvatures reach Planckian levels, classical physics should no longer be trusted. So far, however, one-loop calculations [60, 61] are are rather inconclusive, as the behaviour of quantum corrections depends crucially on a undetermined length scale, which is introduced into the theory during regularisation. Things look even worse once one allows for a charged core of the black hole. In the absence of any radiative tails, pair production effects lead to the formation of a spacelike $r = 0$ singularity [40] before a Cauchy horizon can form. So far no work has been done to generalize this picture to include gravitational perturbations and it is difficult to guess if pair production or mass inflation wins the race.

Possible answers to these questions might come from the analysis of two dimensional string inspired black holes [62]. These two-dimensional so called dilaton black holes classically exhibit mass inflation [63]. The (in four dimensions) notoriously difficult quantum calculation generally become more tractable in two dimensions. In fact, results for the uncharged case have already been obtained [64] and indicate, that vacuum polarisation effects lead to a much stronger singularity than in the classical case, indicating that a better theory of quantum gravity is needed.

Considering the charged case is much more difficult, as one now deals with interacting theories which are much harder to treat.

It is however desirable to find some more conclusive answers in the four dimensional case, even for pure vacuum fluctuation effects. The plane wave model considered in Section 3.2 might be a good candidate to perform such calculations. While it describes the mass inflation scenario very accurately it is simpler to work with than the spherical models due to the absence of an electric charge. (An electric charge would lead to a more complicated equation for r^2). However chances are that again a one-loop calculation renders rather inconclusive answers and a full, as of yet unknown, theory of quantum gravity is required.

This opens the door to speculation, as it is not even clear what (classical) singularities mean in this context. Recent work on string duality for example indicates that certain singularities are not at all seen by a propagating string [65]: propagation in a singular region of spacetime is, from the point of view of the string, equivalent to propagation in a region of weak gravity.

On top of that, certain ideas [66] claiming to solve the famous black hole information puzzle require the existence of (as we have seen classically forbidden) tunnels to other information-hungry baby universes.

So presumably quantum gravity still has some surprises in store and only time will tell which of these existing theories will survive. But despite this "quantum uncertainty" it is felt that our understanding of the (classical) black hole interior is near completion, whereas the quantum picture will provide us still with many hours of exciting physics.

Appendices

A Spherical Spacetimes

In this appendix we briefly review spherically symmetric spacetimes. A spacetime is called spherically symmetric, if it admits the group SO(3) as an isometry group such that the group orbits are spacelike two-manifolds.

From this definition one then deduces [7] that the metric can always be written in the form

$$ds^2 = g_{ab}dx^a dx^b + r^2(x^a)(d\varphi^2 \sin^2(\vartheta) + d\vartheta^2) \qquad a = 1, 2, \tag{A.1}$$

where φ and ϑ are the usual angular coordinates, the x^a's are two arbitrary coordinates and g_{ab} is a pseudo-Riemannian two-metric.

One easily calculates the Ricci tensor to be

$$\begin{aligned} {}^{(4)}R_{ab} &= {}^{(2)}R_{ab} - 2r_{;ab}/r & \text{(A.2)} \\ R_{\vartheta\vartheta} &= \sin^{-2}(\vartheta)R_{\varphi\varphi} = 1 - (r\Box r + r^{,a}r_{,a}), & \text{(A.3)} \end{aligned}$$

where ; denotes the *two* dimensional covariant derivative associated with g_{ab} and $\Box := g^{ab}\,{}^2\nabla_a\,{}^2\nabla_b$.

From this one calculates the Ricci scalar to be

$${}^{(4)}R = {}^{(2)}R + 2(1 - 2r\Box r - r^{,a}r_{,a})/r^2. \tag{A.4}$$

It is convenient to split the Coulomb contribution $E^\mu_\nu = e^2 diag(-1, -1, 1, 1)/8\pi r^4$ from the total energy momentum tensor ($e = const.$). Einstein's equations then read $G_{\mu\nu} = 8\pi(T_{\mu\nu} + E_{\mu\nu})$. We can now decompose $T_{\mu\nu}$ into $T_{ab} = {}^4T_{ab}$ and $T^\varphi_\varphi = T^\vartheta_\vartheta = P$ where P denotes the transverse pressure.

$T_{\mu\nu}$ and $E_{\mu\nu}$ are separately conserved. Thus the conservation equations take the rather simple form

$$\left(r^2 T^a_b\right)_{;a} = \left(r^2\right)_{,b} P. \tag{A.5}$$

One can now define the scalar quantities f, m and κ by

$$f := r^{,a} r_{,a} =: 1 - \frac{2m}{r} + \frac{e^2}{r^2}, \tag{A.6}$$

$$\kappa := -\left(m - \frac{e^2}{r}\right)/r^2. \tag{A.7}$$

Thus Einstein's equations become

$$r_{;ab} - g_{ab}(\Box r + \kappa) = -4\pi r T_{ab} \tag{A.8}$$

$$\text{and} \qquad \Box r - \frac{e^2}{r^3} - \frac{1}{2} r\, {}^{(2)}R = 8\pi r P. \tag{A.9}$$

Taking the trace of equation (A.8) and replacing $\Box r$ in (A.8) and (A.9) finally gives

$$r_{;ab} + g_{ab}\kappa = -4\pi r(T_{ab} - g_{ab}T) \tag{A.10}$$

$$\text{and} \qquad {}^{(2)}R - 4\frac{m}{r^3} + 6\frac{e^2}{r^4} = 8\pi(T - 2P), \tag{A.11}$$

where $T = T^a_a$. For comparison with the static case it is convenient to introduce the following compact notation. First we note that

$$\kappa = -\frac{1}{2}\left.\frac{\partial f}{\partial r}\right|_{m=const.}.$$

Similarly equation (A.11) can now be rewritten as

$${}^{(2)}R - 2\left.\frac{\partial \kappa}{\partial r}\right|_{m=const.} = 8\pi(T - 2P). \tag{A.12}$$

Note that these partial differentiations with respect to r don't assume r to be a coordinate.

B Computing Ricci components: some intermediate details

For the convenience of enterprising readers who wish to derive the Ricci components (5.64)–(5.66) for themselves, we record here some intermediate steps of the computations.

Computation of ${}^{(4)}R_{ab}$ from (5.101) requires evaluation of

$$\begin{aligned}\widetilde{\nabla}_\beta(e^\alpha_{(a)}\widetilde{\nabla}_\alpha e^\beta_{(b)}) &= -e^{-\lambda}(\widetilde{D}_A + K_A)K^A_{ab}\\ (\widetilde{\nabla}_\beta e^\alpha_{(a)})(\widetilde{\nabla}_\alpha e^\beta_{(b)}) &= \frac{1}{2}(\lambda_{,a}\lambda_{,b} + e^{-2\lambda}\omega_a\omega_b) - 2e^{-\lambda}K_{A(a}{}^d\widetilde{K}^A{}_{b)d},\end{aligned}$$

which can be verified from (5.92) and (5.67).

Computation of R_{AB} from (5.100) requires

$$\begin{aligned}\ell_{(A)\alpha|\beta}\ell^{\beta|\alpha}_{(B)} &= (D_A\lambda)(D_B\lambda) - \frac{1}{2}\eta_{AB}(D_E\lambda)(D^E\lambda)\\ &\quad + K_{Aab}K^{ab}_B - \frac{1}{2}e^\lambda\eta_{AB}(\lambda_{,a}\lambda^{,a} + e^{-2\lambda}\omega^a\omega_a)\end{aligned}$$

which follows from (5.93), (5.67) and (5.72).

Finally, computation of R_{Aa} requires

$$\begin{aligned}(\widetilde{\nabla}_\beta e^\alpha_{(a)})\ell^\beta_{(A)|\alpha} &= \frac{1}{2}\lambda_{,a}D_A\lambda + \left(K_{Aab} + \frac{1}{2}\Delta K_{Aab}\right)\lambda^{,b}\\ &\quad + \frac{1}{2}\epsilon_{AB}e^{-\lambda}(\omega_a D^B\lambda + \Delta K^B_{ab}\,\omega^b)\end{aligned}$$

in which

$$\Delta K_{Aab} \equiv \widetilde{K}_{Aab} - K_{Aab} = s_{Ab;a}.$$

C The operator D_A: commutation rules and other properties

In Sec. 5.3 we gave two definitions—(5.21) and (5.24)—for the operator D_A. It is straightforward to show their equivalence. We have

$$[e_{(a)}, e_{(b)}] = 0, \qquad [\partial x/\partial u^A, e_{(b)}] = 0,$$

since the Lie bracket of two holonomic vectors vanishes (cf (5.14)). In combination with (5.9), this yields

$$[\ell_{(A)}, e_{(b)}] = -[s^a_A e_{(a)}, e_{(b)}] = (\partial_b s^a_A)e_{(a)}. \tag{C.1}$$

Hence, for any 2-vector X^b,

$$\mathcal{L}_{\ell_{(A)}}(X^b e_{(b)}) = \left\{(\partial_A - \mathcal{L}_{s^a_A})X^b\right\} e_{(b)} \tag{C.2}$$

which proves the equivalence of (5.24) and (5.21) when applied to X^b.

This argument is easily extended. For instance, for the 2-metric g_{ab}, the definition (5.24) gives

$$\begin{aligned} D_A g_{ab} &= e^{\alpha}_{(a)}\, e^{\beta}_{(b)} \mathcal{L}_{\ell_{(A)}} g_{\alpha\beta} = 2 e^{\alpha}_{(a)}\, e^{\beta}_{(b)} \ell_{(A)(\alpha|\beta)} \\ &= 2K_{Aab} \end{aligned}$$

by (5.16), which agrees with the form (5.23) obtained from the definition (5.21). (Strictly speaking, (5.24) requires that the projector $\Delta_{\alpha\beta} \equiv e_{(a)\alpha}\, e^{(a)}_{\beta}$ should replace $g_{\alpha\beta}$ in the first equality above. But, according to the completeness relation (5.11), the difference involves the Lie derivative of $\ell^{(A)}_{\alpha}\ell_{(A)\beta}$, which is linear homogeneous in $\ell_{(A)}$ and projects to zero.)

Commutation relations for D_A follow most easily from the definition (5.24). For a scalar field f,

$$2D_{[B}D_{A]}f = [\mathcal{L}_{\ell_{(B)}}, \mathcal{L}_{\ell_{(A)}}]f = \mathcal{L}_{[\ell_{(B)},\ell_{(A)}]}f = \epsilon_{AB}\omega^a \partial_a f,$$

where we have recalled the well-known result that the commutator of two Lie derivatives is the Lie derivative of the commutator (i.e., Lie bracket), and made use of (5.19).

Consider next the operation on a 2-vector X^a. We have from (5.24),

$$\begin{aligned} D_B D_A X^a &= e^{(a)}_{\beta} \mathcal{L}_{\ell_{(B)}} (e^{\beta}_{(b)} D_A X^b) \\ &= e^{(a)}_{\beta} \mathcal{L}_{\ell_{(B)}} \{\Delta^{\beta}_{\alpha} \mathcal{L}_{\ell_{(A)}} (e^{\alpha}_{(a)} X^a)\}. \end{aligned}$$

The projection tensor Δ^{β}_{α} can be replaced by δ^{β}_{α}, because the Lie derivative, operating on the difference, gives terms proportional to $\ell^{\beta}_{(E)}$ or $\ell_{(E)\alpha}$, which project to zero, noting (C.2). Thus,

$$D_B D_A X^a = e^{(a)}_{\alpha} \mathcal{L}_{\ell_{(B)}} \mathcal{L}_{\ell_{(A)}} (e^{\alpha}_{(a)} X^a).$$

We can now proceed exactly as for the scalar case to derive the commutator. The result (generalized to an arbitrary 2-tensor) is

$$[D_B, D_A] X^{a\ldots}_{b\ldots} = \epsilon_{AB} \mathcal{L}_{\omega^a} X^{a\ldots}_{b\ldots}.$$

In particular,

$$[D_B, D_A] g_{ab} = 2\epsilon_{AB} \omega_{(a;b)}.$$

Recalling (B3), this may be written

$$D_{[B}K_{A]ab} = \frac{1}{2}\,\epsilon_{AB}\,\omega_{(a;b)},$$

which was used in (5.52). It contracts to

$$D_{[B}K_{A]} = \frac{1}{2}\,\epsilon_{AB}\,\omega^{a}{}_{;a}.$$

These last two identities also play a role in symmetrizing—or, more properly, recognizing the implicit symmetry of—the raw expressions for R_{AB} and R_{AaBb} that emerge from the Ricci commutation relations. The manifestly symmetric expressions listed in (5.28) and Sec. 5.13 have been symmetrized with the aid of these identities.

To conclude, we note the rule for commuting D_A and the two-dimensional covariant derivative ∇_a. The commutator $[D_A, \nabla_a]$, applied to any 2-tensor, is formed by a pattern similar to its two-dimensional covariant derivative, but with Γ^a_{bc} replaced by

$$D_A\Gamma^a_{bc} = 2K_{A(b;c)}{}^{a} - K_{Abc}{}^{;a}.$$

As examples:

$$\begin{aligned}
[D_A, \nabla_a]X^b &= X^d D_A\Gamma^b_{da}, \\
[D_A, \nabla_a g_{bc}] &= -2(D_A\Gamma^d_{a(b})g_{c)d} = -2K_{Abc;a}
\end{aligned}$$

The justification for the rule is that the partial derivative ∂_a(applied to any two-dimensional geometrical object) commutes with both ∂_A and the two-dimensional Lie derivative $\mathcal{L}_{s^a_A}$, so that, by (5.21),

$$[D_A, \partial_a]\, X^{b\ldots}_{c\ldots} = 0.$$

D Solving the inhomogeneous shear equations

Equations like (3.15) for the shear cannot generally be solved analytically. For the homogeneous case one can at least find a series solution of the form (3.16). But this does not work for the inhomogeneous equations which one encounters for example in the perturbation theory in Chapter 6. In this Appendix we present a method, using

standard results, to formally integrate such equations with the help of the Green function for a more general wave equation. As usual the complete solution is then obtained by adding a solution to the homogeneous equation, so that the sum of the two satisfies the boundary conditions.

To start consider a metric of the form

$$ds^2 = g_{ab}dz^a dz^b + R(z^a)\left(dx^2 + dy^2\right), \quad a = 0, 1. \tag{D.1}$$

(This metric serves merely as a mathematical tool, and has no physical meaning attached to it.)

The four-dimensional d'Alambertian ${}^4\Box$ then reads

$${}^4\Box\phi = \frac{1}{R\sqrt{g}}\left(R\,{}^2\Box\phi + \phi_{,a}R^{,a} + \phi_{,xx} + \phi_{,yy}\right),$$

where $g = -\det g_{ab}$ and ${}^2\Box$ is the wave operator associated with g_{ab}.

For example choosing $g_{ab}dz^a dz^b = 2dudv$ gives

$$R\,{}^4\Box\phi = 2R\phi_{,uv} + R_{,u}\phi_{,v} + R_{,v}\phi_{,u} + \phi_{,xx} + \phi_{,yy}$$

which is, up to the x and y derivatives exactly equation (3.12). Choosing $g_{ab}dz^a dz^b = d\chi^2 - dR^2$ similarly gives

$${}^4\Box\phi = 2\left(\phi_{,\chi\chi} - \phi_{,RR} - \frac{\chi_{,R}}{R}\right) + \frac{1}{R}\left(\phi_{,xx} + \phi_{,yy}\right)$$

which, again up to the x and y derivatives, is equation (3.15).

To construct the Green function for the operator ${}^4\Box$ we solve

$${}^4\Box\phi_k = 0 \tag{D.2}$$

for the its modes ϕ_k. The metric (D.1) induces a scalar product

$$(f, g) = i\int d\Sigma^\mu f^* \overset{\leftrightarrow}{\partial}_\mu g = i\int dxdy \int d\sigma^a f^* \overset{\leftrightarrow}{\partial}_a g, \tag{D.3}$$

with respect to which we normalize the modes ϕ_k.

To solve equation (D.2) we make the Ansatz

$$\phi_{k\omega} = \psi_{k\omega}e^{i\omega_m x^m}, \quad m = 2, 3$$

where $x^2 = x$ and $x^3 = y$. Equation (D.2) then becomes

$$\frac{1}{R}\left(R\,{}^2\Box\psi_{k\omega} + \psi_{k\omega,a}R^{,a} + \omega^m\omega_m\psi_{k\omega}\right) = 0 = \Box\psi_{k\omega} + \frac{\omega_m\omega^m}{R}\psi_{k\omega}.$$

For $\omega_m = 0$ the functions $\psi_{k\omega}$ reduce to the complete set of orthonormal modes of the operator $\Box := {}^2\Box + R^{;a}\partial_a$, which we require to be normalized with respect to the inner product

$$(f,g) = i\int d\sigma^a f^* \overset{\leftrightarrow}{\partial}_a g. \tag{D.4}$$

Note that this is nothing but the inner product (D.3) without the "volume" integral over the $x-y$ space. This makes of course sense, as the operator $\Box$ does not contain any derivatives with respect to x and y.

In terms of the standard mode expansion the Pauli-Jordan function for the operator ${}^4\Box$ is given by

$$\Delta(x,x') = \int dkd^2\omega \left[\psi_{k\omega}(x)\psi^*_{k\omega}(x')e^{i\omega_m(x^m-x'^m)} + \psi^*_{k\omega}(x)\psi_{k\omega}(x')e^{-i\omega_m(x^m-x'^m)}\right].$$

Thus for any timelike coordinate x^0 the (retarded) Green function

$$G(x,x') = \Theta(x^0-x'^0)\Delta(x,x'),$$

satisfies

$${}^4\Box G(x,x') = -\frac{1}{R\sqrt{g}}\delta^4(x-x').$$

Thus a particular solution of the inhomogeneous equation $\Box\phi(z^2) = j(z^a)$ is given by treating ϕ as a solution of the equation ${}^4\Box\phi(z^2) = j(z^a)$. Thus

$$\phi(z^a) = \int R\sqrt{g}d^2z'dx'dy'j(z'^a)G(x,x').$$

As the source does not depend on x and y the only contribution to the corresponding Fourier modes come from the $\omega_m = 0$ modes.We can now interchange the $k-\omega$ integration and the $x'-y'$ integration. The latter can be performed explicitly thanks to the x and y independence of $j(z^a)$. We find

$$\begin{aligned}\phi(z^a) &= (2\pi)^2\int R\sqrt{g}d^2z'j(z'^a)\Theta(z^0-z'^0)\\ &\qquad \int dkd^2\omega\left\{\Psi_{k\omega}(z^a)\Psi^*_{k\omega}(z'^a)e^{i\omega_m x^m} + c.c.\right\}\delta^2(\omega_m)\\ &= (2\pi)^2\int R\sqrt{g}d^2z'j(z'^a)\Theta(z^0-z'^0)\int dk\left(\alpha_k(z^a)\alpha^*_k(z'^a) + c.c.\right). \end{aligned}\tag{D.5}$$

Note, that $F(z^a,z'^a) = R(z'^a)\int dk\left(\alpha_k(z^a)\alpha^*_k(z'^a) + c.c.\right)$ is *not* the Green function of $\Box$, as it fails to be symmetric in z and z'. However (D.5) produces the desired solution of the equation $\Box\phi = j$.

Bibliography

[1] B. Carter, Phys. Rev. **141** (1966), 1242.

[2] R. Penrose, in *Battelle Rencontres*, ed.s C.M. de Witt and J.A. Wheeler, (1968), W. A. Benjamin , p. 222.

[3] M. Simpson and R. Penrose, Int. J. Theo. Phys. **7** (1973), 183.

[4] R.A. Matzner, V.D. Sandberg and N. Zamorano, Phys. Rev. D **19**, (1979) 2821.

[5] R.M. Wald, *General Relativity*, (1984), University of Chicago Press.

[6] C.W. Misner, K.S. Thorne and J.A. Wheeler, *Gravitation*, (1973), Freeman.

[7] N. Straumann, *General Relativity and Relativistic Astrophysics*, (1988), Springer Verlag.

[8] Karl Schwarzschild, Sitzungsberichte der Preussischen Akademie der Wissenschaften Berlin, Kl Math. Phys. Tech. (1916) 189.

[9] J.R. Oppenheimer and H. Snyder, Phys. Rev. **56** (1939), 455.

[10] R. Price, Phys. Rev. **D5** (1972), 2419; Astroph. J. **244** (1978), 643.

[11] P.C. Vaidya Curr. Sci. **12** (1943), 183; Proc. Indian Acad. Sci. **A33** (1951), 264; Nature **171** (1953), 171.

[12] W.A. Hiscock, Physics Letters A **83** (1981),110.

[13] E. Poisson and W. Israel, Phys. Rev. Let. **63** (1989), 1663; Phys. Lett. B **233** (1989), 74.

[14] A. Ori, Phys. Rev. Lett. **67** (1991), 789.

[15] A. Bonanno, Preprint Alberta-Thy-16-94-A, July 1995; gr-qc/9507047.

[16] U. Yurtsever, Class. Quantum Grav.**10** (1993), L17.

[17] N.Y. Gnedin and M.L. Gnedin, Sov. Astron. **36** (1992), 216.

[18] M.L. Gnedin and N.Y. Gnedin, Class. Quantum Grav. **10** (1993), 1083.

[19] Y. Gursel, V.D. Sandberg, I.D. Novikov and A.A. Starobinskiĭ, Phys. Rev. **D19** (1979), 413;

[20] Y. Gursel, I.D. Novikov, V.D. Sandberg and A.A. Starobinskiĭ, Phys. Rev.**D 20** (1979), 1260.

[21] A. Bonanno, S. Droz, S.M. Morsink and W. Israel Phys. Rev. **D50** (1994), 7372; Can. J. Phys. **72** (1994), 755, Erratum: Can. J. Phys. **73** (1995), 251; A. Bonanno, S. Droz, S.M. Morsink and W. Israel, Proc. Roy. Soc. in Press.

[22] P.R. Brady, S. Droz, W. Israel and S.M. Morsink, preprint Alberta-Thy-19-95, gr-qc/9510040, submitted to Class. Quant. Grav. (1995).

[23] M.D. Kruskal, Phys. Rev. **119** (1960), 1743.

[24] W. Israel: "Dark stars: The evolution of an idea" in *300 Years of Gravitation*, (1987), 199, Cambridge University Press.

[25] S. Chandrasekar, Phil. Mag. **11** (1931), 592.

[26] G.D. Birkhoff, Relativity and Modern Physics, (1923) Harward University Press.

[27] Roeland P. van der Marel, To appear in: Highlights of Astronomy, Vol. **10**, Proc. of the XXIInd General Assembly of the IAU, The Hague, August 1994, ed. J. Bergeron, Kluwer Academic Publishers.

[28] I.D. Novikov and V.P. Frolov, *Physics of Black Holes* (1989), Kluwer Academic Publishers.

[29] C. Gundlach, R.H. Price and J. Pullin, Phys. Rev. **D49** (1994), 883; Phys. Rev. **D49** (1994), 890.

[30] M. Heusler, S. Droz and N. Straumann: Phys. Lett. **B285** (1992), 21; M. Heusler, Class. Quantum Grav. **12** (1995), 2021.

[31] E.T. Newman et al. J. Math. Phys. **6** (1965), 918.

[32] R. Kerr, Phys. Rev. Lett. **11** (1963), 237.

[33] G. Ellis and S. Hawking, *The Large Scale Structure of Space-Time*, (1973) Cambridge University Press.

[34] S. Chandrasekhar and J.B. Hartle, *Proc. R. Soc. London* **A384** (1982), 301.

[35] D.A. Konkowski and T.M. Helliwell, Phys. Rev. D **50** (1994), 841.

[36] V.A. Belinskii, E.M. Lifshitz and I.M. Khalatnikov, Advances in Physics **19** (1970), 525; C. Misner, Phys. Rev. Lett. **22** (1969), 1071.

[37] E. Poisson and W. Israel, Phys. Rev. D **41** (1990), 1796.

[38] A. Ori, Phys. Rev. Lett. **68** (1992), 2117.

[39] R. Herman and W.A. Hiscock, Phys. Rev. D**46** (1992), 1863.

[40] I. D. Novikov and A. A. Starobinskiĭ, Sov. Phys. JETP **51** (1980), 1.

[41] S. Chandrasekhar, *The Mathematical of Theory Black Holes* (1983), Oxford University Press.

[42] R.A. Isaacson, Phys. Rev. **160** (1968), 1263; **160** (1968), 1272.

[43] P.R. Brady and J.D. Smith, Phys. Rev. Lett. **75** (1995), 1256.

[44] Arnowitt R, Deser S and Misner C W (1962) *Gravitation: an Introduction to Current Research*, ed. Witten (New York: Wiley) Chap. 7.

[45] R.A. d'Inverno and J. Smallwood , Phys. Rev. D **22** (1980), 1233; C.G. Torre, Class. Quantum Grav. **3** (1986), 773; D. McManus, J. Gen. Rel. Grav. **24** (1992), 65; S.A. Hayward, Class. Quantum Grav. **10** (1993), 779; R.A. d'Inverno and J.A.G. Vickers,Class. Quantum Gravity (1995), **12**, 753.

[46] R. Geroch, A. Held and R. Penrose, J. Math. Phys. **14** (1973), 874.

[47] R.K. Sachs, J. Math. Phys. **3** (1962), 908; G. Dautcourt, Ann. Physik **12** (1963), 202; R.J. Penrose, Gen. Rel. Grav. (1980) **12** 225; H. Friedrich, Proc. Roy. Soc. A **375** (1981), 169; J.M. Stewart and H. Friedrich, Proc. Roy. Soc. A **384** (1982); A.D. Rendall, Proc. Roy. Soc. A **427** (1990), 221; J.M. Stewart *Advanced General Relativity* (Cambridge: Cambridge Univ. Press) (1990), Chap. 4.

[48] W.G. Unruh, G. Hayward, W. Israel and D. McManus, Phys. Rev. Letters **62** (1989), 2897.

[49] W. Israel, Phys. Rev. Letters **56** (1986), 789; W. Israel, Phys. Rev. Letters **57** (1986), 397; W. Israel, Can. J. Phys. **64** (1986), 120; S.A. Hayward, Phys. Rev. D **49** (1994), 6467; S.A. Hayward, Class. Quantum Grav. **11** (1994), 3025; P.R. Brady and C.M. Chambers, Phys. Rev. D **51** (1995), 4177.

[50] P.A.M. Dirac, Rev. Mod. Phys. **21** (1949), 392; F. Rohrlich, Acta Phys. Austriaca Suppl. **8** (1971), 277; V.P. Frolov, Fortschr. Physik **26** (1978), 455; J.N. Goldberg, Found. Physics **15**(1985), 439; M.E. Convery, C.C. Taylor and J.W. Jun, Phys. Rev. D **51** (1995), 4445.

[51] E. Verlinde and H. Verlinde *String Quantum Gravity and Physics at the Planck Energy Scale* ed. N. Sanchez (Singapore: World Scientific) (1993), p. 262; R. Kallosh Phys. Let. **B275** (1992), 284.

[52] J.L. Synge *Relativity: The General Theory* (Amsterdam: North-Holland) (1960), p. 1.

[53] R.M. Wald *General Relativity* (Chicago: Univ. of Chicago Press) (1984), p. 218.

[54] H. Bondi, M.G.J. van der Burg and A.W.K. Metzner, Proc. Roy. Soc. A **269** (1962), 21.

[55] R.A. d'Inverno and J. Stachel, J. Math. Phys. **19** (1978), 2447.

[56] A. Ori and E.É. Flanagan, preprint gr-qc/9508066

[57] P.R. Brady and C.M. Chambers, gr-qc/9501025; Phys. Rev. D **51**, (1995), 4177.

[58] P.R. Brady, Quantum Aspects of Black hole interiors; Ph.D. thesis (1993).

[59] F.A.E. Pirani, Introduction to Gravitational Radiation Theory, in *Lectures on General Relativity; Brandeis Summer Institute in theoretical Physics*, A. Trautmann, F.A.E. Pirani, H. Bondi (1964) Prentice-Hall, New Jersey.

[60] R. Balbinot and E. Poisson, Phys. Rev. Lett. **70** (1993), 13.

[61] W. Anderson, P.R. Brady, W. Israel and S.M. Morsink, Phys. Rev. Lett. **70**, (1993) 1041.

[62] V.P. Frolov, Phys. Rev. **D46** (1992), 5383.

[63] S. Droz, Phys. Lett. **A191**,(1994) 211.

[64] R. Balbinot and P.R. Brady, Class. Quantum Grav. **11** (1994), 1763.

[65] M. Perry, Lectures given at the 46th Scottish University Summer School on General Relativity, Aberdeen (1995).

[66] A. Strominger, preprint UCSBTH-94-34; hep-th/9410187; Talk given at the Seventh Marcel Grossman Meeting on General Relativity, Stanford CA, (1994).